

Implications of mirror neutrinos for early universe cosmology

R. Foot* and R. R. Volkas†

School of Physics, Research Centre for High Energy Physics, The University of Melbourne, Parkville 3052, Australia

(Received 30 June 1999; published 26 January 2000)

The exact parity model (EPM) is, in part, a theory of neutrino mass and mixing that can solve the atmospheric, solar and LSND anomalies. The central feature of the neutrino sector is three pairs of maximally mixed ordinary and mirror neutrinos. It has been shown that inter-family ordinary-mirror neutrino oscillations can generate large neutrino asymmetries in the epoch of the early universe immediately prior to big bang nucleosynthesis (BBN). The large neutrino asymmetries generically suppress the production of mirror neutrinos, and a sufficiently large ν_e asymmetry can directly affect light element synthesis through nuclear reaction rates. In this paper we present a detailed calculation of neutrino asymmetry evolution driven by the six-flavor EPM neutrino sector, focusing on implications for BBN.

PACS number(s): 98.80.Cq, 14.60.St, 11.30.Er, 26.35.+c

I. INTRODUCTION

It has been known for a long time, but not widely appreciated, that parity can be a symmetry of nature if the particle content is doubled [1–4]. In this circumstance, for each ordinary particle there is a mirror particle of exactly the same mass as the corresponding ordinary particle. The mirror particles interact with each other in exactly the same way that ordinary particles interact with themselves. The mirror particles are not copiously produced in any laboratory experiments because they either do not couple, or couple extremely weakly, to the ordinary particles. In the modern language of gauge theory, the mirror particles are all gauge singlets under the standard model $G = \text{SU}(3)_c \otimes \text{SU}(2)_L \otimes \text{U}(1)_Y$ gauge interactions. Instead, the mirror particles interact with a set of mirror gauge particles. This is mathematically described by a doubled gauge symmetry of the theory; that is, G is extended to $G \otimes G$. (The ordinary particles are of course singlets under the mirror gauge symmetry.) Parity is conserved because the mirror particles experience $V+A$ mirror weak interactions instead of the usual $V-A$ weak interactions.

The ordinary and mirror sectors can interact with each other in a number of ways. All of these interactions apart from gravity can be controlled by *a priori* arbitrary parameters. Apart from the irremovable gravitational interaction, there are three other ways in which ordinary and mirror particles can interact with each other. Two of these are photon-mirror photon (and Z -mirror- Z) kinetic mixing [3,5] and Higgs-boson-mirror-Higgs-boson mass mixing [3]. If one demands that the reasonably successful big bang nucleosynthesis (BBN) predictions not be greatly disturbed, then it seems unlikely that these interactions can have observable laboratory implications. See Refs. [6,7] for details.¹

*Email address: foot@physics.unimelb.edu.au

†Email address: r.volkas@physics.unimelb.edu.au

¹In particular extensions of the exact parity idea, neutral gauge boson kinetic mixing and/or Higgs boson mixing may not be controlled by an independent arbitrary parameter. For instance, in exact parity extensions of grand unified models such as $\text{SU}(5)$ the kinetic mixing parameter is calculable as a function of other parameters in the theory [5].

Neutrinos provide a third possible interaction between the ordinary and mirror sectors. *If neutrinos have mass, then mass mixing between ordinary and mirror neutrinos is possible. This leads to very important experimental tests of the exact parity idea.* We call the $G \otimes G$ extension of the standard model the exact parity model (EPM) [3,4]. It is, in part, an explicit theory of neutrino mass and mixing. It is a candidate for the standard model extension called for by solar, atmospheric and accelerator neutrino experiments that strongly suggest the existence of neutrino oscillations. Ongoing and future terrestrial experiments, such as SuperKamio-kande, the Sudbury Neutrino Observatory (SNO), Borexino, the long and short base line neutrino oscillation searches and other experiments, will in the next few years provide important new clues in the search for a theory of neutrino mass and mixing, and will further test the proposed EPM resolution of all of the anomalies.

Of course, if mirror matter exists, then there should be dramatic implications for astrophysics and cosmology as well as particle physics. Some studies [2] suggest that mirror matter is an interesting candidate for dark matter. In fact, there is some evidence that mirror stars may have already been discovered in the MACHO experiments [8]. Another exciting possibility is that gamma ray bursts may be due to collapsing or merging mirror stars [9]. Of direct relevance to the present paper, however, is the observation that early universe cosmology, through big bang nucleosynthesis, structure formation and in the near future through detailed cosmic microwave background measurements, should provide important new information about the cosmological role of neutrino physics. This information may thus also provide a test of the EPM. Indeed, the purpose of this paper is to perform a detailed study of the early universe cosmology of the EPM, with particular emphasis on BBN. Before embarking on this analysis, we will briefly review why the EPM supplies an interesting theory of neutrino mass and mixing, and therefore why some effort to study its early universe cosmology is justified.

It was pointed out several years ago [4] that the EPM provides an interesting theory of neutrino mass for one simple reason: the exact parity symmetry between the ordinary and mirror sectors forces an ordinary neutrino ν_α (α

$=e,\mu,\tau$) to be maximally mixed² with its mirror partner ν'_α . It is certainly *very interesting* that the atmospheric neutrino observations of SuperKamiokande [11] and other experiments [12] point to the muon-neutrino being maximally mixed with another flavor ν_x . It is known that ν_x cannot be the ν_e [13], which leaves $\nu_x=\nu_\tau$ and $\nu_x=\nu_s$ as the viable possibilities [14,15], where the subscript s denotes a sterile neutrino. The EPM provides a natural candidate for ν_x , namely the mirror muon-neutrino ν'_μ . As far as terrestrial experiments are concerned, the ν'_μ is a sterile flavor.

Since the confirmation of atmospheric ν_μ disappearance by SuperKamiokande, a significant amount of theoretical effort has gone into trying to explain the large mixing angle observed. This work has focussed almost entirely on the $\nu_x=\nu_\tau$ possibility. It is interesting to note that in the immediate past, small interfamily mixing, as observed for the quark sector, was considered to be natural also for the lepton sector. With the advent, in particular, of the beautiful SuperKamiokande results, this theoretical prejudice is now being criticized. Our proposal is completely different from any current effort to realize large $\nu_\mu-\nu_\tau$ mixing. *We simply argue that the connection between exact parity symmetry and ordinary-mirror neutrino maximal mixing is an especially elegant and simple explanation of the large mixing angle observed in the atmospheric neutrino experiments.* Since this points to ν_x being ν_s rather than ν_τ , a neutral current atmospheric neutrino measurement is vital [16].

Intriguingly, there is independent experimental evidence for large angle neutrino oscillations from another set of measurements: maximal mixing between the electron-neutrino and some other flavor is well motivated by the solar neutrino problem [4,17,18]. In the EPM, the ‘‘other flavor’’ is of course the mirror electron-neutrino ν'_e . Such a scenario leads to an energy independent 50% solar ν_e day-time flux reduction³ for a squared mass difference greater than about 3×10^{-10} eV², and to a ‘‘just-so’’ picture for a squared

²Of course this result only holds if the parity symmetry is *not broken* by the vacuum. In Ref. [3] it was shown that this occurs for a large range of parameters with just the minimal Higgs sector of one Higgs doublet and one mirror Higgs doublet. It was explained in Ref. [10] that if additional Higgs scalars exist, then the parity symmetry can be spontaneously broken with the mirror electroweak symmetry breaking scale left as a free parameter. It was argued in Ref. [10] that such a scenario could be motivated by the neutrino anomalies. Of course the implications for neutrino experiments and early universe cosmology of the model in Ref. [10] are quite different from the minimal case considered in the present paper, where the parity symmetry is *not* broken by the vacuum.

³In a very interesting recent paper, Guth, Randall and Serna [19] have pointed out that an energy-dependent day-night effect in general exists for solar neutrinos even if the vacuum mixing is maximal, thus correcting a misconception shared by the present authors and some of the rest of the community. It is *not correct* to conclude that maximal oscillations out of the ‘‘just-so’’ regime always lead to a completely energy independent suppression, because the night-time rate is in general energy-dependent due to matter effects in the Earth.

mass difference in the approximate range⁴ $\text{few}\times 10^{-11}\rightarrow 3\times 10^{-10}$ eV². The most recent solar neutrino data, compared with the most recent solar model calculations [22], show that four out of the five solar neutrino experiments observe close to a 50% flux deficit. (The chlorine experiment sees a greater than 50% deficit.) The detailed implications of the solar neutrino situation, though surely indicative of ν_e oscillations, is not at present as clear as the atmospheric neutrino situation. For various reasons, more experiments are needed: the relatively low Chlorine result needs to be checked by another experiment, and the cause and existence of the apparent distortion of the ‘‘boron’’ neutrino energy spectrum require further investigation. Of particular relevance for the EPM, we will presumably soon find out from SNO whether the solar neutrino flux contains a significant sterile component.

Notice that no mention was made of the Liquid Scintillator Neutrino Detector (LSND) observations [23] in advocating the existence of what are essentially light sterile neutrinos. It has become commonplace to motivate light sterile neutrinos from the inability of three-flavor oscillations to simultaneously resolve the atmospheric, solar and LSND anomalies. We have used this argument ourselves. We would, however, like to emphasize that our obsession with the EPM arose from the maximal mixing feature, long before the advent of LSND.

Let us turn, then, to the cosmological implications of mirror neutrinos. The distinction between mirror neutrinos and strictly sterile neutrinos, which is totally unimportant for terrestrial, atmospheric and solar neutrinos, is of some significance in the early universe. This issue will be discussed in depth in later sections. For the purposes of these introductory remarks, however, the distinction need not be made. Many of the qualitative features of sterile neutrino early universe cosmology pertain also to mirror neutrinos.

In recent years, the physics of active-sterile neutrino oscillations during and before the BBN epoch has been re-examined [24–29]. Prior to this re-analysis, it had been concluded that light sterile neutrinos were cosmologically disfavored for much of parameter space [30]. Focusing on the $\nu_\mu\rightarrow\nu_s$ solution to the atmospheric neutrino problem by way of concrete example, it had been concluded that the oscillation parameters required would lead to the ν_s being thermally equilibrated prior to BBN, thus increasing the expansion rate of the universe and worsening agreement between theory and primordial light element abundance measurements. However, it was subsequently realized [24] that the explosive production of large neutrino-antineutrino asymmetries or chemical potentials by the active-sterile oscillations themselves had not been properly taken into account in the early studies. Large neutrino asymmetries generically suppress active-sterile oscillations by making the

⁴There is also an interesting ‘‘window’’ around $\delta m^2\sim 5\times 10^{-10}$ eV² [20] which leads to an approximate energy integrated flux reduction of 50% and can also explain the distortion of high energy $E\gtrsim 13$ MeV boron neutrinos suggested by recent SuperKamiokande data [21].

effective mixing angle in matter very small [31]. Detailed numerical work has shown that, for a large region of parameter space, the generation through the oscillations themselves of large neutrino asymmetries suppresses the production of sterile neutrinos sufficiently for the expansion rate of the universe during BBN to be essentially unaffected [25,28].

Furthermore, unless the mixing between the electron-neutrino and the other neutrinos is really tiny, one expects an asymmetry to develop for ν_e 's [26]. This has a direct effect on the rates of the weak interaction processes $\nu_e n \rightarrow e^- p$ and $\bar{\nu}_e p \rightarrow e^+ n$ which help to determine the neutron to proton ratio during BBN. A detailed calculation within a particular neutrino mass and mixing scenario is required to work out the magnitude of this effect. It has been shown for two different ‘‘3 active plus 1 sterile neutrino models’’ that the generation of a ν_e asymmetry can be important [26,27]. In Sec. V, we will for the first time explore this effect for mirror rather than strictly sterile neutrinos.

Aspects of the early universe cosmology of mirror neutrinos were discussed in Ref. [32]. The present paper improves and extends this analysis. Reference [32] focussed solely on what we can call ‘‘high temperature neutrino asymmetry evolution.’’ (We will explain precisely what we mean by this designation later on.) It showed that the $\nu_\mu \rightarrow \nu'_\mu$ and $\nu_e \rightarrow \nu'_e$ solutions to the atmospheric and solar neutrino problems, respectively, were compatible with BBN for a large range of parameters. In Ref. [32], the calculations were carried out in the ‘‘static approximation.’’ In the present work we improve on these calculations by using the full quantum kinetic equations, rather than the above approximation. In addition, we also analyze the ‘‘low temperature neutrino asymmetry evolution’’ that occurs immediately prior and during BBN. The size and evolution of the ν_e asymmetry will be the main issue here.

Finally, let us remark that the neutrino phenomenology of the EPM is very similar to some models employing pseudo-Dirac neutrinos [33]. Many of the implications for early universe cosmology will be qualitatively similar to the EPM. There are of course quantitative differences because the mirror weak interactions play an important role in the early universe through their impact on the matter potential and also because they affect the momentum distribution of the mirror neutrinos. We focus on the mirror neutrino scenario in this paper because it is arguably much more elegant from a model building point of view. (For example, the seesaw mechanism can be invoked to understand the smallness of both the neutrino and mirror neutrino masses [4].) It is also theoretically very well motivated because it restores parity as an unbroken symmetry of nature.

The outline of this paper is as follows: In Sec. II we define and motivate the neutrino mass and mixing parameters which we will use in our subsequent analysis. We also very briefly review the neutrino asymmetry amplification phenomenon. In Sec. III the quantum kinetic equations for ordinary-mirror neutrino oscillations are defined and discussed. In Sec. IV we compute the region of parameter space where the $\nu_\tau \leftrightarrow \nu'_\mu$ oscillations generate L_{ν_τ} and $L_{\nu'_\mu}$ asymmetries in such a way that the maximal $\nu_\mu \leftrightarrow \nu'_\mu$ oscillations

cannot significantly populate the mirror ν'_μ states. The main issue here is whether or not the $\nu_\mu \leftrightarrow \nu'_\mu$ oscillations can produce compensating L_{ν_μ} and $L_{\nu'_\mu}$ asymmetries such that the matter term for $\nu_\mu \leftrightarrow \nu'_\mu$ oscillations becomes unimportant. In Sec. V the low temperature evolution of the neutrino asymmetries is studied in detail. The main issue here is the effect of the oscillations on BBN. In Secs. VI and VII we comment on the implications of the EPM for the hot plus cold dark matter scenario and the anisotropy of the cosmic microwave background. Section VIII is a conclusion.

II. OVERVIEW AND ORIENTATION

The analysis of neutrino oscillations in the early universe is complicated. In order to avoid the pedagogical danger of becoming mired in the full technical detail, we present first a short overview.

There are six light neutrino flavors in the exact parity model: the three ordinary neutrinos $\nu_{e,\mu,\tau}$ and their mirror partners $\nu'_{e,\mu,\tau}$, respectively. In the absence of interfamily mixing, the most general neutrino mass matrix consistent with parity symmetry for each generation is contained in [4]

$$\mathcal{L}_{\text{mass}} = [\bar{\nu}_L, (\bar{\nu}'_R)^c] \begin{pmatrix} m_1 & m_2 \\ m_2 & m_1^* \end{pmatrix} \begin{bmatrix} (\nu_L)^c \\ \nu'_R \end{bmatrix} + \text{H.c.} \quad (1)$$

We have assumed Majorana masses for definiteness and simplicity, and one should note that the parity symmetry interchanges ν_L with $\gamma_0 \nu'_R$. The quantity m_2 must be real, while m_1 may be complex. However, the phase of m_1 can, without loss of generality, be absorbed by the neutrino and mirror neutrino fields. In the phase redefined basis, the mass matrix is diagonalized by the orthogonal transformation

$$\begin{bmatrix} \nu_- \\ \nu_+ \end{bmatrix}_R = \frac{1}{\sqrt{2}} \begin{pmatrix} 1 & -1 \\ 1 & 1 \end{pmatrix} \begin{bmatrix} (\nu_L)^c \\ \nu'_R \end{bmatrix}. \quad (2)$$

We see that the mass eigenstates (ν_\pm) are maximal combinations of the weak eigenstates (and vice versa). Obviously it follows that if, as in the quark sector, the mixing between the generations is nonzero but small, then each pair of weak eigenstates,

$$(\nu_e, \nu'_e), \quad (\nu_\mu, \nu'_\mu), \quad (\nu_\tau, \nu'_\tau), \quad (3)$$

is approximately given by an orthogonal pair of maximal mixtures of the appropriate pair of mass eigenstates. We use the notation

$$\nu_{e+}, \quad \nu_{e-}, \quad \nu_{\mu+}, \quad \nu_{\mu-}, \quad \nu_{\tau+}, \quad \nu_{\tau-} \quad (4)$$

for the mass eigenstates. The subscript in the above equation is used to indicate the pair of states which relate to the corresponding weak eigenstates. In the limit of no mixing between the generations,

$$\begin{aligned}
|\nu_\tau\rangle &= \frac{1}{\sqrt{2}}(|\nu_{\tau+}\rangle + |\nu_{\tau-}\rangle), & |\nu'_\tau\rangle &= \frac{1}{\sqrt{2}}(|\nu_{\tau+}\rangle - |\nu_{\tau-}\rangle), \\
|\nu_\mu\rangle &= \frac{1}{\sqrt{2}}(|\nu_{\mu+}\rangle + |\nu_{\mu-}\rangle), & |\nu'_\mu\rangle &= \frac{1}{\sqrt{2}}(|\nu_{\mu+}\rangle - |\nu_{\mu-}\rangle), \\
|\nu_e\rangle &= \frac{1}{\sqrt{2}}(|\nu_{e+}\rangle + |\nu_{e-}\rangle), & |\nu'_e\rangle &= \frac{1}{\sqrt{2}}(|\nu_{e+}\rangle - |\nu_{e-}\rangle).
\end{aligned} \tag{5}$$

Of course the exact expressions for ν_α and ν'_α ($\alpha = e, \mu, \tau$) will in general be a linear combination of all possible mass eigenstates when mixing between generations exists. This means that all possible oscillations modes among the six neutrino flavors are in general expected to occur. The assumption of small mixing between the generations, together with the necessarily maximal mixing between the ordinary and mirror neutrinos of a given generation, implies that intergenerational modes such as $\nu_\tau \leftrightarrow \nu'_\mu$ or $\nu_\mu \leftrightarrow \nu_e$ will have much smaller amplitudes than the $\nu_\alpha \leftrightarrow \nu'_\alpha$ modes (in vacuum). The analysis to follow will only consider the region of parameter space where vacuum mixing between generations is small.

In order to proceed, we also have to make a guess about the pattern of mass eigenvalues. We will suppose that the neutrino sector is qualitatively identical to the quark and charged-lepton sectors, with the masses displaying the standard hierarchy. We will further assume, most of the time, that the mass splitting between the parity partners within a given family is smaller than the interfamily mass splitting. Putting this together, we have the mass pattern

$$m_{\nu_{\tau+}} \simeq m_{\nu_{\tau-}} \gg m_{\nu_{\mu+}} \simeq m_{\nu_{\mu-}} \gg m_{\nu_{e+}} \simeq m_{\nu_{e-}}. \tag{6}$$

The LSND result suggests that the $e - \mu$ mass splittings are of the order of 1 eV or so, although we will also consider smaller mass splittings. If the $e - \mu$ mass difference is of the order of 1 eV, then to maintain the assumed mass hierarchy the ν_τ and ν'_τ masses should be larger than or about a few eV. A mass in the few eV range would of course make ν_τ a hot dark matter particle. Cosmological closure puts an upper bound of about 40 eV on m_{ν_τ} . Analogy with the quark sector suggests that neutrinos in adjacent families, $e - \mu$ and $\mu - \tau$, should mix more strongly than $e - \tau$. Furthermore, one might guess that $\alpha - \beta / \alpha' - \beta'$ mixing should be stronger than $\alpha' - \beta / \alpha - \beta'$ mixing if one believes that the more ‘‘closely related’’ are the neutrinos the more strongly they should mix. (Also observe that the parity symmetry forces the $\alpha - \beta$ and $\alpha' - \beta'$ mixing angles to be equal, similarly the $\alpha' - \beta$ and $\alpha - \beta'$ mixing angles.) Putting these guesses together with the $\nu_e \rightarrow \nu'_e$ solution to the solar neutrino problem and the $\nu_\mu \rightarrow \nu'_\mu$ solution to the atmospheric neutrino problem, we arrive at the parameter space region⁵

$$m_{\nu_{e+}}, m_{\nu_{e-}} \ll 1 \text{ eV},$$

$$\begin{aligned}
10^{-11} \text{ eV}^2 &\leq |\delta m_{ee}^2| \\
&\equiv |m_{\nu_{e+}}^2 - m_{\nu_{e-}}^2| \lesssim 10^{-3} \text{ eV}^2,
\end{aligned}$$

$$m_{\nu_{\mu+}}, m_{\nu_{\mu-}} \lesssim \text{few eV},$$

$$\begin{aligned}
10^{-3} \text{ eV}^2 &\leq |\delta m_{\mu\mu}^2| \\
&\equiv |m_{\nu_{\mu+}}^2 - m_{\nu_{\mu-}}^2| \lesssim 10^{-2} \text{ eV}^2,
\end{aligned}$$

$$\text{few eV} \lesssim m_{\nu_{\tau+}}, \quad m_{\nu_{\tau-}} \lesssim 40 \text{ eV},$$

$$|\delta m_{\tau\tau}^2| \equiv |m_{\nu_{\tau+}}^2 - m_{\nu_{\tau-}}^2| \ll 1 \text{ eV}^2, \tag{7}$$

with a mixing angle pattern as described above.

We wish to calculate the effect on early universe cosmology of neutrino oscillations within the EPM. A full six-flavor analysis is a daunting task, even with the parameter space restrictions discussed above. Fortunately, the physics of the problem allows some simplifications to be made without sacrificing too much in the way of rigor. In particular, we can build on what we already know about the early universe cosmology of active-sterile neutrino oscillations.

It is useful to start by identifying four qualitatively different epochs:

- (1) the quantum Zeno epoch, where neutrino oscillations are completely damped;
- (2) the high-temperature epoch, where large neutrino asymmetries are initially generated;
- (3) the low-temperature epoch, where decoherence can be neglected; and
- (4) the big bang nucleosynthesis epoch, where neutrino oscillations impact on light element synthesis.

We now very briefly, and qualitatively, discuss these epochs in turn. The mathematics needed to fully explain this cosmological history is available in previous publications and in later sections of this paper.

A. Quantum Zeno epoch

Neutrino oscillations in the early universe are always to some extent damped through collisions with the background medium. As we look back toward the big bang, the collision rate increases as T^5 (below the electroweak phase transition). At sufficiently high temperatures, collisions occur so frequently that quantum coherent oscillatory behavior cannot develop. The neutrino ensemble is frozen with respect to its flavor content (quantum Zeno effect). In addition, the finite temperature contributions to the effective matter potentials for many of the oscillation modes are high enough to render the associated matter mixing angles extremely small. So even with collisions artificially switched off, many of the oscillation modes would have tiny amplitudes.

⁵If $3 \times 10^{-5} \leq |m_{ee}^2| / \text{eV}^2 \leq 10^{-3}$, then the electron neutrino oscillations will have potentially observable effects for atmospheric neutrinos. See Ref. [34] for details.

B. High-temperature epoch

As the temperature decreases, collisional damping is reduced, and partially incoherent evolution of the neutrino ensemble begins. For simplicity, we will in this and the next subsection very briefly review the evolution of the α -like lepton number in the somewhat artificial case where only the $\nu_\alpha \leftrightarrow \nu_s$ mode is operative. It was shown in Ref. [24] that under the influence of this mode⁶ the α -like lepton number L_{ν_α} evolves as per

$$\frac{dL_{\nu_\alpha}}{dt} \simeq C \left(L_{\nu_\alpha} + \frac{\eta}{2} \right). \quad (8)$$

The α -like lepton number is defined by

$$L_{\nu_\alpha} \equiv \frac{n_{\nu_\alpha} - n_{\bar{\nu}_\alpha}}{n_\gamma} \quad (9)$$

and is synonymously called the “ α -like neutrino asymmetry.” The quantity n_i is the number density for species i . Equation (8) holds provided that (i) the squared mass difference $\delta m_{\alpha s}^2$ between the neutrinos obeys $|\delta m_{\alpha s}^2| \gtrsim 10^{-4} \text{ eV}^2$ and (ii) L_{ν_α} is small. The quantity η is set by the relic nucleon number densities and is expected to be small: $\eta/2 \sim 10^{-10}$. The term C is a function of time t (or equivalently temperature T). At high temperature it turns out that C is negative, so that $(L_{\nu_\alpha} + \eta/2) \simeq 0$ is an approximate fixed point. However, if $\delta m_{\alpha s}^2 < 0$ [our δm^2 convention is defined in Eq. (15) below], then C changes sign at a particular temperature $T = T_c$, estimated to be [24]

$$T_c \sim 16 \left(\frac{-\delta m_{\alpha s}^2 \cos 2\theta_{\alpha s}}{\text{eV}^2} \right)^{1/6} \text{ MeV}. \quad (10)$$

At this temperature, rapid exponential growth of neutrino asymmetry occurs, unless $\sin^2 2\theta_{\alpha s}$ is very tiny [see Eq. (11) below]. The generation of neutrino asymmetry occurs because the $\nu_\alpha \rightarrow \nu_s$ oscillation probability is different from the $\bar{\nu}_\alpha \rightarrow \bar{\nu}_s$ oscillation probability due to the matter effects in a CP asymmetric background. As the asymmetry is created, the background becomes more CP asymmetric because the neutrino asymmetries contribute to the CP asymmetry of the background. This leads to a period of runaway exponential growth of the neutrino asymmetry for a large range of parameters⁷ [25,32] summarized by

⁶For the purposes of this introductory discussion, the distinction between mirror and sterile neutrinos will often be neglected.

⁷In the region of parameter space where $|\delta m_{\alpha s}^2| \ll 10^{-4} \text{ eV}^2$, the evolution of the neutrino asymmetry is dominated by oscillations between collisions and the lepton number tends to be oscillatory [35–37].

$$\delta m_{\alpha s}^2 < 0 \quad \text{with} \quad |\delta m_{\alpha s}^2| \gtrsim 10^{-4} \text{ eV}^2,$$

$$10^{-10} \lesssim \sin^2 2\theta_{\alpha s} \lesssim \text{few} 10^{-5} \left[\frac{\text{eV}^2}{|\delta m_{\alpha s}^2|} \right]^{1/2}$$

for ordinary-sterile oscillations,

$$10^{-10} \lesssim \sin^2 2\theta_{\alpha s} \lesssim \text{few} 10^{-4} \left[\frac{\text{eV}^2}{|\delta m_{\alpha s}^2|} \right]^{1/2}$$

for ordinary-mirror oscillations. (11)

(The upper bound in the above equation comes from a constraint on the effective number of neutrino flavors, $N_{\nu, \text{eff}}$, during BBN. We have used $N_{\nu, \text{eff}} - 3 \lesssim 0.6$ in this equation for illustrative purposes.) *We want to emphasize and to state very clearly the following fact: Provided the oscillation parameters are in the large range given in Eq. (11), the ordinary-sterile (or mirror) neutrino oscillations will generate, at the temperature T_c , a significant neutrino asymmetry (or chemical potential) from the tiny seed CP asymmetry of the background plasma. There is no choice about this, a point sometimes misunderstood in the literature: the large neutrino asymmetry will inevitably be generated.* Once generated, neutrino asymmetries in turn contribute to the effective matter potentials and generically suppress oscillations by inducing small effective mixing angles. For typical oscillation parameter values within our scenario, the explosive neutrino asymmetry growth begins while collisions still dominate the evolution (though they now do not completely damp the oscillations). Note that the evolution of lepton number for $T < T_c$ is approximately independent of the initial neutrino asymmetries provided that they are not too big (that is, less than about 10^{-5}). This is because of the approximate fixed point structure which sees $L_{\nu_\alpha} \rightarrow -\eta/2$ for $T > T_c$.

C. Low-temperature epoch

While neutrino asymmetries develop and evolve, the collision rate continues to decrease in a T^5 fashion. Eventually the flavor evolution of the neutrino ensemble becomes dominated by coherent processes rather than decoherence-inducing collisions. This observation is of practical importance, because the evolution equations then reduce to Mikheyev-Smirnov-Wolfenstein (MSW) form. If the dynamics satisfies the adiabatic condition, then the evolution becomes particularly simple. Actually, it turns out that adiabaticity indeed holds for the parameter space of Eq. (11). The low temperature evolution of the asymmetry is then approximately independent of the vacuum mixing angle in the small vacuum mixing angle region. Staying with our example of a $\nu_\alpha - \nu_s$ system in isolation, it has been computed that the “final” value of the asymmetry arises at the temperature [26]

$$T_\nu^f \simeq 0.5 \left(\frac{|\delta m_{\alpha s}^2|}{\text{eV}^2} \right)^{1/4} \text{ MeV}. \quad (12)$$

The magnitude of the final value was calculated to be [26]

$$\begin{aligned} L_{\nu_\alpha}^f &\approx 0.29h \quad \text{for } |\delta m_{\alpha s}^2|/eV^2 \gtrsim 1000, \\ L_{\nu_\alpha}^f &\approx 0.23h \quad \text{for } 3 \lesssim |\delta m_{\alpha s}^2|/eV^2 \lesssim 1000, \\ L_{\nu_\alpha}^f &\approx 0.35h \quad \text{for } 10^{-4} \lesssim |\delta m_{\alpha s}^2|/eV^2 \lesssim 3, \end{aligned} \quad (13)$$

where $h \equiv (T_\nu/T_\gamma)^3$. Similar results also hold for ordinary-mirror neutrino oscillations.

D. Big bang nucleosynthesis epoch

At temperatures of a few MeV, weak interaction rates start to become smaller than the expansion rate of the universe. This causes the ordinary neutrinos to fall out of kinetic and chemical equilibrium with the background plasma. It also signals the onset of the BBN epoch because of the end of nuclear statistical equilibrium. For the typical parameter space of interest in the EPM, we will show that a significant electron neutrino asymmetry is generated by and during during this epoch. This will have important implications for BBN, and one of the major goals of this paper to compute this effect.

III. QUANTUM KINETIC EQUATIONS FOR ORDINARY-MIRROR NEUTRINO OSCILLATIONS

Before we begin in earnest, we need to say something about the thermodynamics of the mirror particles. Because the mirror particles interact among themselves just like the ordinary particles, the mirror particles can be described by a temperature T' (and chemical potentials, which we assume are initially negligible). In fact, the ordinary and mirror particles form two weakly coupled thermodynamic systems. As in our previous paper [32], we will suppose that there is an *asymmetry* between the temperature of the mirror plasma and the temperature of the ordinary plasma so that $T' \ll T$. Of course, if $T' = T$, then a neutrino asymmetry would not be expected to develop. The energy density of the mirror sector would then double the expansion rate of the universe. In this case the reasonably successful BBN predictions would be lost. However, one should remember that exact microscopic symmetry does not imply exact macroscopic symmetry. In reality, if the ordinary and mirror particles are only in very weak thermal contact, there is no compelling reason for $T' = T$. Note that the assumption that $T' \ll T$ does *not* imply that the amount of mirror baryonic matter in the universe today is less than ordinary baryonic matter. The origin of baryon number (and mirror baryon number) is not understood at the moment, so no definite conclusions can be drawn regarding the amount of mirror baryonic matter (and hence mirror stars and so on) in the universe today. Actually there are strong astrophysical arguments for the existence of a large amount of dark matter in the universe, and this suggests that the mirror baryon number is comparable or even greater than the

ordinary baryon number. However, as far as the early⁸ universe is concerned, the precise value of the mirror baryon number should be unimportant since the energy density will be dominated by the relativistic degrees of freedom (neutrinos, electrons or positrons and photons). Thus, when we use the term ‘‘mirror matter’’ below, we will be referring to the ‘‘light’’ mirror particles, that is the mirror electrons or positrons, mirror photons and mirror neutrinos, since these are the mirror particles which affect the expansion rate of the *early* universe.

We now discuss the quantum kinetic equations (QKEs) for a two-flavor subsystem consisting of an ordinary neutrino ν_α and a mirror neutrino ν'_β . We will not, in this work, provide an exhaustive discussion of the derivation of the QKEs or their meaning, since this territory is well covered in previous papers [29,38–40]. We will, however, provide a complete discussion of the special features mirror neutrinos bring to the QKEs (by contrast to strictly sterile neutrinos). Note that two-flavor subsystems will be used as building blocks for the full six-flavor system in a later section.

We will focus on evolution during the temperature regime $m_e \lesssim T \lesssim m_\mu$. The plasma therefore consists of (i) the relativistic ordinary particles $\nu_e, \bar{\nu}_e, \nu_\mu, \bar{\nu}_\mu, \nu_\tau, \bar{\nu}_\tau, e^-, e^+$ and γ , (ii) the nonrelativistic ordinary protons and neutrons (and the nonrelativistic mirror protons and neutrons discussed above), and (iii) whatever amount of mirror matter gets created through ordinary-mirror neutrino oscillations. The character of the mirror matter in the plasma depends on how much of it is created through oscillations. If a sufficiently tiny amount is created, then the mirror electromagnetic and mirror weak interactions among the mirror neutrinos will take place at a rate that is smaller than the expansion rate of the universe. In this case, the mirror neutrino distributions will not be of Fermi-Dirac form, and mirror electrons, positrons and photons will not be created. When the amount of mirror matter exceeds a certain level, mirror electromagnetic and mirror weak interactions among the mirror neutrinos become larger than the expansion rate. In this case, the mirror neutrinos produced through oscillations quickly assume a distribution of Fermi-Dirac form, and equilibrium distributions of mirror electrons, mirror positrons and mirror photons get excited in the plasma. The full plasma thus consists of two weakly coupled thermodynamic systems: the aforementioned ordinary particles at temperature T and the corresponding mirror particles at a smaller temperature T' . For the case where mirror species contribute negligibly to the expansion rate of the universe, we have earlier shown [32] that the inequality

$$T' \gtrsim 2 \left(\frac{T}{\text{MeV}} \right)^{2/5} \text{ MeV} \quad (14)$$

must be obeyed to ensure that the mirror self-interactions are sufficiently fast to thermally equilibrate the mirror species.

⁸By ‘‘early’’ we mean the time during and earlier than the BBN epoch.

Our notation and convention for ordinary-mirror neutrino two state mixing are as follows. The weak eigenstates ν_α and ν'_β are linear combinations of two mass eigenstates ν_a and ν_b ,

$$\begin{aligned}\nu_\alpha &= \cos \theta_{\alpha\beta'} \nu_a + \sin \theta_{\alpha\beta'} \nu_b, \\ \nu'_\beta &= -\sin \theta_{\alpha\beta'} \nu_a + \cos \theta_{\alpha\beta'} \nu_b,\end{aligned}\quad (15)$$

where $\theta_{\alpha\beta'}$ is the vacuum mixing angle. We define $\theta_{\alpha\beta'}$ so that $\cos 2\theta_{\alpha\beta'} > 0$ and we adopt the convention that $\delta m_{\alpha\beta'}^2 \equiv m_b^2 - m_a^2$.

Recall that the α -type neutrino asymmetry is defined by

$$L_{\nu_\alpha} \equiv \frac{n_{\nu_\alpha} - n_{\bar{\nu}_\alpha}}{n_\gamma}.\quad (16)$$

We also need to define an α -type mirror neutrino asymmetry,

$$L_{\nu'_\alpha} \equiv \frac{n_{\nu'_\alpha} - n_{\bar{\nu}'_\alpha}}{n_\gamma},\quad (17)$$

In the above equation, n_γ is the number density of *ordinary* photons.

Note that when we refer to ‘‘neutrinos,’’ sometimes we will mean neutrinos and/or antineutrinos and/or mirror neutrinos and/or mirror anti-neutrinos. We hope the correct meaning will be clear from the context.

The evolution of the ensemble of ν_α and ν'_β neutrinos is described by a density matrix $\rho_{\alpha\beta'}$ which obeys the QKEs. A similar density matrix $\bar{\rho}_{\alpha\beta'}$ describes the antineutrinos. These density matrices [38,40] are conveniently parametrized by

$$\begin{aligned}\rho_{\alpha\beta'}(p) &= \frac{1}{2} [P_0(p)I + \mathbf{P}(p) \cdot \boldsymbol{\sigma}], \\ \bar{\rho}_{\alpha\beta'}(p) &= \frac{1}{2} [\bar{P}_0(p)I + \bar{\mathbf{P}}(p) \cdot \boldsymbol{\sigma}],\end{aligned}\quad (18)$$

where I is the 2×2 identity matrix, the ‘‘polarization vector’’ $\mathbf{P}(p) = P_x(p)\hat{\mathbf{x}} + P_y(p)\hat{\mathbf{y}} + P_z(p)\hat{\mathbf{z}}$ and $\boldsymbol{\sigma} = \sigma_x\hat{\mathbf{x}} + \sigma_y\hat{\mathbf{y}} + \sigma_z\hat{\mathbf{z}}$, with σ_i being the Pauli matrices.⁹

The quantity p is the magnitude of the neutrino 3-momentum or energy. It will be understood that the density matrices and the quantities $P_i(p)$ also depend on time t or, equivalently, temperature T . (For the situation of negligible mirror energy density, the time-temperature relation for $m_e \lesssim T \lesssim m_\mu$ is $dt/dT = -M_p/5.5T^3$, where $M_p \approx 1.22 \times 10^{22}$ MeV is the Planck mass).

We will normalize the density matrices so that the momentum distributions of $\nu_\alpha(p)$ and $\nu'_\beta(p)$ are given by

$$N_{\nu_\alpha}(p) = \frac{1}{2} [P_0(p) + P_z(p)] N^{\text{eq}}(p, T, 0),$$

$$N_{\nu'_\beta}(p) = \frac{1}{2} [P_0(p) - P_z(p)] N^{\text{eq}}(p, T, 0),\quad (19)$$

where

$$N^{\text{eq}}(p, T, \mu) \equiv \frac{1}{2\pi^2} \frac{p^2}{1 + \exp\left(\frac{p - \mu}{T}\right)}\quad (20)$$

is the Fermi-Dirac distribution with chemical potential μ and temperature T . Note that P_0 is related to the total number of ν_α 's and ν'_β 's of momentum p ,

$$P_0(p) = \frac{N_{\nu_\alpha}(p) + N_{\nu'_\beta}(p)}{N^{\text{eq}}(p, T, 0)},\quad (21)$$

while $P_z(p)$ is related to the difference,

$$P_z(p) = \frac{N_{\nu_\alpha}(p) - N_{\nu'_\beta}(p)}{N^{\text{eq}}(p, T, 0)}.\quad (22)$$

Similar expressions pertain to antineutrinos. The ‘‘transverse’’ components $P_{x,y}(p)$ and $\bar{P}_{x,y}(p)$ measure the degree of quantal coherence in the ensemble. Note that in subsequent expressions we will suppress the independent variables for notational clarity unless there is a chance of confusion.

The time evolution of P_0 and \mathbf{P} is governed by three effects: coherent $\nu_\alpha \leftrightarrow \nu'_\beta$ oscillations, decoherence inducing collisions, and repopulation of ν_α and ν'_β states from the background plasma. These effects are incorporated in the quantum kinetic equations [40,29]

$$\begin{aligned}\frac{\partial \mathbf{P}}{\partial t} &= \frac{\partial \mathbf{P}}{\partial t} \Big|_{\nu_\alpha \leftrightarrow \nu'_\beta} + \frac{\partial \mathbf{P}}{\partial t} \Big|_{\text{coll}} + \frac{\partial \mathbf{P}}{\partial t} \Big|_{\text{repop}}, \\ \frac{\partial P_0}{\partial t} &= \frac{\partial P_0}{\partial t} \Big|_{\nu_\alpha \leftrightarrow \nu'_\beta} + \frac{\partial P_0}{\partial t} \Big|_{\text{coll}} + \frac{\partial P_0}{\partial t} \Big|_{\text{repop}},\end{aligned}\quad (23)$$

where

$$\begin{aligned}\frac{\partial \mathbf{P}}{\partial t} \Big|_{\nu_\alpha \leftrightarrow \nu'_\beta} &= \mathbf{V}_{\alpha\beta'} \times \mathbf{P}, \\ \frac{\partial \mathbf{P}}{\partial t} \Big|_{\text{coll}} &= -D\mathbf{P}_T \quad \text{where } \mathbf{P}_T \equiv P_x\hat{\mathbf{x}} + P_y\hat{\mathbf{y}}, \\ \frac{\partial \mathbf{P}}{\partial t} \Big|_{\text{repop}} &= (R_{\nu_\alpha} - R_{\nu'_\beta})\hat{\mathbf{z}},\end{aligned}\quad (24)$$

and

⁹Note that our previous papers used a different definition of \mathbf{P} through the equation $\rho = \frac{1}{2} P_0(p) [I + \mathbf{P}(p) \cdot \boldsymbol{\sigma}]$ rather than Eq. (18). The difference is just a matter of convention.

$$\left. \frac{\partial P_0}{\partial t} \right|_{\nu_\alpha \leftrightarrow \nu'_\beta} = 0, \quad \left. \frac{\partial P_0}{\partial t} \right|_{\text{coll}} = 0, \quad \left. \frac{\partial P_0}{\partial t} \right|_{\text{repop}} = R_{\nu_\alpha} + R_{\nu'_\beta}. \quad (25)$$

We will explicitly define the new terms appearing above shortly. But before doing so, we remark that the general form of the above equations is reasonably easy to understand. The $\mathbf{V} \times \mathbf{P}$ term leads to the precession of the polarization vector without change in its length. The $-D\mathbf{P}_T$ decoherence term causes P_x and P_y to decrease in length ($D > 0$), which quantifies the rate of loss of quantal coherence. The function $R_i(p)$ is related to the repopulation rate for a particle of species i with momentum p . The functions $P_{x,y}$ are unaffected by repopulation because they measure quantal coherence only. On the other hand, P_z , being proportional to the difference in the momentum distributions of the two neutrino flavors as per Eq. (22), receives a contribution proportional to the difference in the repopulation rates. The function P_0 obviously remains unchanged under $\nu_\alpha \leftrightarrow \nu'_\beta$ oscillations, and it plays no role in quantifying loss of coherence. Since it is related to the sum of momentum distributions as per Eq. (21), its time derivative from repopulation is related to the sum of the repopulation rates.

Similar equations are satisfied for the antineutrino functions \bar{P}_0 and $\bar{\mathbf{P}}$, with the substitutions

$$\mathbf{V}_{\alpha\beta'} \rightarrow \bar{\mathbf{V}}_{\alpha\beta'}, \quad D \rightarrow \bar{D}, \quad R_i \rightarrow \bar{R}_i. \quad (26)$$

We now explicitly define the terms appearing in these equations.

The function $\mathbf{V}_{\alpha\beta'}$, which is related to the effective matter potential, drives the coherent aspect of the evolution of the density matrix. Importantly, $\mathbf{V}_{\alpha\beta'}$ depends on the neutrino and mirror neutrino asymmetries. It is given by [38,40]

$$\mathbf{V}_{\alpha\beta'} = \beta \hat{\mathbf{x}} + \lambda \hat{\mathbf{z}}, \quad (27)$$

where β and λ are

$$\beta(p) = \frac{\delta m_{\alpha\beta'}^2}{2p} \sin 2\theta_{\alpha\beta'},$$

$$\lambda(p) = -\frac{\delta m_{\alpha\beta'}^2}{2p} [\cos 2\theta_{\alpha\beta'} - b(p) \pm a(p)], \quad (28)$$

in which the $+$ ($-$) sign corresponds to neutrino (antineutrino) oscillations. The dimensionless variables $a(p)$ and $b(p)$ contain the matter effects [41], being the matter potential divided by $\delta m_{\alpha\beta'}^2/2p$. For $\nu_\alpha \leftrightarrow \nu'_\beta$ oscillations $a(p)$ and $b(p)$ are given by [42]

$$a(p) \equiv -\frac{4\zeta(3)\sqrt{2}G_F T^3 L^{(\alpha\beta')} p}{\pi^2 \delta m_{\alpha\beta'}^2},$$

$$b(p) \equiv -\frac{4\zeta(3)\sqrt{2}G_F T^4 A_\alpha p^2}{\pi^2 \delta m_{\alpha\beta'}^2 M_W^2}, \quad (29)$$

where $\zeta(3) \approx 1.202$ is the Riemann zeta function of 3, G_F is the Fermi constant, M_W is the W -boson mass, $A_e \approx 17$ and $A_{\mu,\tau} \approx 4.9$ (for $m_e \lesssim T \lesssim m_\mu$). The expression for $b(p)$ is valid provided that the plasma has a negligible component of mirror energy density. The quantity $L^{(\alpha\beta')}$ is given by

$$L^{(\alpha\beta')} = L^{(\alpha)} - L'^{(\beta)}, \quad (30)$$

where

$$L^{(\alpha)} = L_{\nu_\alpha} + L_{\nu_e} + L_{\nu_\mu} + L_{\nu_\tau} + \eta,$$

$$L'^{(\beta)} = L_{\nu'_\beta} + L_{\nu'_e} + L_{\nu'_\mu} + L_{\nu'_\tau} + \eta'. \quad (31)$$

Recall that the term η is due to the asymmetry of the electrons and nucleons and is expected to be very small, $\eta \sim 5 \times 10^{-10}$. The mirror analogue, η' , will also be taken to be very small. For antineutrinos, the corresponding function $\bar{V}_{\alpha\beta'}$ is obtained by the substitution $L^{(\alpha\beta')} \rightarrow -L^{(\alpha\beta')}$. The MSW resonance conditions are given by

$$\lambda(p_{\text{res}}) = 0, \quad (32)$$

where p_{res} is the resonance momentum.

The term $D(p)$ is the decoherence or damping function. When the number density of mirror species is much less than the number density of ordinary species, it is given by [39]

$$D(p) \approx \frac{\Gamma(p)}{2}, \quad (33)$$

where $\Gamma(p)$ is the total collision rate of a ν_α neutrino of momentum p with the background plasma.¹⁰ From Refs. [29,43] it is given by

$$\Gamma(p) = y_\alpha G_F^2 T^5 \left(\frac{p}{\langle p \rangle} \right), \quad (34)$$

where $\langle p \rangle \approx 3.15T$ is the average momentum of the ordinary neutrinos, $y_e \approx 4.0$ and $y_{\mu,\tau} \approx 2.9$ (for the $m_e \lesssim T \lesssim m_\mu$ epoch we are considering). The total collision rate for a ν'_β mirror neutrino of momentum p is, roughly,

$$\Gamma'(p) \approx \begin{cases} \left(\frac{T'}{T} \right)^4 \Gamma(p) & \text{if } T' \text{ obeys Eq. (14),} \\ 0 & \text{otherwise.} \end{cases} \quad (35)$$

In the presence of neutrino asymmetries, the collision rates for neutrinos and antineutrinos differ. The collision rates quoted above hold when the asymmetries are small, with the antineutrino rate being approximately equal to the neutrino rate in that limit. Note that in the parameter space regime we are considering, neutrino asymmetries do not become large until temperatures are sufficiently low that collisions can be

¹⁰If the number density of mirror species is significant, $D(p)$ must also include the collision rate of ν'_β 's with the background mirror particles.

approximately neglected. Therefore, the dependence of the collision rates on the neutrino asymmetries is never of practical importance.

The repopulation functions R_{ν_α} and $R_{\nu'_\beta}$ are given by

$$\begin{aligned} R_{\nu_\alpha} &\approx \Gamma \left[K_{\nu_\alpha} - \frac{1}{2}(P_0 + P_z) \right], \\ R_{\nu'_\beta} &\approx \Gamma' \left[K_{\nu'_\beta} - \frac{1}{2}(P_0 - P_z) \right], \end{aligned} \quad (36)$$

where

$$\begin{aligned} K_{\nu_\alpha}(p) &\equiv \frac{N^{\text{eq}}(p, T, \mu_{\nu_\alpha})}{N^{\text{eq}}(p, T, 0)}, \\ K_{\nu'_\beta}(p) &\equiv \frac{N^{\text{eq}}(p, T', \mu_{\nu'_\beta})}{N^{\text{eq}}(p, T, 0)}, \end{aligned} \quad (37)$$

with μ_i being the chemical potential for species i . For antineutrinos, μ_{ν_α} is replaced by $\mu_{\bar{\nu}_\alpha}$ in the above equation. The approximate equality sign in Eq. (36) indicates that the right-hand side is not an exact result. It holds when all species are in thermal equilibrium apart from ν_α and ν'_β , which are instead approximately in equilibrium. [See Ref. [40] for the exact form of Eq. (25).] The two terms R_{ν_α} and $R_{\nu'_\beta}$ are due to the repopulation of ν_α states by ordinary weak interactions, and the repopulation of ν'_β states by mirror weak interactions, respectively.

In order to integrate Eqs. (24) and (25), we need to relate the chemical potentials appearing in Eqs. (36) and (37) to the asymmetries appearing in Eq. (24). In general, for a distribution in thermal equilibrium,

$$L_{\nu_\alpha} = \frac{1}{4\zeta(3)} \int_0^\infty \frac{x^2 dx}{1 + e^{x - \tilde{\mu}_\alpha}} - \frac{1}{4\zeta(3)} \int_0^\infty \frac{x^2 dx}{1 + e^{x - \tilde{\mu}_\alpha^-}}, \quad (38)$$

where $\tilde{\mu}_\alpha \equiv \mu_{\nu_\alpha}/T$ and $\tilde{\mu}_\alpha^- \equiv \mu_{\bar{\nu}_\alpha}/T$. Expanding out the above equation,

$$L_{\nu_\alpha} \approx \frac{1}{24\zeta(3)} [\pi^2(\tilde{\mu}_\alpha - \tilde{\mu}_\alpha^-) + 6(\tilde{\mu}_\alpha^2 - \tilde{\mu}_\alpha^{-2}) \ln 2 + (\tilde{\mu}_\alpha^3 - \tilde{\mu}_\alpha^{-3})]. \quad (39)$$

This is an exact equation for $\tilde{\mu}_\alpha = -\tilde{\mu}_\alpha^-$; otherwise it holds to a good approximation provided that $\tilde{\mu}_\alpha, \tilde{\mu}_\alpha^- \lesssim 1$. For $T \gtrsim T_{\text{dec}}^\alpha$, where $T_{\text{dec}}^e \approx 2.5$ MeV and $T_{\text{dec}}^{\mu, \tau} \approx 3.5$ MeV are the chemical decoupling temperatures, $\mu_{\nu_\alpha} \approx -\mu_{\bar{\nu}_\alpha}$ because inelastic processes such as $\nu_\alpha \bar{\nu}_\alpha \leftrightarrow e^+ e^-$ and $e^+ e^- \leftrightarrow \gamma \gamma$ are rapid enough to make $\tilde{\mu}_\alpha + \tilde{\mu}_\alpha^- \approx \tilde{\mu}_{e^+} + \tilde{\mu}_{e^-} \approx 0$. However, for $1 \text{ MeV} \lesssim T \lesssim T_{\text{dec}}^\alpha$, weak interactions are rapid enough to approximately thermalize the neutrino momentum distributions, but not rapid enough to keep the neutrinos in chemical

equilibrium.¹¹ In this case, the value of $\tilde{\mu}_\alpha$ is approximately frozen at $T \approx T_{\text{dec}}^\alpha$ (taking for definiteness $L_{\nu_\alpha} > 0$), while the anti-neutrino chemical potential $\tilde{\mu}_\alpha^-$ continues evolving until $T \approx 1$ MeV. For $T \lesssim 1$ MeV, the exact form for the right-hand side of Eq. (25) should be used.

The neutrino asymmetries that appear in λ , R and their antineutrino analogues are in principle calculated from the density matrices. Recall that the neutrino asymmetry is defined in Eq. (16). The number density of ν_α is

$$n_{\nu_\alpha} = \int_0^\infty N_{\nu_\alpha} dp = \int_0^\infty \frac{1}{2} (P_0 + P_z) N^{\text{eq}}(p, T, 0) dp, \quad (40)$$

so that

$$L_{\nu_\alpha} = \frac{1}{2n_\gamma} \int_0^\infty [(P_0 + P_z) - (\bar{P}_0 + \bar{P}_z)] N^{\text{eq}}(p, T, 0) dp. \quad (41)$$

Although it is in a strict technical sense redundant, it is useful to derive an equation for the rate of change of lepton number. It is given by

$$\frac{dL_{\nu_\alpha}}{dt} = \frac{d}{dt} \left(\frac{n_{\nu_\alpha} - n_{\bar{\nu}_\alpha}}{n_\gamma} \right). \quad (42)$$

Thus, using Eq. (19),

$$\frac{dL_{\nu_\alpha}}{dt} = \frac{1}{2n_\gamma} \int_0^\infty \left[\frac{\partial P_0}{\partial t} + \frac{\partial P_z}{\partial t} - \frac{\partial \bar{P}_0}{\partial t} - \frac{\partial \bar{P}_z}{\partial t} \right] N^{\text{eq}}(p, T, 0) dp. \quad (43)$$

This equation can be further simplified using the QKEs and the fact that the repopulation does not directly affect the lepton number to obtain

$$\frac{dL_{\nu_\alpha}}{dt} = \frac{1}{2n_\gamma} \int_0^\infty \beta (P_y - \bar{P}_y) N^{\text{eq}}(p, T, 0) dp. \quad (44)$$

In our numerical work, this equation is the one actually used to calculate the lepton number that appears in the QKEs. Note for future reference that a limiting case of these equations will take center stage when we come to study the Low temperature epoch.

The last piece of information needed is the evolution equation for the mirror sector temperature T' . This is obtained by using a conservation of energy argument that was first presented in Ref. [32]. It goes as follows: Consider $\nu_\alpha \rightarrow \nu'_\beta$ oscillations with the mirror interactions felt by ν'_β artificially switched off. The energy density of the ν'_β and $\bar{\nu}'_\beta$ states is then given by

¹¹The chemical and thermal decoupling temperatures are so different because the inelastic collision rates are much less than the elastic collision rates. See, for example, Ref. [43] for a list of the collision rates.

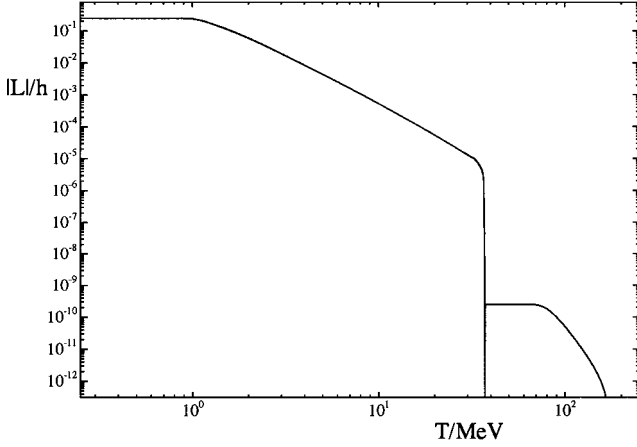


FIG. 1. $|L_{\nu_\tau}|/h$ (where $h \equiv T_\nu^3/T_\gamma^3$) versus temperature for $\nu_\tau \leftrightarrow \nu'_\mu$ oscillations with $\delta m^2 = -50$ eV² and $\sin^2 2\theta = 10^{-8}$.

$$\begin{aligned} \rho_{\nu'_\beta} &= \int_0^\infty (N_{\nu'_\beta} + N_{\bar{\nu}'_\beta}) p dp \\ &= \frac{1}{2} \int_0^\infty (P_0 - P_z + \bar{P}_0 - \bar{P}_z) p N^{\text{eq}}(p, T, 0) dp. \end{aligned} \quad (45)$$

Now switch on the mirror self-interactions. They will quickly distribute this energy density among all of the relevant mirror species: the three mirror neutrinos and antineutrinos, the mirror electrons and positrons, and the mirror photon. However, the energy density that is being fed into the mirror sector by ordinary-mirror oscillations is still given by the right-hand side of Eq. (45). The rate at which energy density is being transferred from the ordinary to the mirror sector is therefore equal to the time rate of change of the right-hand side of Eq. (45) due to *oscillations only*. Therefore we conclude that

$$\begin{aligned} \left. \frac{d\rho'}{dt} \right|_{\nu_\alpha \leftrightarrow \nu'_\beta} &= \frac{1}{2} \int_0^\infty \left. \frac{\partial}{\partial t} \right|_{\nu_\alpha \leftrightarrow \nu'_\beta} \\ &\quad \times (P_0 - P_z + \bar{P}_0 - \bar{P}_z) p N^{\text{eq}}(p, T, 0) dp \end{aligned} \quad (46)$$

where $\rho' \equiv 3\rho_{\nu'_\beta} + \rho_{e'} + \rho_{\gamma'}$ is the total energy density in mirror species. The complete evolution equation for T' is obtained by combining Eq. (46) with the cosmological redshifting of T' . To this end, consider the quantity γ_ρ where

$$\gamma_\rho \equiv \frac{\rho'}{\rho} = \left(\frac{T'}{T} \right)^4, \quad (47)$$

with $\rho = \frac{43}{4} (\pi^2/30) T^4$ being the total energy density due to ordinary species. This ratio of energy densities does not redshift. Its total rate of change can therefore be calculated from Eqs. (46), (24) and (25) to yield

$$\frac{d\gamma_\rho}{dt} \simeq -\frac{1}{2\rho} \int_0^\infty \beta (P_y + \bar{P}_y) p N^{\text{eq}}(p, T, 0) dp, \quad (48)$$

which is the required evolution equation for T' . Note that we implicitly assumed in the above derivation that the redistribution of mirror energy density from ν'_β 's to the other mirror species did not affect the expansion rate of the universe. This is a good approximation provided that the mirror energy density is small, that is $\gamma_\rho \ll 1$. This is generally expected to be the case since $\delta N_{\nu, \text{eff}} \leq 0.6 \Rightarrow \gamma_\rho \leq 0.1$.

We end this section with an example of the evolution of neutrino asymmetry generated by two flavor ordinary-mirror neutrino oscillations. In Fig. 1 the evolution of the τ -like asymmetry is plotted. For our present illustrative purpose, we have considered the evolution of L_{ν_τ} under the influence of the $\nu_\tau - \nu'_\mu$ oscillation mode only. The parameter point $\delta m^2_{\tau\mu'} = -50$ eV² and $\sin^2 2\theta_{\tau\mu'} = 10^{-8}$ has been chosen. The initial L_{ν_τ} is set to zero. Notice that L_{ν_τ} evolves from zero to a value which approximately cancels the baryon asymmetry by $T \approx 70$ MeV. The asymmetry then remains constant until the critical temperature $T_c \approx 38$ MeV when explosive growth begins. Shortly thereafter, the explosive growth phase gives way to power law T^{-4} growth. During the power law phase, the high temperature epoch evolves into the low temperature epoch. Of course the behavior shown in Fig. 1 is quite general and in fact quite similar to ordinary-sterile neutrino oscillations. The latter have already been studied in some detail in previous papers [24–26, 28, 29]. Finally note that we have plotted $|L_{\nu_\tau}|$. This is because L_{ν_τ} changes sign at the critical temperature (the reason for this behavior has been discussed in Ref. [25]). For values of $\sin^2 2\theta$ large enough, our numerical results indicate that the sign of L_{ν_τ} initially oscillates and thus the final sign of the asymmetry may be random. This may lead to different regions of space having different neutrino asymmetries (as suggested earlier in Ref. [24]). Also it should be mentioned that the effect of statistical fluctuations on lepton number asymmetry is an important open problem, and consequently it is also possible that the sign of the asymmetry may turn out to be random even for small values of $\sin^2 2\theta$. For the purposes of the present paper, we acknowledge the indeterminate nature of the asymmetry by considering the two possible signs in all our numerical work.

In the next section we will discuss the high temperature epoch in the EPM. Our main goal there will be to demonstrate the consistency of the $\nu_\mu \rightarrow \nu'_\mu$ solution to the atmospheric neutrino problem with BBN for a range of parameters.

IV. HIGH TEMPERATURE EPOCH: CONSISTENCY OF THE $\nu_\mu \rightarrow \nu'_\mu$ SOLUTION OF THE ATMOSPHERIC NEUTRINO ANOMALY WITH BBN

Previous work has shown that the QKEs for ordinary-mirror (or ordinary-sterile) oscillations will imply the explosive creation of neutrino asymmetries provided some fairly mild restrictions on the oscillation parameter space are imposed. In particular, the $\delta m^2_{\alpha\beta'}$ involved must be negative, and the vacuum mixing angle $\theta_{\alpha\beta'}$ must be in the approximate range

$$10^{-10} \lesssim \sin^2 2\theta_{\alpha\beta'} \lesssim \text{few} \times 10^{-4} \left(\frac{\text{eV}^2}{|\delta m_{\alpha\beta'}^2|} \right)^{1/2}. \quad (49)$$

The lower bound comes from the requirement that the oscillation mode be sufficiently strong,¹² while the upper bound was derived in Ref. [32] from the requirement that $\nu_\alpha \rightarrow \nu'_\beta$ oscillations, considered in isolation, not spoil BBN [Eq. (49) takes for definiteness that $\delta N_{\nu, \text{eff}} \lesssim 0.6$]. Once created, the large neutrino asymmetry or asymmetries will suppress other ordinary-sterile oscillation modes for a range of parameters.

For the generic parameter space region considered here (see Sec. II), the oscillation modes

$$\nu_\tau \rightarrow \nu'_\mu, \quad \nu_\tau \rightarrow \nu'_e, \quad \nu_\mu \rightarrow \nu'_e \quad (50)$$

could all satisfy the above criteria. We will call these the ‘‘lepton number creating modes.’’ The other oscillation modes, including the $\nu_\mu \rightarrow \nu'_\mu$ mode that hypothetically solves the atmospheric neutrino problem, tend to destroy a linear combination of asymmetries.

Lepton number amplification begins at a critical temperature T_c , given roughly by

$$T_c \approx 16 \left(-\frac{\delta m^2 \cos 2\theta}{\text{eV}^2} \right)^{1/6} \text{ MeV}, \quad (51)$$

where the oscillation parameters pertain to the two-flavor lepton number creating mode responsible. The mode with the largest $|\delta m^2|$ will therefore be expected to create lepton number first, provided its vacuum mixing angle is in the range of Eq. (49). Within the scenario of Sec. II, the $\nu_\tau \rightarrow \nu'_\mu$ and $\nu_\tau \rightarrow \nu'_e$ modes will have the largest δm^2 values. Which, if either, of them dominates lepton number creation depends on their specific oscillation parameters. For the sake of a plausible example, we will suppose that $\nu_\tau \rightarrow \nu'_\mu$ dominates, even though $\nu_\tau \rightarrow \nu'_e$ has a slightly larger δm^2 . This is because we expect $\theta_{\tau e'} \ll \theta_{\tau \mu'}$, as per Sec. II. Basically, we will work in the parameter space region where $\theta_{\tau e'}$ is negligibly tiny.

So we are led to consider the four flavor subsystem

$$\begin{array}{c} \nu_\mu \leftrightarrow \nu'_\mu \\ \updownarrow \quad \boxtimes \quad \updownarrow \\ \nu_\tau \leftrightarrow \nu'_\tau \end{array} \quad (52)$$

Further, we decompose this four flavor system into the two flavor subsystems indicated by the arrows above. Some discussion of the justification for this sort of decomposition can be found in Ref. [29]. Heuristically, it is expected that this simplifying assumption is justified because the MSW resonance momenta of each of the oscillation modes are generally different. The ordinary-ordinary and mirror-mirror modes are governed by the same mixing angle $\theta_{\mu\tau}$, and the

modes $\nu_\tau \rightarrow \nu'_\mu$ and $\nu_\mu \rightarrow \nu'_\tau$ are both governed by another mixing angle $\theta_{\tau\mu'}$, while the $\nu_{\tau,\mu} \rightarrow \nu'_{\tau,\mu}$ modes are maximally mixed. The squared mass difference $\delta m_{\mu\mu'}^2$ is set by the atmospheric neutrino data to be in the range quoted in Eq. (7). The other mass parameters, $\delta m_{\tau\mu'}^2$ and $\delta m_{\tau\tau'}^2$, are free, subject to the restrictions discussed in Sec. II and summarized in Eq. (7).

For simplicity and the sake of the example, we will set $|\delta m_{\tau\tau'}^2|$ to be so small that the associated oscillation mode can be neglected.¹³ The precise value of the mixing angle $\theta_{\mu\tau}$ is unimportant, provided it is small. The $\nu_\mu \leftrightarrow \nu_\tau$ mode has almost no effect until lepton number is large (here ‘‘large’’ means greater than about 10^{-2}), because of the approximately equal number densities of the two species involved. In the high temperature epoch being considered in this section, lepton number will always be small. For a given $\delta m_{\mu\mu'}^2$ we are therefore effectively left with two free parameters: $\theta_{\tau\mu'}$ and $\delta m_{\tau\mu'}^2$. Our task is to find the region of this parameter space for which the $\nu_\mu \rightarrow \nu'_\mu$ solution to the atmospheric neutrino problem is consistent with BBN. For the EPM,¹⁴ this calculation was first performed in Ref. [32] within the static approximation. We improve on this approach here through the use of the QKEs.

We now write down the equations we must solve. We begin by introducing three two-flavor density matrices

$$\begin{aligned} \rho_{\tau\mu'} &\equiv \frac{1}{2}(P_0 + \sigma \cdot \mathbf{P}), & \rho_{\mu\mu'} &\equiv \frac{1}{2}(Q_0 + \sigma \cdot \mathbf{Q}), \\ \rho_{\mu\tau'} &\equiv \frac{1}{2}(S_0 + \sigma \cdot \mathbf{S}), \end{aligned} \quad (53)$$

for the three significant oscillation modes

$$\nu_\tau \leftrightarrow \nu'_\mu, \quad \nu_\mu \leftrightarrow \nu'_\mu, \quad \nu_\mu \leftrightarrow \nu'_\tau, \quad (54)$$

respectively. Since ν'_μ is common to the first pair of modes, and ν_μ is common to the second pair, we have the constraints

$$\begin{aligned} \frac{N_{\nu'_\mu}}{N^{\text{eq}}(p, T, 0)} &= \frac{1}{2}(P_0 - P_z) = \frac{1}{2}(Q_0 - Q_z), \\ \frac{N_{\nu_\mu}}{N^{\text{eq}}(p, T, 0)} &= \frac{1}{2}(Q_0 + Q_z) = \frac{1}{2}(S_0 + S_z). \end{aligned} \quad (55)$$

Extending the two flavor case discussed in the previous section, the time derivatives of the functions $P_0, Q_0, S_0, \mathbf{P}, \mathbf{Q}$

¹³This will be the case provided that $|\delta m_{\tau\tau'}^2| \leq |\delta m_{\mu\mu'}^2|$. If $|\delta m_{\tau\tau'}^2|$ is much larger than $|\delta m_{\mu\mu'}^2|$, then the resulting ‘‘allowed region’’ will be significantly reduced.

¹⁴For the case of strictly sterile neutrinos, this calculation was done in the static approximation in Ref. [25] and by numerically integrating the quantum kinetic equations in Ref. [28].

¹²But note that the vacuum oscillation amplitude can still be tiny.

and \mathbf{S} are observed to receive contributions from each of the three oscillation modes, from decohering collisions, and from repopulation. Denoting a generic function by F , we have that

$$\frac{\partial F}{\partial t} = \frac{\partial F}{\partial t} \Big|_{\nu_\tau \rightarrow \nu'_\mu} + \frac{\partial F}{\partial t} \Big|_{\nu_\mu \rightarrow \nu'_\mu} + \frac{\partial F}{\partial t} \Big|_{\nu_\mu \rightarrow \nu'_\tau} + \frac{\partial F}{\partial t} \Big|_{\text{coll}} + \frac{\partial F}{\partial t} \Big|_{\text{repop}}. \quad (56)$$

From the two-flavor formalism described in Sec. III we have that

$$\begin{aligned} \frac{\partial \mathbf{P}}{\partial t} \Big|_{\nu_\tau \rightarrow \nu'_\mu} + \frac{\partial \mathbf{P}}{\partial t} \Big|_{\text{coll}} &= \mathbf{V}_{\tau\mu'} \times \mathbf{P} - D\mathbf{P}_T, \\ \frac{\partial \mathbf{Q}}{\partial t} \Big|_{\nu_\mu \rightarrow \nu'_\mu} + \frac{\partial \mathbf{Q}}{\partial t} \Big|_{\text{coll}} &= \mathbf{V}_{\mu\mu'} \times \mathbf{Q} - D\mathbf{Q}_T, \\ \frac{\partial \mathbf{S}}{\partial t} \Big|_{\nu_\mu \rightarrow \nu'_\tau} + \frac{\partial \mathbf{S}}{\partial t} \Big|_{\text{coll}} &= \mathbf{V}_{\mu\tau'} \times \mathbf{S} - D\mathbf{S}_T. \end{aligned} \quad (57)$$

It is also clear that

$$\begin{aligned} \frac{\partial P_0}{\partial t} \Big|_{\nu_\tau \rightarrow \nu'_\mu} &= \frac{\partial P_0}{\partial t} \Big|_{\text{coll}} = 0, \\ \frac{\partial Q_0}{\partial t} \Big|_{\nu_\mu \rightarrow \nu'_\mu} &= \frac{\partial Q_0}{\partial t} \Big|_{\text{coll}} = 0, \\ \frac{\partial S_0}{\partial t} \Big|_{\nu_\mu \rightarrow \nu'_\tau} &= \frac{\partial S_0}{\partial t} \Big|_{\text{coll}} = 0. \end{aligned} \quad (58)$$

We also obviously know that

$$\begin{aligned} \frac{\partial \mathbf{P}}{\partial t} \Big|_{\nu_\mu \rightarrow \nu'_\tau} &= \frac{\partial P_0}{\partial t} \Big|_{\nu_\mu \rightarrow \nu'_\tau} = 0, \\ \frac{\partial \mathbf{S}}{\partial t} \Big|_{\nu_\tau \rightarrow \nu'_\mu} &= \frac{\partial S_0}{\partial t} \Big|_{\nu_\tau \rightarrow \nu'_\mu} = 0. \end{aligned} \quad (59)$$

Consider now the contribution of $\nu_\mu \rightarrow \nu'_\mu$ oscillations to the evolution of \mathbf{P} and P_0 . First of all, the transverse components $P_{x,y}$ receive no contribution,

$$\frac{\partial P_{x,y}}{\partial t} \Big|_{\nu_\mu \rightarrow \nu'_\mu} = 0, \quad (60)$$

because they are affected only by decohering collisions. The evolution of P_z and P_0 can be obtained from Eq. (55) by noting that

$$\frac{\partial}{\partial t} (P_0 - P_z) \Big|_{\nu_\mu \rightarrow \nu'_\mu} = \frac{\partial}{\partial t} (Q_0 - Q_z) \Big|_{\nu_\mu \rightarrow \nu'_\mu} = - \frac{\partial Q_z}{\partial t} \Big|_{\nu_\mu \rightarrow \nu'_\mu},$$

$$\frac{\partial}{\partial t} (P_0 + P_z) \Big|_{\nu_\mu \rightarrow \nu'_\mu} = 0, \quad (61)$$

so that

$$\begin{aligned} \frac{\partial P_0}{\partial t} \Big|_{\nu_\mu \rightarrow \nu'_\mu} &= - \frac{1}{2} \frac{\partial Q_z}{\partial t} \Big|_{\nu_\mu \rightarrow \nu'_\mu}, \\ \frac{\partial P_z}{\partial t} \Big|_{\nu_\mu \rightarrow \nu'_\mu} &= + \frac{1}{2} \frac{\partial Q_z}{\partial t} \Big|_{\nu_\mu \rightarrow \nu'_\mu}, \end{aligned} \quad (62)$$

having used Eq. (58). The expression for $(\partial Q_z / \partial t) \Big|_{\nu_\mu \rightarrow \nu'_\mu}$ is obtained from Eq. (57). Finally, we have that

$$\begin{aligned} \frac{\partial P_{x,y}}{\partial t} \Big|_{\text{repop}} &= 0, \\ \frac{\partial}{\partial t} \frac{1}{2} (P_0 + P_z) \Big|_{\text{repop}} &= \Gamma \left[K_{\nu_\tau} - \frac{1}{2} (P_0 + P_z) \right], \\ \frac{\partial}{\partial t} \frac{1}{2} (P_0 - P_z) \Big|_{\text{repop}} &= \Gamma' \left[K_{\nu'_\mu} - \frac{1}{2} (P_0 - P_z) \right]. \end{aligned} \quad (63)$$

This completes the specification of the evolution equations for \mathbf{P} and P_0 .

The evolution of \mathbf{S} and S_0 due to $\nu_\mu \rightarrow \nu'_\mu$ oscillations and repopulation is handled in a very similar manner to yield

$$\begin{aligned} \frac{\partial S_{x,y}}{\partial t} \Big|_{\nu_\mu \rightarrow \nu'_\mu} &= 0, \\ \frac{\partial S_0}{\partial t} \Big|_{\nu_\mu \rightarrow \nu'_\mu} &= + \frac{1}{2} \frac{\partial Q_z}{\partial t} \Big|_{\nu_\mu \rightarrow \nu'_\mu}, \\ \frac{\partial S_z}{\partial t} \Big|_{\nu_\mu \rightarrow \nu'_\mu} &= + \frac{1}{2} \frac{\partial Q_z}{\partial t} \Big|_{\nu_\mu \rightarrow \nu'_\mu}, \end{aligned}$$

$$\frac{\partial S_{x,y}}{\partial t} \Big|_{\text{repop}} = 0,$$

$$\frac{\partial}{\partial t} \frac{1}{2} (S_0 + S_z) \Big|_{\text{repop}} = \Gamma \left[K_{\nu_\mu} - \frac{1}{2} (S_0 + S_z) \right],$$

$$\frac{\partial}{\partial t} \frac{1}{2} (S_0 - S_z) \Big|_{\text{repop}} = \Gamma' \left[K_{\nu'_\tau} - \frac{1}{2} (S_0 - S_z) \right]. \quad (64)$$

This completes the specification of the evolution equations for \mathbf{S} and S_0 .

Finally, we have to specify the time rate of change of \mathbf{Q} and Q_0 under the influence of $\nu_\tau \leftrightarrow \nu'_\mu$ oscillations, $\nu_\mu \leftrightarrow \nu'_\tau$ oscillations and repopulation. We note first that $Q_{x,y}$ are unaffected by these processes:

$$\left. \frac{\partial Q_{x,y}}{\partial t} \right|_{\nu_\tau \rightarrow \nu'_\mu} = \left. \frac{\partial Q_{x,y}}{\partial t} \right|_{\nu_\mu \rightarrow \nu'_\tau} = \left. \frac{\partial Q_{x,y}}{\partial t} \right|_{\text{repop}} = 0. \quad (65)$$

Then, from Eq. (55) we see that

$$\begin{aligned} \left. \frac{\partial Q_0}{\partial t} \right|_{\nu_\tau \rightarrow \nu'_\mu} &= \frac{1}{2} \left. \frac{\partial}{\partial t} (P_0 - P_z) \right|_{\nu_\tau \rightarrow \nu'_\mu} = -\frac{1}{2} \left. \frac{\partial P_z}{\partial t} \right|_{\nu_\tau \rightarrow \nu'_\mu}, \\ \left. \frac{\partial Q_z}{\partial t} \right|_{\nu_\tau \rightarrow \nu'_\mu} &= -\frac{1}{2} \left. \frac{\partial}{\partial t} (P_0 - P_z) \right|_{\nu_\tau \rightarrow \nu'_\mu} = +\frac{1}{2} \left. \frac{\partial P_z}{\partial t} \right|_{\nu_\tau \rightarrow \nu'_\mu}, \\ \left. \frac{\partial Q_0}{\partial t} \right|_{\nu_\mu \rightarrow \nu'_\tau} &= \frac{1}{2} \left. \frac{\partial}{\partial t} (S_0 + S_z) \right|_{\nu_\mu \rightarrow \nu'_\tau} = +\frac{1}{2} \left. \frac{\partial S_z}{\partial t} \right|_{\nu_\mu \rightarrow \nu'_\tau}, \\ \left. \frac{\partial Q_z}{\partial t} \right|_{\nu_\mu \rightarrow \nu'_\tau} &= \frac{1}{2} \left. \frac{\partial}{\partial t} (S_0 + S_z) \right|_{\nu_\mu \rightarrow \nu'_\tau} = +\frac{1}{2} \left. \frac{\partial S_z}{\partial t} \right|_{\nu_\mu \rightarrow \nu'_\tau}. \end{aligned} \quad (66)$$

Finally,

$$\begin{aligned} \left. \frac{\partial}{\partial t} \frac{1}{2} (Q_0 + Q_z) \right|_{\text{repop}} &= \Gamma \left[K_{\nu_\mu} - \frac{1}{2} (Q_0 + Q_z) \right], \\ \left. \frac{\partial}{\partial t} \frac{1}{2} (Q_0 - Q_z) \right|_{\text{repop}} &= \Gamma' \left[K_{\nu'_\mu} - \frac{1}{2} (Q_0 - Q_z) \right] \end{aligned} \quad (67)$$

specify the remaining repopulation equations.

This completes the list of quantum kinetic equations for our system. Of course, because of the constraints in Eq. (55), some of these equations are redundant.

To use these equations one needs (i) equations connecting neutrino asymmetries with chemical potentials and (ii) an evolution equation for the temperature T' of the mirror plasma. The chemical potentials are calculated in exactly the same way as discussed in Sec. III. The T' evolution equation is obtained by extending the two-flavor derivation of Sec. III in the obvious way. As before, it is best to first imagine that the mirror electroweak interactions are artificially switched off. The energy density in mirror states is then entirely due to the ν'_μ and ν'_τ species:

$$\begin{aligned} \rho_{\nu'_\mu} + \rho_{\nu'_\tau} &= \int_0^\infty (N_{\nu'_\mu} + N_{\bar{\nu}'_\mu} + N_{\nu'_\tau} + N_{\bar{\nu}'_\tau}) p dp \\ &= \frac{1}{2} \int_0^\infty (P_0 - P_z + \bar{P}_0 - \bar{P}_z + S_0 \\ &\quad - S_z + \bar{S}_0 - \bar{S}_z) p N^{\text{eq}}(p, T, 0) dp. \end{aligned} \quad (68)$$

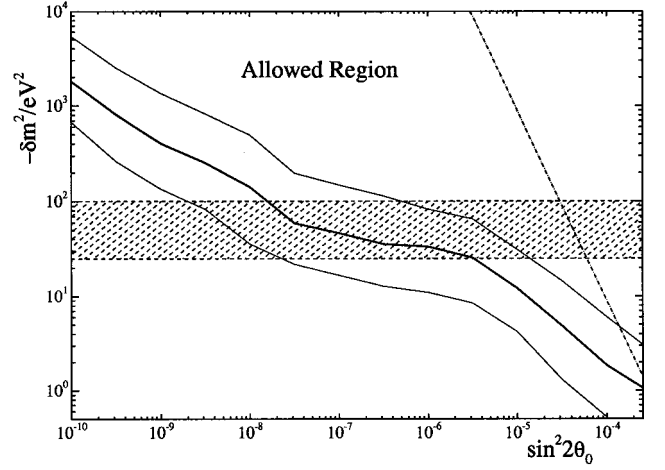


FIG. 2. Region of parameter space in the $\sin^2 2\theta_{\tau\mu'}, -\delta m^2_{\tau\mu'}$ plane where L_{ν_τ} is generated rapidly enough so that the $\nu_\mu \leftrightarrow \nu'_\mu$ oscillations cannot significantly populate the ν'_μ states (for $T \gtrsim 0.4$ MeV). This region, which in the figure is denoted by the “Allowed Region,” includes all of the parameter space above the solid line(s). The top, middle and bottom solid lines correspond to the atmospheric δm^2 values of $\delta m^2_{\mu\mu'}/eV^2 = 10^{-2}$, $10^{-2.5}$ and 10^{-3} , respectively. The dash-dotted line is the nucleosynthesis bound, Eq. (49), which takes $\delta N_{\nu, \text{eff}} \lesssim 0.6$ for definiteness, and the shaded region is the hot dark matter region indicated from some studies of structure formation (see Sec. VI).

With mirror electroweak interactions now switched on, this energy density is distributed among all of the relevant mirror species. The rate at which energy density is being transferred from the ordinary to the mirror sector is thus

$$\begin{aligned} \left. \frac{d\rho'}{dt} \right|_{\text{osc}} &= \frac{1}{2} \int_0^\infty \left. \frac{\partial}{\partial t} \right|_{\text{osc}} (P_0 - P_z + \bar{P}_0 - \bar{P}_z \\ &\quad + S_0 - S_z + \bar{S}_0 - \bar{S}_z) p N^{\text{eq}}(p, T, 0) dp, \end{aligned} \quad (69)$$

where ρ' is the total energy density in mirror species, and

$$\left. \frac{d}{dt} \right|_{\text{osc}} \equiv \left. \frac{d}{dt} \right|_{\nu_\tau \rightarrow \nu'_\mu} + \left. \frac{d}{dt} \right|_{\nu_\mu \rightarrow \nu'_\tau} + \left. \frac{d}{dt} \right|_{\nu'_\mu \rightarrow \nu'_\mu}. \quad (70)$$

Introducing γ_p as per Eq. (47) and using the QKEs we obtain

$$\begin{aligned} \frac{d\gamma_p}{dt} &= -\frac{1}{2\rho} \int_0^\infty [\beta_{\tau\mu'} (P_y + \bar{P}_y) + \beta_{\mu\mu'} (Q_y + \bar{Q}_y) \\ &\quad + \beta_{\mu\tau'} (S_y + \bar{S}_y)] p N^{\text{eq}}(p, T, 0) dp \end{aligned} \quad (71)$$

as the T' evolution equation, where

$$\begin{aligned} \beta_{\tau\mu'} &\equiv \frac{\delta m^2_{\tau\mu'}}{2p} \sin 2\theta_{\tau\mu'}, \quad \beta_{\mu\mu'} \equiv \frac{\delta m^2_{\mu\mu'}}{2p}, \\ \beta_{\mu\tau'} &\equiv \frac{\delta m^2_{\mu\tau'}}{2p} \sin 2\theta_{\tau\mu'}. \end{aligned} \quad (72)$$

Note that $\beta_{\tau\mu'} \approx -\beta_{\mu\tau'}$ because $\delta m_{\tau\mu'}^2 \approx -\delta m_{\mu\tau'}^2$ for the parameter space of interest.

We first present the main result of numerically solving the above equations. After doing so, we will provide a physical description of what lies behind the mathematics. The main result is displayed in Fig. 2, which shows the region of $(\delta m_{\tau\mu'}^2, \sin^2 2\theta_{\tau\mu'})$ parameter space which is consistent with big bang nucleosynthesis for various values of $\delta m_{\mu\mu'}^2$, motivated by the atmospheric neutrino anomaly. The allowed region lies above the relevant solid line (which corresponds to a particular $\delta m_{\mu\mu'}^2$) and to the left of the dash-dotted line. The solid lines arise from solving the QKEs, while the dash-dotted line is the upper bound quoted in Eq. (49) applied to the lepton number creating mode $\nu_{\tau\leftrightarrow\nu'_\mu}$. For the sake of definiteness, we have adopted $\delta N_{\nu, \text{eff}} \lesssim 0.6$ as the BBN bound on the expansion rate of the universe (expressed as an equivalence to additional relativistic neutrino flavors, as is customary). Of course, at the present time there is some confusion regarding the value of this bound, due to conflicting primordial element abundance measurements. The value of 0.6 was chosen for illustrative purposes only. The position of the dash-dotted line depends on the $\delta N_{\nu, \text{eff}}$ chosen. The solid lines, on the other hand, define sharp transition regions. Below the lines, the mirror sector comes into thermal equilibrium because of the eventual copious production of ν'_μ from $\nu_\mu \rightarrow \nu'_\mu$ oscillations. Above the lines, essentially no mirror matter is produced by this oscillation mode. Of course, the closer one gets to the dash-dotted line, the more mirror matter is produced by the $\nu_\tau \rightarrow \nu'_\mu$ mode. For $\sin^2 2\theta_{\tau\mu'} \lesssim 10^{-5}$ the results obtained here using the QKEs are almost identical to those obtained earlier using the static approximation. The results differ at large values of the mixing angle mainly because lepton number is created rapidly enough to spoil the validity of the static approximation.¹⁵

The importance of Fig. 2 lies in its demonstration that the $\nu_\mu \rightarrow \nu'_\mu$ solution in the EPM to the atmospheric neutrino problem is cosmologically consistent for a large region of oscillation parameter space. Furthermore, most of this region sees the ν_τ having a cosmologically interesting mass. In particular, note that the hot dark matter region marked as a shaded band in Fig. 2 has a significant overlap with the allowed region from BBN (we will discuss more about the dark matter region in Sec. VI). It is also interesting to note that the BBN allowed region implied by the $\nu_\mu \rightarrow \nu'_\mu$ solution to the atmospheric neutrino problem is larger than the corresponding region [25,28] obtained when ν'_μ is replaced by a strictly sterile neutrino. The production of sterile neutrinos tends to delay the onset of the rapid exponential growth [25] which means that by the time it occurs the $\nu_\mu \leftrightarrow \nu'_\mu$ oscillations can destroy $L^{(\mu\mu')}$ more efficiently since they are not

damped so much by the collisions. In the case of the mirror neutrino ν'_μ , the mirror electroweak interactions have the effect of reducing their number density, so the production of lepton number is not delayed. Of course a ν_τ in the eV mass region is currently being searched for in the short base line Nomad-Chorus experiments. Such experiments are extremely important to test for the eV tau neutrino which is suggested by Fig. 2. Unfortunately, we cannot predict $\sin^2 2\theta_{\tau\mu}$, so these experiments will either discover $\nu_{\tau\leftrightarrow\nu_\mu}$ oscillations or constrain $\sin^2 2\theta_{\tau\mu}$.

Before closing this section, we will discuss some of the numerical details of performing the above computation, which will entail also a discussion of the physics of the result.

MSW resonances play a key role in the evolution of the system. It is instructive to examine the connection between the neutrino asymmetries and the resonance momenta of the three important two-flavor modes within our system. Note, first of all, that the effective potentials of the three modes depend on different linear combinations of neutrino asymmetries:

$$\begin{aligned} L^{(\tau\mu')} &= 2L_{\nu_\mu} + 3L_{\nu_\tau} - L_{\nu'_\mu}, \\ L^{(\mu\mu')} &= 3L_{\nu_\mu} + 2L_{\nu_\tau} - L_{\nu'_\mu}, \\ L^{(\mu\tau')} &= 4L_{\nu_\mu} + 3L_{\nu_\tau} + L_{\nu'_\mu}, \end{aligned} \quad (73)$$

where we have set $L_{\nu_e} = L_{\nu'_e} = 0$, and we have used conservation of lepton number¹⁶

$$L_{\nu_e} + L_{\nu_\mu} + L_{\nu_\tau} + L_{\nu'_e} + L_{\nu'_\mu} + L_{\nu'_\tau} = 0, \quad (74)$$

to eliminate $L_{\nu'_\tau}$. The lepton number creating mode $\nu_\tau \rightarrow \nu'_\mu$ generates a nonzero L_{ν_τ} , which means that $L^{(\mu\mu')}$ is also nonzero. The latter quantity then suppresses $\nu_\mu \rightarrow \nu'_\mu$ oscillations, provided that it grows sufficiently quickly for a sufficiently long period of time. This is not inevitable, because the effect of the lepton number destroying mode $\nu_\mu \rightarrow \nu'_\mu$ is to try to destroy $L^{(\mu\mu')}$ through the creation of nonzero values for L_{ν_μ} and $L_{\nu'_\mu}$ to compensate the nonzero L_{ν_τ} and $L_{\nu'_\mu}$ produced by the $\nu_\tau \rightarrow \nu'_\mu$ oscillations. The essence of the calculation presented above is the determination of when $L^{(\mu\mu')}$ is driven to zero, and when it is not. This depends on the oscillation parameters, as summarized in Fig. 2.

The resonance momenta for the $\nu_\tau \rightarrow \nu'_\mu$ mode and its antimatter analogue are given by

¹⁵A complete discussion of the static approximation can be found in Refs. [25,29]. In particular, it was shown in Ref. [29] that the static approximation is an adiabatic-like approximation for partially incoherent oscillations in the small vacuum mixing angle parameter regime.

¹⁶Of course the sum of lepton numbers need not be exactly zero. However, we can set the sum to zero without loss of generality provided that the sum is not large.

$$\begin{aligned} \frac{p_{\tau\mu'}}{T} &= \frac{1}{2} \left[\frac{a_0 L^{(\tau\mu')}}{b_0 T^2} \right. \\ &\quad \left. + \sqrt{\left(\frac{a_0 L^{(\tau\mu')}}{b_0 T^2} \right)^2 + \frac{4|\delta m_{\tau\mu'}^2| \cos 2\theta_{\tau\mu'}}{b_0 T^6}} \right], \\ \frac{\bar{p}_{\tau\mu'}}{T} &= \frac{1}{2} \left[-\frac{a_0 L^{(\tau\mu')}}{b_0 T^2} \right. \\ &\quad \left. + \sqrt{\left(\frac{a_0 L^{(\tau\mu')}}{b_0 T^2} \right)^2 + \frac{4|\delta m_{\tau\mu'}^2| \cos 2\theta_{\tau\mu'}}{b_0 T^6}} \right]. \end{aligned} \quad (75)$$

The p - and T -independent quantities a_0 and b_0 are defined through

$$a(p) \equiv -a_0 \frac{T^3 L^{(\alpha\beta')}_p}{\delta m_{\alpha\beta'}^2}, \quad b(p) \equiv -b_0 \frac{T^4 p^2}{\delta m_{\alpha\beta'}^2}, \quad (76)$$

leading to

$$a_0 = \frac{4\sqrt{2}\zeta(3)G_F}{\pi^2}, \quad b_0 = \frac{4\sqrt{2}\zeta(3)G_F A_\alpha}{\pi^2 M_W^2}. \quad (77)$$

In the following we will consider the $L^{(\tau\mu')} > 0$ case for definiteness.¹⁷ Before the rapid exponential creation of lepton number (that is for $T > T_c$), the neutrino and antineutrino resonance momenta for the lepton number creating modes are equal. As $L^{(\tau\mu')}$ gets exponentially created, the neutrino resonance momentum $p_{\tau\mu'}$ moves rapidly to infinity, while the antineutrino resonance momentum $\bar{p}_{\tau\mu'}$ remains at a value of order T . Numerical calculations show that $\bar{p}_{\tau\mu'}/T$ typically takes a value in the range 0.2–0.6 at $T \approx T_c/2$ where T_c is the critical temperature at which lepton number creation begins. These observations are important, because they mean that $\nu_\tau \rightarrow \nu'_\mu$ oscillations are unimportant after the creation of lepton number, while $\bar{\nu}_\tau \rightarrow \bar{\nu}'_\mu$ oscillations remain very important. This is simply because the neutrino resonance momentum has moved to the tail of the Fermi-Dirac distribution, while the antineutrino resonance momentum is within the body of the distribution. (Note that these observations will play a central role in the next section.)

The resonance momenta for the $\nu_\mu \rightarrow \nu'_\mu$ and $\bar{\nu}_\mu \rightarrow \bar{\nu}'_\mu$ modes are given by

$$\frac{p_{\mu\mu'}}{T} = \frac{a_0 L^{(\mu\mu')}}{b_0 T^2}, \quad \frac{\bar{p}_{\mu\mu'}}{T} = 0 \quad \text{if } L^{(\mu\mu')} > 0,$$

$$\frac{p_{\mu\mu'}}{T} = 0, \quad \frac{\bar{p}_{\mu\mu'}}{T} = -\frac{a_0 L^{(\mu\mu')}}{b_0 T^2} \quad \text{if } L^{(\mu\mu')} < 0. \quad (78)$$

In the region of parameter space where $L^{(\mu\mu')}$ is not driven to zero, we see that $p_{\mu\mu'}/T$ gets driven to infinity (staying with the $L_{\nu_\tau} > 0$ case), while $\bar{p}_{\mu\mu'}/T$ stays at zero. In the region of parameter space where $L^{(\mu\mu')}$ gets destroyed, we see that $p_{\mu\mu'}/T$ moves from zero to a finite value as L_{ν_τ} gets created, and then moves back towards zero as the compensating L_{ν_μ} is induced. There is a sharp transition between these two possibilities for the evolution of $p_{\mu\mu'}/T$, with the boundary given by the solid lines in Fig. 2. Above the solid line $L^{(\mu\mu')}$ is created early enough and is large enough so that the ν'_μ is never significantly populated by $\nu_\mu \leftrightarrow \nu'_\mu$ oscillations, these oscillations being heavily suppressed by the matter effects resulting from the large $L^{(\mu\mu')}$. Below the solid line the ν'_μ states would eventually become populated by $\nu_\mu \leftrightarrow \nu'_\mu$ oscillations in the temperature range $6 \lesssim T/\text{MeV} \lesssim 10$. Furthermore, the other mirror particles would also become populated due to the mirror weak interactions, which would effectively double the energy density of the universe prior to the BBN epoch.

The $\nu_\mu \rightarrow \nu'_\tau$ and $\bar{\nu}_\mu \rightarrow \bar{\nu}'_\tau$ resonance momenta are given by

$$\begin{aligned} \frac{p_{\mu\tau'}}{T} &= \frac{1}{2} \left[\frac{a_0 L^{(\mu\tau')}}{b_0 T^2} \right. \\ &\quad \left. \pm \sqrt{\left(\frac{a_0 L^{(\mu\tau')}}{b_0 T^2} \right)^2 - \frac{4|\delta m_{\mu\tau'}^2| \cos 2\theta_{\tau\mu'}}{b_0 T^6}} \right], \\ \frac{\bar{p}_{\mu\tau'}}{T} &= \frac{1}{2} \left[-\frac{a_0 L^{(\mu\tau')}}{b_0 T^2} \right. \\ &\quad \left. \pm \sqrt{\left(\frac{a_0 L^{(\mu\tau')}}{b_0 T^2} \right)^2 - \frac{4|\delta m_{\mu\tau'}^2| \cos 2\theta_{\tau\mu'}}{b_0 T^6}} \right]. \end{aligned} \quad (79)$$

Because the sign of $\delta m_{\mu\tau'}^2$ is positive, we see a qualitatively different behavior for these resonance momenta compared to their mirror reflections in the $\nu_\tau + \nu'_\mu$ subsystem. Before the creation of lepton number, there are no solutions to the resonance conditions. If lepton number evolves to the point where

$$\left(\frac{a_0 L^{(\mu\tau')}}{b_0 T^2} \right)^2 = \frac{4|\delta m_{\mu\tau'}^2|}{b_0 T^6}, \quad (80)$$

then (taking the $L^{(\mu\tau')} > 0$ case) $\nu_\mu \leftrightarrow \nu'_\tau$ comes on resonance at a finite value of the momentum, while $\bar{\nu}_\mu \leftrightarrow \bar{\nu}'_\tau$ never comes on resonance. In the region of parameter space where L_{ν_τ} dominates, it is easy to show that this point occurs when

¹⁷A discussion of the overall sign of the asymmetries created can be found in Ref. [25].

$$\frac{p_{\mu\tau'}}{T} \approx \frac{1}{3} \frac{p_{\mu\mu'}}{T} \approx 2. \quad (81)$$

Thus by the time sufficient L_{ν_τ} and $L_{\nu'_\mu}$ asymmetries have been generated by $\nu_\tau \leftrightarrow \nu'_\mu$ oscillations for the $\nu'_\tau \leftrightarrow \nu_\mu$ oscillations to have a resonance momentum, the $\nu'_\mu \leftrightarrow \nu_\mu$ oscillation resonance momentum is already into the tail of the distribution (for the parameter space where negligible L_{ν_μ} has been created by $\nu_\mu \leftrightarrow \nu'_\mu$ oscillations).¹⁸ For low temperatures, $T \lesssim T_c/3$, the b term in the matter potential can be approximately neglected and the resonance momentum can be derived from $a(p) \approx \cos 2\theta_{\mu\tau'}$, leading to

$$\frac{p_{\mu\tau'}}{T} \approx \frac{\delta m_{\mu\tau'}^2 \cos 2\theta_{\mu\tau'}}{a_0 T^4 L^{(\mu\tau')}}. \quad (82)$$

Observe that the effect of the $\nu_\mu \leftrightarrow \nu'_\tau$ oscillations is to decrease $|L^{(\mu\tau')}|$ and hence to *increase* $p_{\mu\tau'}/T$. By the time $T \sim T_c/2$, the resonance momentum has reached $p_{\mu\tau'}/T \sim 15$. We mention this here because it will be important in the following section.

The observations about the evolution of resonance momenta made above are relevant to the numerical integration of the quantum kinetic equations. Because this integration is CPU time consuming, we employ the useful time saving approximation of integrating the oscillation and collision driven aspects of the evolution in the region around the MSW resonances. Since the precise details and justification of this have been covered in Ref. [28], we will not repeat the discussion here.

V. LOW TEMPERATURE AND BBN EPOCHS: EFFECT OF OSCILLATIONS ON LIGHT ELEMENT ABUNDANCES

A. Introduction

The primordial deuterium to hydrogen (D/H) ratio can be used to give a sensitive determination of the baryon to photon ratio η which, given the estimated primordial ${}^4\text{He}$ mass fraction, can be used to infer the effective number of light neutrino flavors $N_{\nu,\text{eff}}$ during the BBN epoch. This value can then be compared with the predictions for $N_{\nu,\text{eff}}$ from various models of particle physics to find out which ones are compatible with standard BBN. For example, the minimal standard model predicts $N_{\nu,\text{eff}} = 3$. At the present time, most estimates favor $N_{\nu,\text{eff}} < 3.6$ and some estimates favor $N_{\nu,\text{eff}} < 3.0$ [44]. Of course, even if a model of particle physics is

shown to be incompatible with BBN, this does not necessarily mean that the model is incorrect, since it is also possible that one of the standard assumptions of BBN may not be correct [45].

For gauge models with mirror or sterile neutrinos, one in general expects $N_{\nu,\text{eff}} \neq 3$. In fact, $N_{\nu,\text{eff}}$ may be less than 3 or greater than 3. The prediction for $N_{\nu,\text{eff}}$ depends on the oscillation parameters in a given model. One possible consequence of ordinary-mirror (or ordinary-sterile) neutrino oscillations is the excitation of mirror neutrino states, which typically leads to an increase in the expansion rate of the universe and thereby also increases $N_{\nu,\text{eff}}$. Another possible consequence of ordinary-mirror neutrino oscillations is the dynamical generation of an electron-neutrino asymmetry. This also has important implications for BBN, as it directly affects the reaction rates which determine the neutrino to proton (n/p) ratio just before nucleosynthesis. If the electron neutrino asymmetry is positive, then it will decrease $N_{\nu,\text{eff}}$, while if it is negative, then it will increase $N_{\nu,\text{eff}}$.

The neutron to nucleon ratio, $X_n(t)$, is related to the primordial helium mass fraction, Y_p , by¹⁹

$$Y_p = 2X_n \quad (83)$$

just before nucleosynthesis. The evolution of $X_n(t)$ is governed by the equation

$$\frac{dX_n}{dt} = -\lambda(n \rightarrow p)X_n + \lambda(p \rightarrow n)(1 - X_n), \quad (84)$$

where the reaction rates are approximately

$$\begin{aligned} \lambda(n \rightarrow p) &\approx \lambda(n + \nu_e \rightarrow p + e^-) + \lambda(n + e^+ \rightarrow p + \bar{\nu}_e), \\ \lambda(p \rightarrow n) &\approx \lambda(p + e^- \rightarrow n + \nu_e) + \lambda(p + \bar{\nu}_e \rightarrow n + e^+), \end{aligned} \quad (85)$$

and depend on the momentum distributions of the species involved. The processes in Eq. (85) for determining $n \leftrightarrow p$ are only important for temperatures above about 0.4 MeV. Below this temperature the weak interaction rates freeze out and neutron decay becomes the dominant factor affecting the n/p ratio. An excess of ν_e over $\bar{\nu}_e$, due to the creation of a positive L_{ν_e} would change the rates for the processes in Eq. (85). The effect of this would be to reduce the n/p ratio, and hence reduce Y_p . Neutron decay is not significantly altered by lepton asymmetries. It is quite well known that a small change in Y_p due to the modification of ν_e and $\bar{\nu}_e$ distributions does not impact significantly on the other light element abundances (see for example Ref. [47]). A small modification to the expansion rate, using the convenient unit $N_{\nu,\text{eff}}$, primarily affects only Y_p , with [48]

$$\delta Y_p \approx 0.012 \times \delta N_{\nu,\text{eff}}. \quad (86)$$

¹⁸Actually, in the pseudo-Dirac case [33] where there are no mirror interactions the $\nu_\mu + \nu'_\tau$ oscillation system is more important. The reason is that, in the pseudo-Dirac case, these oscillations destroy *exactly* the same combination of lepton numbers as does the $\nu_\mu \leftrightarrow \nu'_\mu$ mode; that is, in this case $L^{(\mu\tau')} = L^{(\mu\mu')}$. Thus, in the pseudo-Dirac alternative to the mirror scenario, the $\nu_\mu \leftrightarrow \nu'_\tau$ oscillations can help the $\nu_\mu \leftrightarrow \nu'_\mu$ oscillations destroy $L^{(\mu\mu')}$, which means that the ‘‘allowed region’’ can be significantly reduced.

¹⁹For a review of helium synthesis, see for example Ref. [46].

In Appendix A we describe in detail how we compute the effect on Y_p due to the modified ν_e and $\bar{\nu}_e$ distributions.

In two previous papers [26,27], we studied the implications for BBN of oscillations within two distinct four-neutrino-flavor models which featured the three ordinary neutrinos and one sterile neutrino. In Ref. [26], a model with the mass hierarchy $m_{\nu_\tau} \gg m_{\nu_\mu}, m_{\nu_e}, m_{\nu_s}$ was considered. In this case $\bar{\nu}_\tau \leftrightarrow \bar{\nu}_s$ oscillations resulted in an excess of ν_τ over $\bar{\nu}_\tau$ (in the case where $L_{\nu_\tau} > 0$), thereby generating a large tau-neutrino asymmetry. It was shown that if $\bar{\nu}_\tau - \bar{\nu}_e$ oscillations also occurred, then some of the tau-neutrino asymmetry was reprocessed into an electron-neutrino asymmetry. The effective number of neutrino flavors found in Ref. [26] was either 2.5 or 3.4, depending on the ambiguity for the sign of the asymmetry and hence the prediction for $N_{\nu, \text{eff}}$ (Ref. [25] discusses the sign ambiguity issue). For a positive asymmetry, $\delta N_{\nu, \text{eff}} \approx -0.5$ was obtained over a range of mass differences $|\delta m_{\tau s}^2| \sim 10\text{--}1000 \text{ eV}^2$, while for a negative asymmetry the result was $\delta N_{\nu, \text{eff}} \approx +0.4$. Later, in a separate paper with Bell [27], we considered another four-neutrino model where ν_τ and ν_μ were taken to be approximately maximal combinations of two nearly degenerate mass eigenstates, ν_1 and ν_2 , with $m_{\nu_1}, m_{\nu_2} \gg m_{\nu_e}, m_{\nu_s}$. In that case, we found $N_{\nu, \text{eff}} \approx 2.7$ or 3.1 depending on the sign of the asymmetry.

As the above paragraph illustrates, the prediction for $N_{\nu, \text{eff}}$ is a model dependent quantity. In the next section we will estimate $N_{\nu, \text{eff}}$ in the EPM for various illustrative parameter ranges.

B. Low temperature neutrino asymmetry evolution in the EPM: Case 1

We now study the ‘‘low temperature’’ evolution of the number distributions and lepton numbers in the EPM. As discussed in Sec. II, by ‘‘low temperature’’ we mean the regime succeeding the exponential growth epoch. In this regime, the evolution of the neutrino ensemble is dominated by coherent effects, because the T^5 decrease in the damping function D renders negligible the decohering effect of collisions. Repopulation, however, is still important.

Consider, for the moment, two-flavor small angle ordinary-mirror oscillations $\nu_\alpha \leftrightarrow \nu'_\beta$. In the case of undamped evolution, we know from numerical integration of the exact quantum kinetic equations that the adiabatic approximation is valid provided that $\sin^2 2\theta_{\alpha\beta'} \gtrsim 10^{-10}$. Now, coherent adiabatic MSW transitions completely convert $\nu_\alpha \leftrightarrow \nu'_\beta$ at the resonance momentum of these states. For adiabatic two-flavor neutrino oscillations in the early universe it is then quite easy to see that the rate of change of lepton number is governed by the simple equation [26]

$$\frac{dL_{\nu_\alpha}}{dT} = -\frac{dL_{\nu'_\beta}}{dT} = -X \left| \frac{d(p_{\text{res}}/T)}{dT} \right|, \quad (87)$$

where

$$X = \frac{T}{n_\gamma} (N_{\nu_\alpha}^- - N_{\nu'_\beta}^-), \quad (88)$$

and the case $L_{\nu_\alpha} > 0$ has been considered (so that the resonance occurs for antineutrinos). Equation (87) relates the rate of change of lepton number to the speed of the resonance momentum through the neutrino distribution. Reference [29] provides a detailed discussion of how this equation can be derived from Eq. (44) for the case of adiabatic evolution with a narrow resonance width.²⁰ Equation (87) can be simplified using

$$\frac{d(p_{\text{res}}/T)}{dT} = \frac{\partial(p_{\text{res}}/T)}{\partial T} + \frac{\partial(p_{\text{res}}/T)}{\partial L_{\nu_\alpha}} \frac{dL_{\nu_\alpha}}{dT}, \quad (89)$$

from which it follows that

$$\frac{dL_{\nu_\alpha}}{dT} = -\frac{dL_{\nu'_\beta}}{dT} = \frac{fX \frac{\partial(p_{\text{res}}/T)}{\partial T}}{1 - fX \frac{\partial(p_{\text{res}}/T)}{\partial L_{\nu_\alpha}}} = \frac{-4fX p_{\text{res}}/T^2}{1 - \frac{2fX p_{\text{res}}}{T[L^{(\alpha)} - L^{(\beta)}]}}, \quad (90)$$

where $f=1$ for $d(p_{\text{res}}/T)/dt > 0$ [that is for $d(p_{\text{res}}/T)/dT < 0$] and $f=-1$ for $d(p_{\text{res}}/T)/dt < 0$. For the multi-flavor case under analysis, coupled equations based on Eq. (90) will be used.

Of course the evolution of the lepton number can also be described using the QKEs. As mentioned above, they give the same answer provided that the evolution is adiabatic. In the case of non-adiabatic evolution, the QKEs should be used instead of the simple equation (87). For our study of the low temperature evolution of the number distributions and lepton numbers in the EPM, we will make use of the adiabatic approximation encoded in Eq. (90). In fact, it turns out that the evolution of the system in the EPM model is quite complicated. For example, three-flavor effects cannot be ignored, so solving the problem using the quantum kinetic equations would be extremely complicated and (CPU) time consuming.

We first consider the parameter region

$$m_{\nu_{\tau+}} \approx m_{\nu_{\tau-}} \gg m_{\nu_{\mu+}}, m_{\nu_{\mu-}}, m_{\nu_{e+}}, m_{\nu_{e-}}, \quad (91)$$

with

$$m_{\nu_{\mu+}}, m_{\nu_{\mu-}}, m_{\nu_{e+}}, m_{\nu_{e-}} \ll 1 \text{ eV}. \quad (92)$$

We will call this ‘‘case 1.’’ (Later on we will consider another case, case 2, where $m_{\nu_{\mu\pm}} \sim \text{eV}$ as suggested by the LSND results.) In Case 1, the following oscillation modes all have approximately the same $|\delta m^2|$, which we denote as $\delta m_{\text{large}}^2$:

²⁰Note that when collisional decoherence is neglected, the QKEs produce standard Schrödinger-like MSW evolution with repopulation effects added via a Boltzmann approach.

$$\begin{aligned} \nu_\tau \leftrightarrow \nu'_e, \quad \nu_\tau \leftrightarrow \nu'_\mu, \quad \nu'_\tau \leftrightarrow \nu_e, \quad \nu'_\tau \leftrightarrow \nu_\mu, \\ \nu_\tau \leftrightarrow \nu_e, \quad \nu_\tau \leftrightarrow \nu_\mu, \quad \nu'_\tau \leftrightarrow \nu'_e, \quad \nu'_\tau \leftrightarrow \nu'_\mu. \end{aligned} \quad (93)$$

Note that $\delta m_{\text{large}}^2 \simeq m_{\nu_{\tau\pm}}^2$. All the other oscillation modes have much smaller δm^2 values. In fact, for case 1, we will consider the parameter space region where the δm^2 values of all the other oscillation modes are small enough so that they can be approximately neglected for temperatures $T \gtrsim 0.4$ MeV. This last condition means that these modes will not affect the neutron/proton ratio and hence cannot significantly affect BBN.

In the following discussion we consider the case $L_{\nu_\tau} > 0$ for definiteness. This means that the $\bar{\nu}_\tau \leftrightarrow \bar{\nu}'_e$ and $\bar{\nu}_\tau \leftrightarrow \bar{\nu}'_\mu$ oscillations generate L_{ν_τ} while the other oscillations reprocess some of this asymmetry into other flavors. Of course a crucial issue for BBN is to find out how much of this asymmetry is reprocessed to the electron neutrinos, and at what temperature this occurs.

In order to use Eq. (90), we have to employ the resonance conditions to determine the resonance momenta as functions of temperature and the neutrino asymmetries. We begin by noting that the sum of the ordinary and mirror lepton numbers is conserved by the oscillations, and we will suppose that they sum to zero²¹:

$$L_{\nu_e} + L_{\nu_\mu} + L_{\nu_\tau} + L_{\nu'_e} + L_{\nu'_\mu} + L_{\nu'_\tau} = 0. \quad (94)$$

Furthermore, we take as initial conditions that

$$L_{\nu_\mu} \simeq L_{\nu_e}, \quad L_{\nu'_\mu} \simeq L_{\nu'_e}. \quad (95)$$

We will show that this assumption is robust shortly. With the above initial conditions, it follows that the eight oscillation modes of Eq. (93) can be classified together into four groups of two, each group having approximately the same resonance momentum:

$$\begin{aligned} \text{group 1: } & \bar{\nu}_\tau \leftrightarrow \bar{\nu}'_e, \quad \bar{\nu}_\tau \leftrightarrow \bar{\nu}'_\mu, \quad p_{\text{res}} \equiv P_1, \\ \text{group 2: } & \nu'_\tau \leftrightarrow \nu_e, \quad \nu'_\tau \leftrightarrow \nu_\mu, \quad p_{\text{res}} \equiv P_2, \\ \text{group 3: } & \bar{\nu}_\tau \leftrightarrow \bar{\nu}_e, \quad \bar{\nu}_\tau \leftrightarrow \bar{\nu}_\mu, \quad p_{\text{res}} \equiv P_3, \\ \text{group 4: } & \bar{\nu}'_\tau \leftrightarrow \bar{\nu}'_e, \quad \bar{\nu}'_\tau \leftrightarrow \bar{\nu}'_\mu, \quad p_{\text{res}} \equiv P_4. \end{aligned} \quad (96)$$

In the low temperature epoch, the b term in the effective potential can be approximately neglected because it decreases as T^6 . This means that the resonance condition is approximately $a(p) = \pm \cos 2\theta \simeq \pm 1$ for small angle oscillations.

²¹Of course our results do not depend significantly on this assumption. For example, if we put the sum in Eq. (94) equal to a number of the order of the baryon asymmetry, then the resulting analysis will change very little.

For $\nu_\alpha \leftrightarrow \nu'_\beta$ small angle oscillations, the resonance momentum is therefore to a good approximation given by

$$\frac{p_{\text{res}}}{T} = \frac{\delta m_{\alpha\beta'}^2}{a_0 T^4 L^{(\alpha\beta')}}, \quad (97)$$

where we have used the notation defined earlier in Eq. (76). For the four groups of oscillation modes in Eq. (96),

$$\frac{P_i}{T} = \frac{\delta m_{\text{large}}^2}{a_0 T^4 L_i}, \quad (98)$$

where $i = 1, \dots, 4$ and

$$\begin{aligned} L_1 &\equiv L^{(\tau e')} = \frac{7}{2} L_{\nu_\tau} + 5 L_{\nu_e} + \frac{1}{2} L_{\nu'_\tau}, \\ L_2 &\equiv -L^{(e\tau')} = 2 L_{\nu_\tau} + 5 L_{\nu_e} - L_{\nu'_\tau}, \\ L_3 &\equiv L^{(\tau)} - L^{(e)} = L_{\nu_\tau} - L_{\nu_e}, \\ L_4 &\equiv L'^{(\tau)} - L'^{(e)} = L_{\nu'_\tau} - L_{\nu'_e} \\ &= \frac{1}{2} L_{\nu_\tau} + L_{\nu_e} + \frac{3}{2} L_{\nu'_\tau}. \end{aligned} \quad (99)$$

Note that Eqs. (94) and (95) have been used in the above equation to express L_{ν_μ} , $L_{\nu'_\mu}$ and $L_{\nu'_e}$ in terms of the L_{ν_e} , L_{ν_τ} and $L_{\nu'_\tau}$.

In the following discussion we will focus on the parameter space region where all of the oscillations are approximately adiabatic. This is extraordinarily helpful, because adiabatic transitions are independent of the vacuum mixing angles (as long as the mixing angles are much smaller than 1). This means that generic outcomes can be calculated for a reasonably large range of parameters, rather than having to consider small points in oscillation parameter space on a case by case basis. As noted earlier, two flavor subsystems in this epoch of the early universe evolve adiabatically provided that the relevant $\sin^2 2\theta \gtrsim 10^{-10}$. This is not a very stringent requirement. In particular, there will be a large range of parameters where the evolution is both adiabatic and satisfies the experimental and cosmological constraints. Given the parameter region of Eqs. (91) and (92), consistency with BBN constrains $\sin^2 2\theta_{\tau\mu'}$ to be²²

$$\sin^2 2\theta_{\tau\mu'} \lesssim \text{few} \times 10^{-4} \left(\frac{eV^2}{\delta m_{\text{large}}^2} \right)^{1/2}, \quad (100)$$

while Nomad and Chorus constrain $\sin^2 2\theta_{\tau\mu}$ to be [49]

$$\sin^2 2\theta^{\tau\mu} \lesssim 10^{-3} \text{ for } \delta m_{\text{large}}^2 \gtrsim 40 \text{ eV}^2. \quad (101)$$

²²Note that $\sin^2 2\theta_{\tau\mu'} = \sin^2 2\theta_{\tau'\mu}$ from the parity symmetry.

We now discuss the effects of each of the four groups of modes in Eq. (96).

(1) *The $\bar{\nu}_\tau \leftrightarrow \bar{\nu}'_e$ and $\bar{\nu}_\tau \leftrightarrow \bar{\nu}'_\mu$ group 1 modes:* These modes have negative δm^2 values and thus create the relevant lepton numbers L_{ν_τ} , $L_{\nu'_e}$ and $L_{\nu'_\mu}$. It is important to understand that if these two modes have slightly different resonance momenta, say P_1^a and P_1^b , then they generate lepton numbers so that $P_1^a \rightarrow P_1^b$. This is tantamount to ensuring that the initial conditions of Eq. (95) hold, provided that the difference between the initial values of L_{ν_e} and L_{ν_μ} is not too great. To see that the resonance momenta are dynamically driven to coincide, assume that $P_1^a > P_1^b$. This means that the $\bar{\nu}_\tau \leftrightarrow \bar{\nu}'_e$ resonance momentum precedes the $\bar{\nu}_\tau \leftrightarrow \bar{\nu}'_\mu$ resonance momentum. Now, the $\bar{\nu}_\tau \leftrightarrow \bar{\nu}'_e$ oscillations convert all of the resonant $\bar{\nu}_\tau$'s into $\bar{\nu}'_e$'s. The closely following $\bar{\nu}_\tau \leftrightarrow \bar{\nu}'_\mu$ resonance has a much weaker effect, since there are no $\bar{\nu}_\tau$'s left to convert into $\bar{\nu}'_\mu$ states. (For this to be true the resonance momenta must be close enough so that the converted $\bar{\nu}_\tau$ states do not get completely refilled by the weak interactions before the trailing resonance momentum P_1^b passes their momentum value.) Because of the disparity in raw material for processing, $L_{\nu'_e}$ is created much more rapidly than $L_{\nu'_\mu}$. According to Eq. (98), this in turn means that P_1^a increases more slowly relative to P_1^b and thus $P_1^b \rightarrow P_1^a$. Obviously, if we had started with $P_1^b > P_1^a$, then we also would have found that the evolution of lepton numbers is such that $P_1^a \rightarrow P_1^b$. Because the dynamics drives the two resonances in this group to approximately coincide, the system cannot be described in terms of two-flavor oscillations. Instead, three-flavor effects among $\bar{\nu}_\tau$, $\bar{\nu}'_e$ and $\bar{\nu}'_\mu$ effect the adiabatic conversion

$$|\bar{\nu}_\tau\rangle \leftrightarrow \frac{1}{\sqrt{2}}(|\bar{\nu}'_e\rangle + |\bar{\nu}'_\mu\rangle). \quad (102)$$

This means that as P_1 sweeps through the $\bar{\nu}_\tau$ momentum distribution,

$$\begin{aligned} N_{\bar{\nu}'_e}(P_1) &\rightarrow \frac{1}{2} \left[\frac{N_{\bar{\nu}'_e}(P_1)}{2} + \frac{N_{\bar{\nu}'_\mu}(P_1)}{2} + N_{\bar{\nu}_\tau}(P_1) \right], \\ N_{\bar{\nu}'_\mu}(P_1) &\rightarrow \frac{1}{2} \left[\frac{N_{\bar{\nu}'_e}(P_1)}{2} + \frac{N_{\bar{\nu}'_\mu}(P_1)}{2} + N_{\bar{\nu}_\tau}(P_1) \right], \\ N_{\bar{\nu}_\tau}(P_1) &\rightarrow \frac{1}{2} [N_{\bar{\nu}'_e}(P_1) + N_{\bar{\nu}'_\mu}(P_1)]. \end{aligned} \quad (103)$$

In our numerical work the continuous momentum distribution for each flavor is replaced by a finite number of ‘‘cells’’ on a logarithmically spaced mesh. As the momentum P_1 passes a cell, the number density in the cell is modified ac-

ording to Eq. (103).²³ Of course weak interactions will repopulate these cells as they thermalize the neutrino momentum distributions. We will discuss this later.

(2) *The $\nu'_\tau \leftrightarrow \nu_e$ and $\nu'_\tau \leftrightarrow \nu_\mu$ group 2 modes:* These modes have positive δm^2 values. At quite high temperatures, where the group 1 oscillation modes are exponentially creating L_{ν_τ} , the group 2 oscillation modes generate $L_{\nu'_\tau}$, L_{ν_e} and L_{ν_μ} such that $L'^{(\tau)} - L^{(e)} \rightarrow 0$ and $L'^{(\tau)} - L^{(\mu)} \rightarrow 0$. As already discussed in Sec. IV, this makes $P_2/T \gg 1$ at the onset of the low temperature epoch. Our numerical work shows that the initial value of P_2/T is typically about 15 and decreasing by the time $T \sim T_c/2$. The subsequent evolution of P_2/T is a little complicated, but can be roughly understood from Eqs. (89) and (98), which combine to produce

$$\frac{d(P_2/T)}{dT} = -\frac{P_2}{T} \left[\frac{4}{T} + \frac{1}{L_2} \frac{dL_2}{dT} \right] \quad (104)$$

or, equivalently,

$$\frac{d(P_2/T)}{dt} \simeq \frac{P_2}{T} \left[\frac{5.5T^2}{M_p} - \frac{1}{L_2} \frac{dL_2}{dt} \right]. \quad (105)$$

By the time $T \sim T_c/2$, the group 2 modes have driven L_2 to be quite small. The second term in the right-hand side of the above equation therefore dominates, making P_2/T a decreasing function of time. So, at the start of the low temperature epoch, P_2/T slowly decreases, converting ν_e 's and ν_μ 's to ν'_τ 's as it does so. As for the group 1 modes above, it is easy to see that if the two group 2 modes had slightly different resonance momenta, P_2^a and P_2^b , then the dynamics forces $P_2^a \rightarrow P_2^b$. The effect of the three-flavor $\nu_e - \nu_\mu - \nu'_\tau$ subsystem is to convert $|\nu'_\tau\rangle$ to $(1/\sqrt{2})(|\nu_e\rangle + |\nu_\mu\rangle)$. So, as P_2 moves (backward) through the neutrino momentum distribution,

$$\begin{aligned} N_{\nu'_e}(P_2) &\rightarrow \frac{1}{2} \left[\frac{N_{\nu_e}(P_2)}{2} + \frac{N_{\nu_\mu}(P_2)}{2} + N_{\nu'_\tau}(P_2) \right], \\ N_{\nu'_\mu}(P_2) &\rightarrow \frac{1}{2} \left[\frac{N_{\nu_e}(P_2)}{2} + \frac{N_{\nu_\mu}(P_2)}{2} + N_{\nu'_\tau}(P_2) \right], \\ N_{\nu'_\tau}(P_2) &\rightarrow \frac{1}{2} [N_{\nu_e}(P_2) + N_{\nu_\mu}(P_2)]. \end{aligned} \quad (106)$$

The effect of this conversion is to generate significant L_{ν_e} and L_{ν_μ} asymmetries which are negative in sign (given that we have taken $L_{\nu_\tau} > 0$ for definiteness). As the evolution unfolds, at some temperature P_2/T changes direction and begins to increase again. This is due to the gradual increase in L_2 which eventually makes the second term on the right-

²³Note that it is legitimate to consider probabilities, as encoded in the number density distributions, rather than probability amplitudes in effecting the conversion. This is because fully adiabatic transitions are sufficiently ‘‘classical.’’

hand side of Eq. (105) smaller in magnitude than the first term. The full analysis, incorporating all of the modes simultaneously, requires a numerical treatment. We compute the minimum P_2/T to be ~ 6 , which is still in the tail of the distribution. The upshot of this somewhat complicated evolution is that the P_2 resonance momentum does not sweep through the entire momentum distribution, but rather, it sweeps through a significant part of the high momentum tail. In the temperature regime where P_2/T makes the return journey from its minimum value back to high values, the adiabatic MSW transitions have little effect because they simply swap the almost equal number densities of ν'_τ and $\nu_{e,\mu}$ that were created by adiabatic transitions before the turnaround.²⁴ This is of course only true provided that the momentum distribution of ν'_τ states does not get significantly modified by the mirror weak interactions, an issue we will discuss in more detail later.

(3) *The $\bar{\nu}_\tau \leftrightarrow \bar{\nu}_e$ and $\bar{\nu}_\tau \leftrightarrow \bar{\nu}_\mu$ group 3 modes.* These modes, being ordinary-ordinary, are slightly different in character to the ordinary-mirror modes. Their effect is to reprocess some of the L_{ν_τ} into L_{ν_e} and L_{ν_μ} . In the early stages of lepton number creation, all of the ordinary-ordinary modes are unimportant, because they simply swap flavors with almost identical number density distributions. However, eventually the L_{ν_τ} asymmetry created by the group 1 modes is large enough to distort the $\bar{\nu}_\tau$ momentum distribution so that the attendant reduction in the $\bar{\nu}_\tau$ number density relative to that for $\bar{\nu}_{e,\mu}$ allows $\bar{\nu}_\tau \leftrightarrow \bar{\nu}_{e,\mu}$ oscillations to induce non-trivial dynamics: the depletion of $\bar{\nu}_e$ and $\bar{\nu}_\mu$ states at the resonance momentum P_3 . This effect becomes significant when L_{ν_τ} becomes quite large, which occurs roughly when $P_1/T \gtrsim 2$. Now, from Eq. (99) it is evident that $P_3 \sim \frac{1}{2}P_1$ using the fact that L_{ν_τ} is the largest lepton number in the system. This has the important consequence that the overall effect of the group 3 oscillations is not very large because by the time L_{ν_τ} is large, P_3 is already well into the tail of the momentum distribution. This is fortunate, because these oscillations are more complicated to describe. Unlike the group 1 and 2 modes, it is easy to see that if the resonance momenta, P_3^a and P_3^b , of the two modes are slightly different, then they do *not* subsequently evolve to coincide. (The reason is that if, say, the $\bar{\nu}_\tau \leftrightarrow \bar{\nu}_e$ resonance momentum precedes the $\bar{\nu}_\tau \leftrightarrow \bar{\nu}_\mu$ resonance momentum, then the $\bar{\nu}_\tau \leftrightarrow \bar{\nu}_e$ oscillations act to reduce $L^{(\tau e)}$, thereby *increasing* the rate at which this resonance momentum moves relative to the $\bar{\nu}_\tau \leftrightarrow \bar{\nu}_\mu$ resonance momentum.) Note, however, that because of the more influential group 2 oscillations, it follows that P_3^a and P_3^b are at least *approximately* equal. What precisely happens

will then depend on the width of these resonances and whether they overlap or not. This means that the effects will be dependent on the values of the relevant oscillation parameters. In our numerical work we will assume that the resonances overlap, so that $|\bar{\nu}_\tau\rangle \leftrightarrow 1/\sqrt{2}(|\bar{\nu}_e\rangle + |\bar{\nu}_\mu\rangle)$. In this case,

$$\begin{aligned} N_{\bar{\nu}_e}^-(P_3) &\rightarrow \frac{1}{2} \left[\frac{N_{\bar{\nu}_e}^-(P_3)}{2} + \frac{N_{\bar{\nu}_\mu}^-(P_3)}{2} + N_{\bar{\nu}_\tau}^-(P_3) \right], \\ N_{\bar{\nu}_\mu}^-(P_3) &\rightarrow \frac{1}{2} \left[\frac{N_{\bar{\nu}_e}^-(P_3)}{2} + \frac{N_{\bar{\nu}_\mu}^-(P_3)}{2} + N_{\bar{\nu}_\tau}^-(P_3) \right], \\ N_{\bar{\nu}_\tau}^-(P_3) &\rightarrow \frac{1}{2} [N_{\bar{\nu}_e}^-(P_3) + N_{\bar{\nu}_\mu}^-(P_3)]. \end{aligned} \quad (107)$$

We stress that, were the above assumption proved to be invalid, our numerical results would not be greatly affected because the group 3 modes have a relatively weak effect for the reasons discussed above. Finally we note that the L_{ν_e} and L_{ν_μ} asymmetries created by the group 3 modes have the opposite sign to the L_{ν_e} and L_{ν_μ} asymmetries generated by the group 2 modes.

(4) *The $\bar{\nu}'_\tau \leftrightarrow \bar{\nu}'_e$ and $\bar{\nu}'_\tau \leftrightarrow \bar{\nu}'_\mu$ group 4 modes.* These mirror-mirror modes can be neglected because P_4 is always greater than P_1 , and thus the $\bar{\nu}'_{e,\mu}$ states are approximately empty (as is $\bar{\nu}'_\tau$) when the P_4 resonance momentum moves through.

Having understood to some extent the effect of each group of oscillations, it is now time to solve the complete system of coupled equations for the various lepton numbers. These are obtained by a straightforward generalization of the two-flavor case given in Eq. (90). They are

$$\begin{aligned} \frac{dL_{\nu_\tau}}{dT} &= -X_1 \left| \frac{d(P_1/T)}{dT} \right| - X_3 \left| \frac{d(P_3/T)}{dT} \right|, \\ \frac{dL_{\nu_e}}{dT} &= \frac{1}{2} X_3 \left| \frac{d(P_3/T)}{dT} \right| + \frac{1}{2} X_2 \left| \frac{d(P_2/T)}{dT} \right|, \\ \frac{dL_{\nu_\mu}}{dT} &= \frac{dL_{\nu_e}}{dT}, \quad \frac{dL_{\nu'_\tau}}{dT} = -X_2 \left| \frac{d(P_2/T)}{dT} \right|, \\ \frac{dL_{\nu'_e}}{dT} &= \frac{dL_{\nu'_\mu}}{dT} = -\frac{1}{2} \left(\frac{dL_{\nu_\tau}}{dT} + \frac{dL_{\nu'_\tau}}{dT} + \frac{dL_{\nu_e}}{dT} + \frac{dL_{\nu_\mu}}{dT} \right), \end{aligned} \quad (108)$$

where

$$\begin{aligned} X_1 &\equiv \frac{T}{n_\gamma} \left(N_{\bar{\nu}_\tau}^-(P_1) - \frac{1}{2} [N_{\bar{\nu}_e}^-(P_1) + N_{\bar{\nu}_\mu}^-(P_1)] \right), \\ X_2 &\equiv \frac{T}{n_\gamma} \left(\frac{1}{2} [N_{\nu_e}(P_2) + N_{\nu_\mu}(P_2)] - N_{\nu'_\tau}(P_2) \right), \end{aligned}$$

²⁴Actually, in this region, the two resonance momenta $P_2^{a,b}$ are no longer dynamically driven to coincide, making the oscillations somewhat more complicated. However, if the ν'_τ tail is fully populated from the previous evolution of the system, then this complication matters very little.

$$X_3 \equiv \frac{T}{n_\gamma} \left(N_{\bar{\nu}_\tau}(P_3) - \frac{1}{2} [N_{\bar{\nu}_e}(P_3) + N_{\bar{\nu}_\mu}(P_3)] \right). \quad (109)$$

Expanding out Eq. (108) we find

$$\begin{aligned} y_1 \frac{dL_{\nu_\tau}}{dT} &= \alpha + \beta \frac{dL_{\nu_e}}{dT} + \gamma \frac{dL_{\nu'_\tau}}{dT}, \\ y_2 \frac{dL_{\nu_e}}{dT} &= \delta + \rho \frac{dL_{\nu_\tau}}{dT} + \zeta \frac{dL_{\nu'_\tau}}{dT}, \\ y_3 \frac{dL_{\nu'_\tau}}{dT} &= \eta + \theta \frac{dL_{\nu_e}}{dT} + \phi \frac{dL_{\nu_\tau}}{dT}, \end{aligned} \quad (110)$$

where

$$\begin{aligned} y_1 &\equiv 1 - f_1 X_1 \frac{\partial(P_1/T)}{\partial L_{\nu_\tau}} - f_3 X_3 \frac{\partial(P_3/T)}{\partial L_{\nu_\tau}} \\ &= 1 + \frac{7f_1 X_1 P_1}{2TL_1} + \frac{f_3 X_3 P_3}{TL_3}, \\ y_2 &\equiv 1 + \frac{1}{2} f_3 X_3 \frac{\partial(P_3/T)}{\partial L_{\nu_e}} + \frac{1}{2} f_2 X_2 \frac{\partial(P_2/T)}{\partial L_{\nu_e}} \\ &= 1 + \frac{f_3 X_3 P_3}{2TL_3} - \frac{5f_2 X_2 P_2}{2TL_2}, \\ y_3 &\equiv 1 - f_2 X_2 \frac{\partial(P_2/T)}{\partial L_{\nu'_\tau}} = 1 - \frac{f_2 X_2 P_2}{TL_2}, \\ \alpha &\equiv f_1 X_1 \frac{\partial(P_1/T)}{\partial T} + f_3 X_3 \frac{\partial(P_3/T)}{\partial T} \\ &= -4f_1 X_1 P_1 / T^2 - 4f_3 X_3 P_3 / T^2, \\ \beta &\equiv f_1 X_1 \frac{\partial(P_1/T)}{\partial L_{\nu_e}} + f_3 X_3 \frac{\partial(P_3/T)}{\partial L_{\nu_e}} \\ &= \frac{-5f_1 X_1 P_1}{TL_1} + \frac{f_3 X_3 P_3}{TL_3}, \\ \gamma &\equiv f_1 X_1 \frac{\partial(P_1/T)}{\partial L_{\nu'_\tau}} = \frac{-f_1 X_1 P_1}{2TL_1}, \\ \delta &\equiv -\frac{1}{2} f_3 X_3 \frac{\partial(P_3/T)}{\partial T} - \frac{1}{2} f_2 X_2 \frac{\partial(P_2/T)}{\partial T} \\ &= 2f_3 X_3 P_3 / T^2 + 2f_2 X_2 P_2 / T^2, \end{aligned}$$

$$\begin{aligned} \rho &\equiv -\frac{1}{2} f_3 X_3 \frac{\partial(P_3/T)}{\partial L_{\nu_\tau}} - \frac{1}{2} f_2 X_2 \frac{\partial(P_2/T)}{\partial L_{\nu_\tau}} \\ &= \frac{f_3 X_3 P_3}{2TL_3} + \frac{f_2 X_2 P_2}{TL_2}, \\ \zeta &\equiv -\frac{1}{2} f_2 X_2 \frac{\partial(P_2/T)}{\partial L_{\nu'_\tau}} = -\frac{f_2 X_2 P_2}{2TL_2}, \\ \eta &\equiv f_2 X_2 \frac{\partial(P_2/T)}{\partial T} = -4f_2 X_2 P_2 / T^2, \\ \theta &\equiv f_2 X_2 \frac{\partial(P_2/T)}{\partial L_{\nu_e}} = -\frac{5f_2 X_2 P_2}{TL_2}, \\ \phi &\equiv f_2 X_2 \frac{\partial(P_2/T)}{\partial L_{\nu_\tau}} = -\frac{2f_2 X_2 P_2}{TL_2}, \end{aligned} \quad (111)$$

and $f_i = 1$ for $d(P_i/T)/dt > 0$ and $f_i = -1$ for $d(P_i/T)/dt < 0$ ($i = 1, 2, 3$). Solving Eq. (110) we find

$$\begin{aligned} \frac{dL_{\nu_e}}{dT} &= \frac{(\delta y_3 + \zeta \eta)(y_1 y_3 - \gamma \phi) + (\rho y_3 + \phi \zeta)(\alpha y_3 + \gamma \eta)}{(y_2 y_3 - \zeta \theta)(y_1 y_3 - \gamma \phi) - (\rho y_3 + \phi \zeta)(\beta y_3 + \gamma \theta)}, \\ \frac{dL_{\nu_\tau}}{dT} &= \frac{\alpha y_3 + \gamma \eta + (\beta y_3 + \gamma \theta) \frac{dL_{\nu_e}}{dT}}{y_1 y_3 - \gamma \phi}, \\ \frac{dL_{\nu'_\tau}}{dT} &= \frac{1}{y_3} \left[\eta + \theta \frac{dL_{\nu_e}}{dT} + \phi \frac{dL_{\nu_\tau}}{dT} \right]. \end{aligned} \quad (112)$$

We compute the number densities incorporating Eqs. (103)–(107). The repopulation and thermalization of the neutrino momentum distributions is taken into account using the same expression as in the high temperature epoch:

$$\frac{\partial}{\partial t} \frac{N_{\nu_\alpha}(p)}{N^{\text{eq}}(p, T, 0)} \simeq \Gamma_\alpha(p) \left[\frac{N^{\text{eq}}(p, T, \mu_{\nu_\alpha})}{N^{\text{eq}}(p, T, 0)} - \frac{N_{\nu_\alpha}(p)}{N^{\text{eq}}(p, T, 0)} \right], \quad (113)$$

where $\Gamma_\alpha(p)$ is the total collision rate. The chemical potentials are computed from the lepton numbers as per Sec. III.

Observe that the oscillations will necessarily generate a significant number of $\bar{\nu}'_e$, $\bar{\nu}'_\mu$ and ν'_τ mirror neutrino species. We will make the simplifying assumption that there is negligible thermalization of these mirror neutrinos. By this we mean that the mirror weak interactions of these mirror states are weak enough to not appreciably modify the mirror neutrino momentum distributions. We will discuss later the circumstances required for this to be a valid approximation, and the expected effects when it is not valid.

In solving Eq. (112) initial conditions for L_{ν_α} and $L_{\nu'_\alpha}$ for each α must be specified at a temperature, T_{low} , that serves as the initial point for the low temperature epoch. For definiteness we take $T_{\text{low}} = T_c/2$, where T_c is the critical point

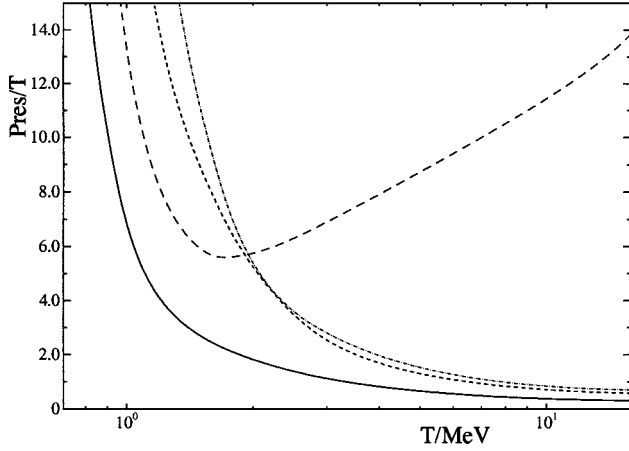


FIG. 3. Evolution of the resonance momenta P_i/T , for the example with $\delta m_{\text{large}}^2 = 50 \text{ eV}^2$. The solid line, long-dashed line, short dashed line, and dash-dotted line correspond to $P_1/T, P_2/T, P_3/T$ and P_4/T respectively.

during the high temperature epoch at which the explosive growth of L_{ν_τ} begins. Our results are quite insensitive to the precise value taken for T_{low} as long as it is high enough for the lepton numbers to be still much less than 1. (This issue is discussed more fully in Ref. [26].) The lepton numbers are related to the resonance momenta by using Eqs. (98) and (99),

$$\begin{aligned} L_{\nu_e} &= \frac{\omega}{24} \left(\frac{2}{P_1} + \frac{1}{P_2} - \frac{9}{P_3} \right), \\ L_{\nu_\tau} &= \frac{\omega}{24} \left(\frac{2}{P_1} + \frac{1}{P_2} + \frac{15}{P_3} \right), \\ L_{\nu'_\tau} &= \frac{\omega}{24} \left(\frac{14}{P_1} - \frac{17}{P_2} - \frac{15}{P_3} \right), \end{aligned} \quad (114)$$

where $\omega \equiv \delta m_{\text{large}}^2 / a_0 T^3$. (The group 4 oscillation modes have been neglected for reasons discussed earlier.) Thus, specifying the values P_i/T at $T = T_{\text{low}}$ completely fixes the values of the lepton numbers at that temperature. From our numerical work, we find that the $T \sim T_{\text{low}}$ values of the resonance momenta P_1 and P_2 are given approximately by

$$P_1/T \sim 0.3, \quad P_2/T \sim 15. \quad (115)$$

These values are approximately independent of the vacuum oscillation parameters as long as the various mixing angles obey $\sin^2 2\theta \gtrsim 10^{-10}$ and provided the δm^2 's lie in the range of interest. Also note that our subsequent numerical work is not very sensitive to the precise initial values of P_1/T and P_2/T provided that P_1/T is small (less than about 0.6) and P_2/T is large (greater than about 10). We also need to specify the initial values of the signs f_i . We take $f_1 = f_3 = 1$ and $f_2 = -1$ at $T = T_{\text{low}}$. Subsequently f_i are evaluated from the previous time step.

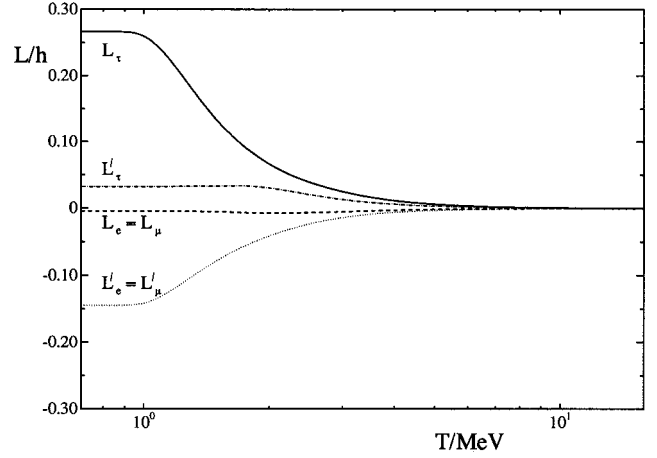


FIG. 4. Evolution of the lepton numbers for the same example as Fig. 3.

In the region during and just after the exponential growth, the initial production of L_{ν_e} and L_{ν_μ} due to the oscillations $\bar{\nu}_\tau \leftrightarrow \bar{\nu}_e$ and $\bar{\nu}_\tau \leftrightarrow \bar{\nu}_\mu$ is suppressed because the number densities of all the ordinary neutrino flavors are almost equal. At $T = T_{\text{low}}$ we find that the creation of lepton number due to these oscillations is approximately negligible. This means that the main contribution to L_{ν_e} , L_{ν_μ} and $L_{\nu'_\tau}$ at $T \sim T_{\text{low}}$ is from $\nu'_\tau \leftrightarrow \nu_{e,\mu}$ oscillations, and thus $L_{\nu'_\tau} \approx -2L_{\nu_e}$. It follows that the initial value for P_3/T can be approximately related to the initial values of P_1/T and P_2/T by

$$\frac{1}{P_3} \approx \frac{18}{33P_1} - \frac{15}{33P_2}. \quad (116)$$

We have solved this system of equations for the illustrative example of $\delta m_{\text{large}}^2 = 50 \text{ eV}^2$. In Fig. 3 we show the evolution of the four resonance momenta P_i/T . The evolution of L_{ν_α} and $L_{\nu'_\alpha}$ for the same $\delta m_{\text{large}}^2$ parameter choice is plotted in Fig. 4 for the $L_{\nu_\tau} > 0$ case.

Let us now turn to the implications of the oscillations for BBN. The change in Y_P due to the neutrino oscillations can be separated into two contributions,

$$\delta Y_P = \delta_1 Y_P + \delta_2 Y_P, \quad (117)$$

where $\delta_1 Y_P$ is the change due to the effect of the modified electron neutrino momentum distributions on the reaction rates, and $\delta_2 Y_P$ is due to the change in the energy density (or equivalently the change in the expansion rate of the universe). The former effect can be determined by numerically integrating the rate equations for the processes given in Eq. (85) using the modified electron neutrino momentum distributions N_{ν_e} and $N_{\bar{\nu}_e}$ as discussed in Appendix A. The latter contribution can be computed from the momentum distributions of the ordinary and mirror neutrinos through

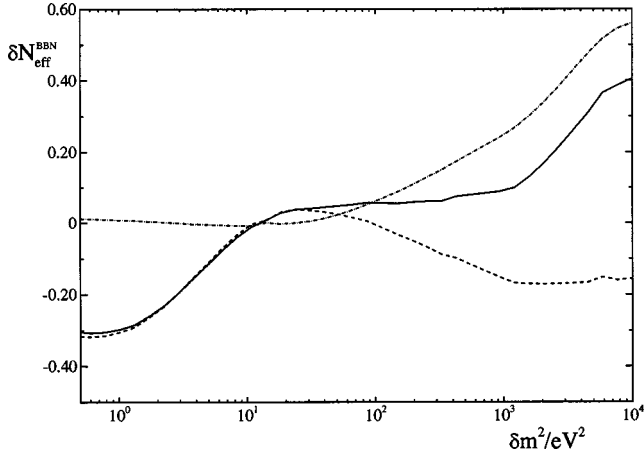


FIG. 5. $\delta N_{\nu, \text{eff}}$ versus $\delta m_{\text{large}}^2$ for case 1 [see Eqs. (91), (92)]. The dashed line is the contribution $\delta_1 N_{\nu, \text{eff}}$ due to the effects of the L_{ν_e} asymmetry while the dash-dotted line is the contribution $\delta_2 N_{\nu, \text{eff}}$ due to the change in the expansion rate. The solid line is the total contribution $\delta_1 N_{\nu, \text{eff}} + \delta_2 N_{\nu, \text{eff}}$. This figure considers the case $L_{\nu_\tau} < 0$.

$$\delta_2 Y_P \approx 0.012 \left(\frac{1}{2\rho_0} \sum_{\alpha=1}^3 \int_0^\infty [N_{\nu_\alpha}(p) + N_{\bar{\nu}_\alpha}(p) + N_{\nu'_\alpha}(p) + N_{\bar{\nu}'_\alpha}(p)] p dp - 3 \right), \quad (118)$$

where

$$\rho_0 \equiv \int_0^\infty N^{\text{eq}}(p, T, 0) p dp = \frac{7\pi^2}{240} T^4 \quad (119)$$

is the energy density of a Weyl fermion at equilibrium with zero chemical potential. [Recall that Eq. (86) can be used to express δY_P , $\delta_1 Y_P$ and $\delta_2 Y_P$ in terms of effective neutrino number, $\delta N_{\nu, \text{eff}}$, $\delta_1 N_{\nu, \text{eff}}$ and $\delta_2 N_{\nu, \text{eff}}$, respectively.] To calculate $\delta_2 Y_P$, we numerically determine the momentum distributions at $T=0.5$ MeV. Because of the approximate kinetic decoupling of neutrinos for temperatures below about 3–4 MeV, large contributions²⁵ to $\delta_2 Y_P$, should they exist, must have been generated earlier. A temperature of 0.5 MeV is therefore a safe place to evaluate the final $\delta_2 Y_P$.

Recall that there is an ambiguity concerning the sign of the L_{ν_τ} lepton asymmetry. We have considered the $L_{\nu_\tau} > 0$ case above for definiteness, but $L_{\nu_\tau} < 0$ is equally likely *a priori*. (See Ref. [25] for further discussion of this.) For the negative L_{ν_τ} case, the roles of particles and anti-particles are reversed for the modes quoted in Eq. (96) and subsequent equations. One consequence of this is that the signs of all the other asymmetries are also reversed. The quantity $\delta_1 Y_P$ will obviously be significantly affected by this ambiguity in sign, while $\delta_2 Y_P$ will not be affected at all. This means that we have two possible values for the overall change in the effective

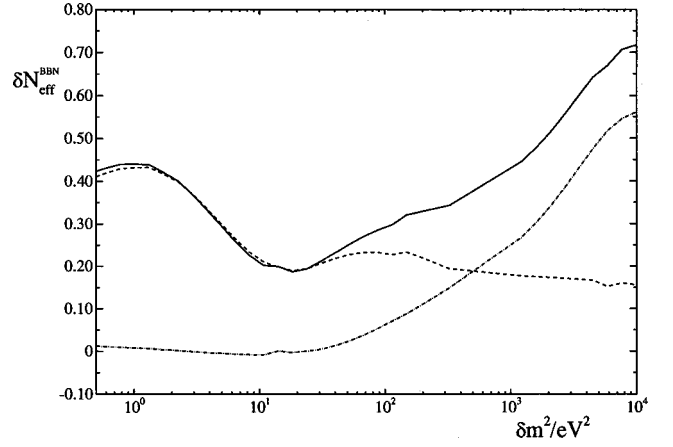


FIG. 6. Same as Fig. 5 except $L_{\nu_\tau} > 0$ is considered.

number of neutrino flavors during BBN. The results of the numerical work is presented in Figs. 5 and 6. Figure 5 treats the $L_{\nu_\tau} < 0$ case (which it turns out means that $L_{\nu_e} > 0$), while Fig. 6 displays the $L_{\nu_\tau} > 0$ case (which implies that $L_{\nu_e} < 0$).

Observe that $\delta_1 Y_P$ is not very large. The main contribution to it is from the modification of the high momentum tail of the ν_e distribution due to the group 2 $\nu'_\tau \leftrightarrow \nu_e$ oscillations. This is partially offset by the modification of the $\bar{\nu}_e$ distribution due to $\bar{\nu}_\tau \leftrightarrow \bar{\nu}_e$ oscillations. It is also evident that $\delta_2 Y_P$ is close to zero for $\delta m_{\text{large}}^2 \lesssim 300$ eV². This is simply because the generation of mirror states, which is dominated by the $\nu_\tau \leftrightarrow \nu'_e$ and $\nu_\tau \leftrightarrow \nu'_\mu$ modes, occurs below the kinetic decoupling temperature for ν_τ 's. This means that the ν_τ states which have converted into mirror states are not repopulated. For larger values of $\delta m_{\text{large}}^2$, the ν_τ states begin to get repopulated, and the energy density increases accordingly. We should also emphasize that our calculations contain approximations. The most important are that the repopulation is handled approximately via Eq. (113) and we have neglected mirror thermalization. Thus, our results have a theoretical uncertainty, which we estimate to be of order $\delta N_{\nu, \text{eff}} \sim 0.3$ (see following discussion).

We now discuss in more detail the effects of mirror neutrino thermalization. Recall that in the foregoing computations, we have included mirror neutrino thermalization via the quantity $\gamma_\rho \equiv (T'/T)^4$ during the high temperature epoch, but neglected it during the low temperature epoch. (Remember that mirror weak interaction rates increase with temperature.) We now discuss when this approximation is valid and the expected effects when it is not.

Given our division of the evolution of the system into high and low temperature epochs, it is convenient to also classify mirror weak interactions into two categories. The first category consists of the interactions of the mirror neutrinos generated during the low temperature epoch with the background mirror neutrinos, electrons and positrons left over from the preceding high temperature epoch [“mirror high- T background” (MHTB)]. The second category is the elastic collisions of the $\bar{\nu}'_e$, $\bar{\nu}'_\mu$ and ν'_τ neutrinos generated

²⁵By “large contributions” we mean $\delta_2 N_{\nu, \text{eff}} \gtrsim 0.10$.

during the low temperature epoch with themselves. We now estimate each of these thermalization rates.

The interaction rate of a mirror neutrino ν'_α of momentum p with the MHTB is approximately given by

$$\Gamma_m(p) = \gamma_\rho \Gamma(p) \approx \gamma_\rho \gamma_\alpha G_F^2 T^5 \left(\frac{p}{3.15T} \right). \quad (120)$$

Now, from the discussion above [see Eq. (96)], the additional mirror neutrino states created during the low temperature epoch consist of the flavors $\bar{\nu}'_e$, $\bar{\nu}'_\mu$ and ν'_τ . Their interactions with the MHTB can be approximately neglected if

$$\frac{\Gamma_m(p)}{H} \lesssim 1 \Rightarrow \gamma_\rho \gamma_\alpha G_F^2 \frac{M_P}{5.5} \left(\frac{p}{3.15T} \right) T^3 \lesssim 1. \quad (121)$$

As summarized in Fig. 3, the resonance momentum P_2/T for the modes producing ν'_τ 's is always higher than the resonance momentum P_1/T for the modes producing $\bar{\nu}'_e$ and $\bar{\nu}'_\mu$. The mirror thermalization effects will therefore be most important for the ν'_τ states. It is also clear that the relatively high momentum ν'_τ states are produced at a higher temperature than $\bar{\nu}'_e$ and $\bar{\nu}'_\mu$ states of a corresponding momentum. The temperature range of interest for the ν'_τ lies between $T_{\text{low}} \approx T_c/2$ and the temperature T_{min} at which P_2/T reaches its minimum value of ≈ 6 .

We can easily numerically compute T_{min} to obtain

$$\frac{T_{\text{min}}}{\text{MeV}} \approx 0.70 \left(\frac{\delta m_{\text{large}}^2}{\text{eV}^2} \right)^{1/4}. \quad (122)$$

We now estimate the effects of thermalization by considering the interaction rate for a ν'_τ with a typical momentum of $p/T \sim 8$ at a temperature around or slightly higher than T_{min} . Although the constraint, Eq. (121), on γ_ρ is stronger for higher values of T , the number of ν'_τ 's produced is lower, so the effects of their thermalization will be correspondingly weaker. The choices made for p/T and T as input for Eq. (121) represent a reasonable ‘‘compromise’’ driven by these considerations. So we estimate that the interactions of ν'_τ with the MHTB can be neglected provided that

$$\gamma_\rho \lesssim \frac{1}{3T_{\text{min}}^3} \sim \left(\frac{\text{eV}^2}{\delta m_{\text{large}}^2} \right)^{3/4}. \quad (123)$$

We now estimate the thermalization rate, due to elastic collisions with themselves and with the $\bar{\nu}'_{e,\mu}$ states produced during the low temperature epoch, of the mirror ν'_τ states produced during the low temperature epoch. We will collectively call the mirror neutrino/antineutrino states produced during the low temperature epoch the ‘‘mirror low- T background’’ (MLTB). Let us denote the collision rate for a ν'_τ of momentum p with the $\bar{\nu}'_{e,\mu}$ (ν'_τ) component of the MLTB by $\Gamma_1(p)$ [$\Gamma_2(p)$]. The relevant collision rates can be obtained from Ref. [43] to yield

$$\Gamma_1(p) \approx 0.13 G_F^2 T^5 \left(\frac{\rho_{\bar{\nu}'_e} + \rho_{\bar{\nu}'_\mu}}{\rho_0} \right) \left(\frac{p}{3.15T} \right),$$

$$\Gamma_2(p) \approx 0.77 G_F^2 T^5 \left(\frac{\rho_{\nu'_\tau}}{\rho_0} \right) \left(\frac{p}{3.15T} \right), \quad (124)$$

where ρ_0 is defined in Eq. (119). So the interactions of the ν'_τ with the $\bar{\nu}'_{e,\mu}$ (ν'_τ) MLTB can be approximately neglected provided that

$$\frac{\Gamma_1}{H} \lesssim 1 \Rightarrow 0.13 G_F^2 T^3 \frac{M_P}{5.5} \left(\frac{\rho_{\bar{\nu}'_e} + \rho_{\bar{\nu}'_\mu}}{\rho_0} \right) \left(\frac{p}{3.15T} \right) \lesssim 1,$$

$$\frac{\Gamma_2}{H} \lesssim 1 \Rightarrow 0.77 G_F^2 T^3 \frac{M_P}{5.5} \left(\frac{\rho_{\nu'_\tau}}{\rho_0} \right) \left(\frac{p}{3.15T} \right) \lesssim 1. \quad (125)$$

Our numerical work shows that $(\rho_{\bar{\nu}'_e} + \rho_{\bar{\nu}'_\mu})/\rho_0 \ll 1$ until quite low temperatures $T/\text{MeV} \lesssim (\delta m_{\text{large}}^2/\text{eV}^2)^{1/4}$. In fact the second condition in Eq. (125), from $\nu'_\tau \nu'_\tau$ elastic collisions, is the more stringent requirement. For this case we can estimate the collision rate by considering a ν'_τ of typical momentum $p/T \sim 8$, which is produced at a temperature $T/\text{MeV} \sim 1.3(\delta m_{\text{large}}^2/\text{eV}^2)^{1/4}$. The ratio of energy densities required is estimated from adiabatic conversion as P_2/T evolves from its initial value to about 8:

$$\frac{\rho_{\nu'_\tau}}{\rho_0} \approx \frac{T^4}{2\pi^2 \rho_0} \int_8^\infty \frac{y^3 dy}{1+e^y} \approx 0.04. \quad (126)$$

Using these numbers we estimate from Eq. (125) that $\nu'_\tau \nu'_\tau$ elastic collisions can be approximately neglected provided that

$$0.05 \left(\frac{\delta m_{\text{large}}^2}{\text{eV}^2} \right)^{3/4} \lesssim 1 \Rightarrow \delta m_{\text{large}}^2 \lesssim 50 \text{ eV}^2. \quad (127)$$

It turns out that this numerical bound is not very sensitive to what we choose for a ‘‘typical’’ P_2/T , so it is fairly robust. Thus, in summary, we conclude that the thermalization of the mirror neutrinos can be approximately neglected provided that

$$\gamma_\rho \lesssim \left(\frac{\text{eV}^2}{\delta m_{\text{large}}^2} \right)^{3/4} \quad \text{and} \quad \delta m_{\text{large}}^2 \lesssim 50 \text{ eV}^2. \quad (128)$$

Let us now discuss what happens when there is significant thermalization of the mirror neutrinos. Let us first consider the case of the ν'_τ states. If they are thermalized, the ν'_τ distribution will be close to an equilibrium distribution given by

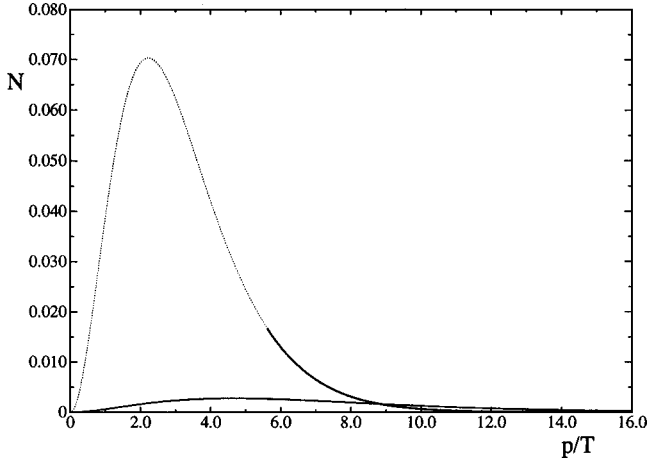


FIG. 7. $N_{\nu'_\tau}^{\text{eq}}$ (bottom solid line) at the temperature $T = T_{\min}$ (see text) for the example of Figs. 3 and 4. The top solid line is the expected distribution of ν'_τ 's if the thermalization due to the mirror weak interactions is neglected. The unit along the vertical axis is MeV^2 .

$$N_{\nu'_\tau}^{\text{eq}} = \frac{1}{2\pi^2} \frac{p^2}{1 + \exp\left(\frac{p - \mu_{\nu'_\tau}}{T_{\nu'_\tau}}\right)}. \quad (129)$$

The elastic ν'_τ collisions with the background ν'_τ conserve both the number density $n_{\nu'_\tau}$ and energy density $\rho_{\nu'_\tau}$, so these quantities can be used to determine the two parameters $\mu_{\nu'_\tau}$ and $T_{\nu'_\tau}$. Now,

$$\begin{aligned} n_{\nu'_\tau} &= \int_0^\infty N_{\nu'_\tau} dp \approx \frac{T_{\nu'_\tau}^3}{\pi^2} e^{\mu_{\nu'_\tau}/T_{\nu'_\tau}}, \\ \rho_{\nu'_\tau} &= \int_0^\infty N_{\nu'_\tau} p dp \approx \frac{3T_{\nu'_\tau}^4}{\pi^2} e^{\mu_{\nu'_\tau}/T_{\nu'_\tau}}. \end{aligned} \quad (130)$$

Thus,

$$T_{\nu'_\tau} = \frac{\rho_{\nu'_\tau}}{3n_{\nu'_\tau}}, \quad \mu_{\nu'_\tau} = T \ln\left(\frac{27\pi^2 n_{\nu'_\tau}^4}{\rho_{\nu'_\tau}^3}\right). \quad (131)$$

Hence, for any T , we can compute $T_{\nu'_\tau}$ and $\mu_{\nu'_\tau}$ by computing $\rho_{\nu'_\tau}$ and $n_{\nu'_\tau}$ from $N_{\nu'_\tau}$. To estimate the effects of the repopulation we use the equation

$$\left. \frac{d}{dt} \frac{N_{\nu'_\tau}(p)}{N^{\text{eq}}(p, T, 0)} \right|_{\text{repop}} \approx \Gamma_2(p) \left[\frac{N_{\nu'_\tau}^{\text{eq}}(p)}{N^{\text{eq}}(p, T, 0)} - \frac{N_{\nu'_\tau}(p)}{N^{\text{eq}}(p, T, 0)} \right], \quad (132)$$

where $\Gamma_2(p)$ is the elastic $\nu'_\tau \nu'_\tau$ collision rate quoted earlier.

The most important effect of the thermalization of the ν'_τ occurs when P_2/T evolves from $P_2/T|_{\min}$ to infinity. For the example of Figs. 3 and 4, namely $\delta m_{\text{large}}^2 = 50 \text{ eV}^2$, we have computed $N_{\nu'_\tau}^{\text{eq}}$ at the temperature T_{\min} . This is shown in Fig. 7 as a function of p/T in order to compare this distribution with the distribution of ν'_τ states which would exist in the absence of ν'_τ thermalization. In this latter case, the MSW transitions that occurred during the previous evolution of P_2/T from about 15 down to about 6 populated the ν'_τ states from the tail of the $\nu_{e,\mu}$ distributions (which have approximately negligible chemical potentials in this region). Furthermore, ordinary weak interactions repopulated the depleted $\nu_{e,\mu}$ tails. This means that, in the absence of mirror thermalization, the journey back from $P_2/T|_{\min}$ to infinity is dynamically inert as the oscillating species always have approximately equal number densities in the resonance region. However, if the ν'_τ 's are thermalized, this is not the case.

Computing the evolution of the system when P_2/T evolves from $P_2/T|_{\min}$ back to high values appears to be problematic. The problem is that in this region the resonance momenta P_2^a and P_2^b for the modes $\nu'_\tau \leftrightarrow \nu_e$ and $\nu'_\tau \leftrightarrow \nu_\mu$, respectively, are not dynamically driven to coincide. Thus, in this case, we might expect different results depending on which resonance momentum goes first. Since the previous evolution of the system was such that the two resonance momenta coincided, it is not clear which resonance momentum will in fact go first. For instance, the result may well depend on a statistical fluctuation, and therefore may be different in different regions of the universe. The physical implication of this would be a spatially dependent Y_p distribution.

We have made some numerical estimates using the prescription given in Eq. (106). Our numerical results indicate that the overall affect of ν'_τ thermalization is not unacceptably large, typically about $\delta N_{\nu_{\text{eff}}} \sim 0.3$ (for the entire range of interest in $\delta m_{\text{large}}^2$). For $L_{\nu'_\tau} > 0$ the effect is positive, that is $\delta N_{\nu_{\text{eff}}} \sim +0.3$, while for $L_{\nu'_\tau} < 0$ the effect is negative, that is $\delta N_{\nu_{\text{eff}}} \sim -0.3$. This essentially results in a theoretical error of this magnitude for the parameter space region which violates the bounds in Eq. (128).

C. Low temperature neutrino asymmetry evolution in the EPM: Case 2

We now consider the case where the ν_μ and ν'_μ masses are not negligible. This is of considerable interest since $m_{\nu_{\mu\pm}} \sim 1 \text{ eV}$ is expected if the LSND anomaly [23] is due to neutrino oscillations. We consider the mass hierarchy

$$m_{\nu_{\tau+}} \approx m_{\nu_{\tau-}} \gg m_{\nu_{\mu+}} \approx m_{\nu_{\mu-}} \gg m_{\nu_{e+}}, m_{\nu_{e-}}. \quad (133)$$

In case 2, there are two δm^2 scales. The modes listed in Eq. (93) have the large $\delta m^2 \equiv \delta m_{\text{large}}^2$, while

$$\nu_\mu \leftrightarrow \nu'_e, \quad \nu_\mu \leftrightarrow \nu_e, \quad \nu'_\mu \leftrightarrow \nu_e, \quad \nu'_\mu \leftrightarrow \nu'_e, \quad (134)$$

plus the associated antiparticle modes have the smaller $\delta m^2 \equiv \delta m_{\text{small}}^2$. The specification of the parameter space of

interest is completed by taking the remaining modes, $\nu_\alpha \leftrightarrow \nu'_\alpha$ for $\alpha = e, \mu, \tau$, to have a negligible δm^2 (much smaller than $\delta m_{\text{small}}^2$).

The four modes in Eq. (134) typically have distinct resonance momenta which we denote as follows:

$$\begin{aligned} \bar{\nu}_\mu \leftrightarrow \bar{\nu}'_\mu, \quad p_{\text{res}} = P_1, \\ \nu'_\mu \leftrightarrow \nu_e, \quad p_{\text{res}} = P_2, \\ \bar{\nu}_\mu \leftrightarrow \bar{\nu}_e, \quad p_{\text{res}} = P_3, \\ \bar{\nu}'_\mu \leftrightarrow \bar{\nu}'_e, \quad p_{\text{res}} = P_4. \end{aligned} \quad (135)$$

The resonance momenta for each of these modes can be obtained from Eq. (97),

$$\frac{p_i}{T} = \frac{\delta m_{\text{small}}^2}{a_0 T^4 L_i}, \quad (136)$$

where $i = 1, \dots, 4$ and

$$\begin{aligned} L_1 &\equiv L^{(\mu)} - L'^{(e)} = 2L_{\nu_\mu} + L_{\nu_\tau} + L_{\nu_e} - 2L_{\nu'_e} - L_{\nu'_\mu} - L_{\nu'_\tau}, \\ L_2 &\equiv -(L'^{(\mu)} - L^{(e)}) \\ &= -2L_{\nu'_\mu} - L_{\nu'_e} - L_{\nu'_\tau} + 2L_{\nu_e} + L_{\nu_\mu} + L_{\nu_\tau}, \\ L_3 &\equiv L^{(\mu)} - L^{(e)} = L_{\nu_\mu} - L_{\nu_e}, \\ L_4 &\equiv L'^{(\mu)} - L'^{(e)} = L_{\nu'_\mu} - L_{\nu'_e}. \end{aligned} \quad (137)$$

Observe that we use the lowercase p_i notation for the $\delta m_{\text{small}}^2$ modes of Eq. (135) and the uppercase P_i notation for the $\delta m_{\text{large}}^2$ modes of Eq. (96).

Since $\delta m_{\text{small}}^2 \ll \delta m_{\text{large}}^2$, it follows that $p_{1,2} \ll P_i$. (Note however that p_3 and p_4 start out being infinitely large because of the $L_{\nu_e} = L_{\nu'_\mu}$ and $L_{\nu'_e} = L_{\nu'_\mu}$ conditions. As we will explain shortly, these two modes have little effect.) For our numerical work, we will consider the parameter space region where the hierarchy between $\delta m_{\text{small}}^2$ and $\delta m_{\text{large}}^2$ is great enough so that $p_{1,2}/T \leq 0.5$ when $P_i/T \geq 10$. Numerically, this corresponds to $\delta m_{\text{large}}^2 \geq 50 \delta m_{\text{small}}^2$. Let us denote by $T = T_x$ the temperature at which the P_i/T are all greater than 10. From Fig. 3 and Eq. (97) it is easy to see that T_x is given by

$$\frac{T_x}{\text{MeV}} \approx 0.3 \left(\frac{\delta m_{\text{large}}^2}{\text{eV}^2} \right)^{1/4}. \quad (138)$$

The evolution of the neutrino ensemble during the low temperature epoch for case 2 therefore breaks up into two temperature regions: $T \geq T_x$ and $T \leq T_x$. When $T \geq T_x$, the evolution of the system is dominated by the $\delta m_{\text{large}}^2$ modes of Eq. (96), because the $\delta m_{\text{small}}^2$ modes are negligible due to their very small resonance momenta. In this temperature region the evolution of the lepton numbers and number densi-

ties can be evaluated using the equations of the previous section. When $T \leq T_x$, the $\delta m_{\text{large}}^2$ modes are no longer effective, because they all have $P_i/T \geq 10$. The $\delta m_{\text{small}}^2$ modes begin to become important. For $\delta m_{\text{small}}^2 \sim 1 \text{ eV}^2$, it follows from Eq. (136) that $p_{1,2}/T \sim 1$ for $T \sim 1 \text{ MeV}$. This means that for $\delta m_{\text{small}}^2$ in the LSND range, the oscillation modes of Eq. (134) become important while the BBN reactions $n \leftrightarrow p$ are still rapid. So these oscillations can potentially influence BBN and therefore should not be ignored.

It turns out that it is not possible to use the adiabatic approximation [as encoded in Eq. (90)] to work out the effects of the oscillation subsystem given in Eq. (134). This is because of the structure of Eq. (136). For example, $\nu'_\mu \leftrightarrow \nu_e$ oscillations create significant L_{ν_e} asymmetry, as p_2/T sweeps through the ν_e momentum distribution. The L_{ν_e} asymmetry becomes so large that $L_2 \rightarrow 0$. This makes the rate of change of p_2/T very large and the system is no longer adiabatic. Because of this complication, we will analyze the effects of the modes in Eq. (134) using the quantum kinetic equations.

We start integrating the QKEs for the subsystem of Eq. (134) at $T = T_x$ with the values of the number distributions N_{ν_α} and $N_{\nu'_\alpha}$, and the lepton numbers L_{ν_α} and $L_{\nu'_\alpha}$ ($\alpha = e, \mu, \tau$) obtained from the evolution equations of the previous subsection. We will not explicitly write down the QKEs for this subsystem here, because their form is obvious once the contents of Sec. IV above have been understood. Nevertheless, for completeness we will include them in Appendix B. The reader, however, should note the following points:

(1) We utilize the approximation that the x and y components of the polarization vectors for the modes of Eq. (134) vanish at $T = T_x$. While this is not expected to actually be

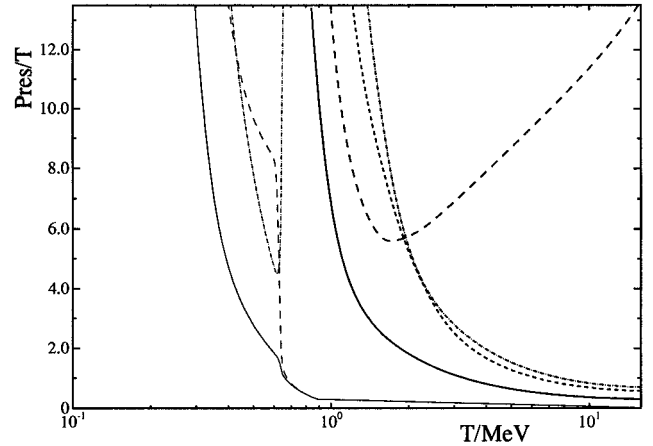


FIG. 8. Evolution of the resonance momenta P_i/T and p_i/T for the example with $\delta m_{\text{large}}^2 = 50 \text{ eV}^2$ and $\delta m_{\text{small}}^2 = 1 \text{ eV}^2$. The bold lines on the right of the figure correspond to the $\delta m_{\text{large}}^2$ modes and the thin lines on the left of the figure correspond to the $\delta m_{\text{small}}^2$ modes. For the bold lines, the solid line, long-dashed line, short-dashed line, and dash-dotted line correspond to $P_1/T, P_2/T, P_3/T$ and P_4/T respectively. For the thin lines, the solid line, long-dashed line and dash-dotted line correspond to $p_1/T, p_2/T$ and $p_3/T = p_4/T$ respectively.

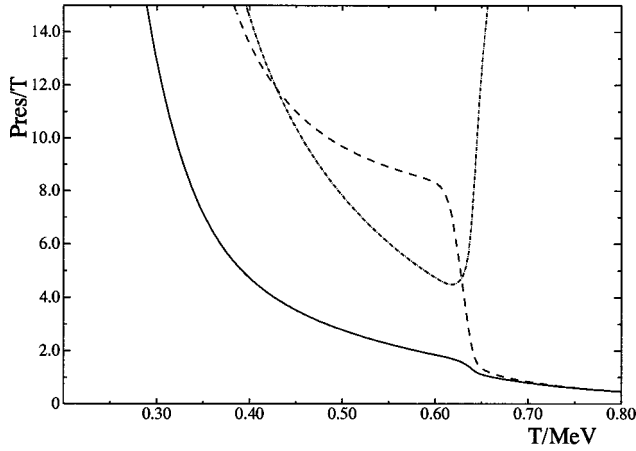


FIG. 9. Magnified version of the left-hand side of Fig. 8.

the case, the subsequent evolution is not sensitive to the particular choices made for the initial values. This is because the resonance momenta for the subsystems are either very small or very large, so the very first stage of the evolution after $T=T_x$ is fairly unimportant. Furthermore, correct values for the x and y components are quickly generated by the QKEs soon after $T=T_x$.

(2) Repopulation and thermalization of the mirror neutrino ensembles have been neglected, consistent with our treatment of the evolution between the end of the high temperature epoch and $T=T_x$. Actually, this is an excellent approximation in this regime, since for typical interesting parameter choices the mirror sector temperature is quite low.

(3) The ordinary-ordinary $\bar{\nu}_\mu \leftrightarrow \bar{\nu}_e$ and mirror-mirror $\nu'_\mu \leftrightarrow \nu'_e$ modes can, to a good approximation, actually be omitted. Recall that the resonance momenta p_3 and p_4 are initially very large, much larger than p_1 and p_2 respectively. Subsequent evolution maintains this hierarchy in the resonance momenta. The $\bar{\nu}_\mu \leftrightarrow \bar{\nu}_e$ mode, with resonance momentum p_1 , is strongly reprocessing lepton number as the resonance moves through the body of the $\bar{\nu}_\mu$ distribution. The coupled $\bar{\nu}_\mu \leftrightarrow \bar{\nu}_e$ mode, on the other hand, sees its resonance

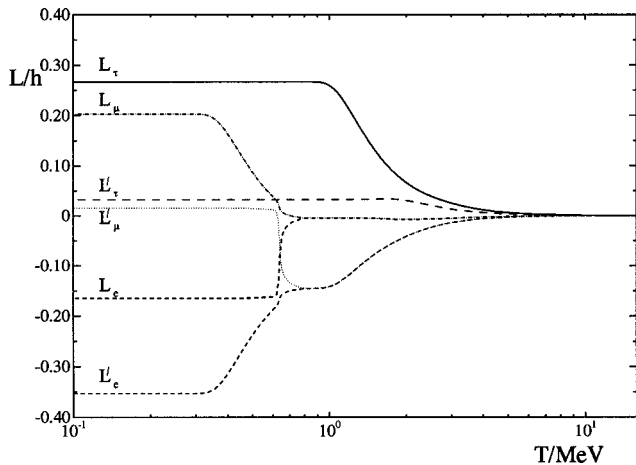


FIG. 10. Evolution of the lepton numbers for the same example as Figs. 8 and 9.

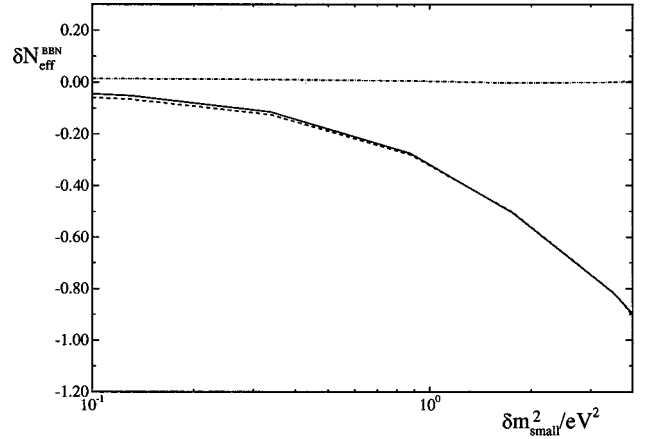
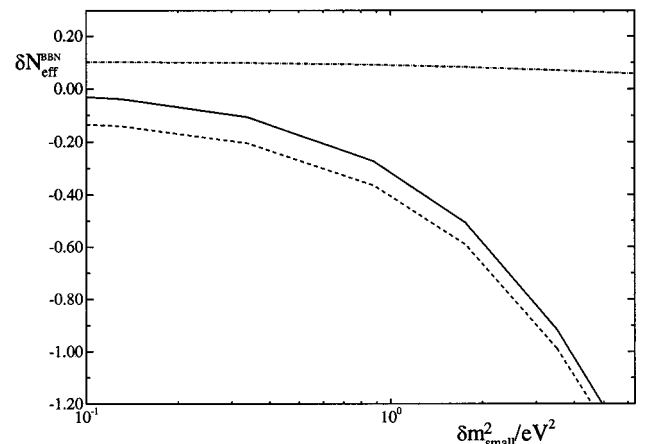


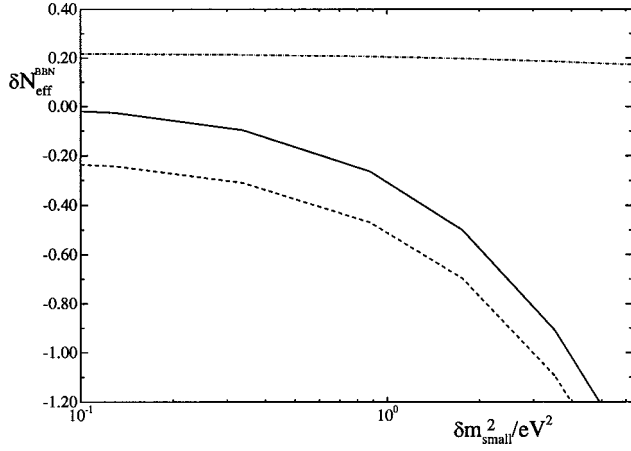
FIG. 11. $N_{\nu,\text{eff}}$ versus $\delta m_{\text{small}}^2$ with $\delta m_{\text{large}}^2 = 50 \text{ eV}^2$. The case $L_{\nu_\tau} < 0$ (which it turns out implies $L_{\nu_e} > 0$) has been considered. The dashed line is the contribution $\delta_1 N_{\nu,\text{eff}}$ due to the effects of the L_{ν_e} asymmetry while the dash-dotted line is the contribution $\delta_2 N_{\nu,\text{eff}}$ due to the change in the expansion rate. The solid line is the total contribution $\delta_1 N_{\nu,\text{eff}} + \delta_2 N_{\nu,\text{eff}}$.

momentum p_3 remain in the tail of the distribution, where it is ineffective because of the essentially identical number densities of $\bar{\nu}_\mu$ and $\bar{\nu}_e$ in the tail. Remember that because weak interaction rates after typical values of T_x are getting quite weak, there is little thermalization of the reprocessed e and μ asymmetries created at low momenta p_1 . In other words, the p_3 resonance barely “knows” the asymmetry is there.

In Figs. 8 and 9 we plot the evolution of the resonance momenta, P_i/T and p_i/T for an illustrative example. We choose $\delta m_{\text{large}}^2 = 50 \text{ eV}^2$, $\delta m_{\text{small}}^2 = 1 \text{ eV}^2$ and all of the vacuum mixing angles to be 10^{-8} . We emphasize that our results should be approximately independent of the vacuum mixing angles as long as $10^{-10} \lesssim \sin^2 2\theta \ll 1$. In Fig. 10 we plot the evolution of all of the asymmetries for the same example.

The effect of the oscillations on BBN is given in Figs. 11–16. In Fig. 11 we have plotted $N_{\nu,\text{eff}}$ versus $\delta m_{\text{small}}^2$, with $\delta m_{\text{large}}^2 = 50 \text{ eV}^2$ and $L_{\nu_\tau} < 0$. Figures 12 and 13 are similar

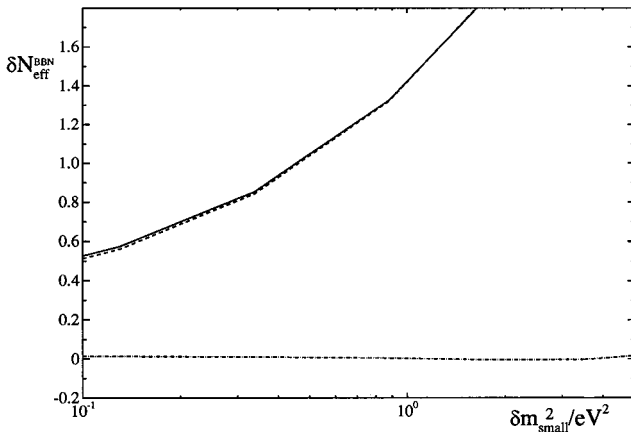
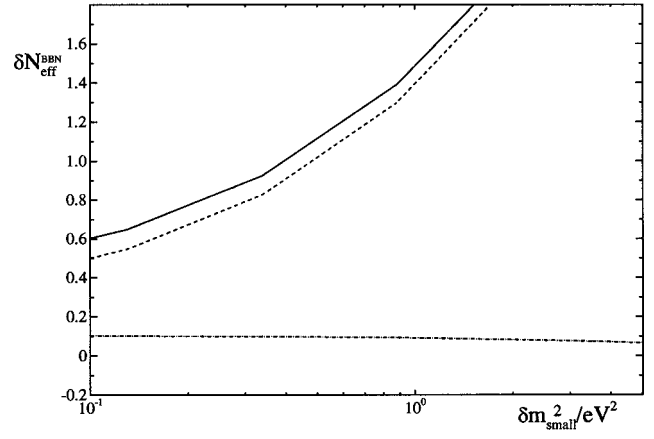

 FIG. 12. Same as Fig. 11 except $\delta m_{\text{large}}^2 = 200 \text{ eV}^2$.

FIG. 13. Same as Fig. 11 except $\delta m_{\text{large}}^2 = 800 \text{ eV}^2$.

except $\delta m_{\text{large}}^2 = 200$ and 800 eV^2 , respectively. Figures 14–16 are the same as Figs. 11–13 except that the opposite sign asymmetries have been considered. *It is very important to note that the effect of a nonzero $\delta m_{\text{small}}^2$ is considerable. In particular, as Figs. 11–13 illustrate, $N_{\nu, \text{eff}}$ depends sensitively on $\delta m_{\text{small}}^2$, with negative corrections to $N_{\nu, \text{eff}}$ equal to about one effective neutrino flavor achieved for $\delta m_{\text{small}}^2$ values in the few eV^2 range.* In Figs. 14–16 observe that L_{ν_e} has a large effect even at very low values compared to the corresponding effect in Figs. 11–13. This asymmetry is due to the neutron/proton mass difference.

Recall that Figs. 11–16 have not included the effects of mirror neutrino thermalization. As already discussed, these effects should be significant for the modes with $\delta m^2 = \delta m_{\text{large}}^2$ if $\delta m_{\text{large}}^2 \gtrsim 50 \text{ eV}^2$. The thermalization of mirror neutrinos should have negligible effect for the modes with $\delta m^2 = \delta m_{\text{small}}^2$ because they are only important when the temperature is typically less than about 1 MeV. As discussed earlier, our rough estimate of the effect of the mirror thermalization is about $\delta N_{\nu, \text{eff}} \sim 0.3$. For $L_{\nu_\tau} < 0$ ($L_{\nu_\tau} > 0$), the effect of mirror thermalization should be to *decrease (increase)* $\delta N_{\nu, \text{eff}}$ by of order -0.3 ($+0.3$).

As mentioned above, the numerical results were obtained

FIG. 14. Same as Fig. 11 except $L_{\nu_\tau} > 0$ (and hence $L_{\nu_e} < 0$) is considered.FIG. 15. Same as Fig. 12 except $L_{\nu_\tau} > 0$ (and hence $L_{\nu_e} < 0$) is considered.

using the parameter choice $\sin^2 2\theta_{\mu e'} = 10^{-8}$. Actually we expect the results to be quite insensitive to $\sin^2 2\theta_{\mu e'}$ as long as $\sin^2 2\theta_{\mu e'} \ll 1$. The reason is that the amount of L_{ν_e} that gets created is already close to the maximal amount possible. That is, after its rapid creation (which is at $T \sim 0.6 \text{ MeV}$ in the example in Fig. 8), the quantity $L^{(e\mu')} \sim 0$. Increasing $\sin^2 2\theta_{\mu e'}$ cannot increase the amount of L_{ν_e} much since it is already close to the maximum possible. Also, it cannot be created much earlier. Thus, the results shown in Figs. 11–16 should be approximately independent of $\sin^2 2\theta_{\mu e'}$.²⁶

Finally, we should remark that the results of this section indicate that the bounds obtained in Sec. IV can be evaded somewhat. The reason is that even if $\delta N_{\nu, \text{eff}} \approx 1.5$ from the high temperature population of mirror states from the $\nu_\tau \rightarrow \nu'_\mu$ oscillations, this can be compensated by a $\delta N_{\nu, \text{eff}} \sim -1.0$ from the low temperature generation of a large L_{ν_e} asymmetry.

VI. IMPLICATIONS FOR HOT DARK MATTER

In the scenario considered in this paper, where $\nu_\mu \leftrightarrow \nu'_\mu$ oscillations solve the atmospheric neutrino anomaly, a BBN bound of $N_{\nu, \text{eff}} \lesssim 3.6$ implies $m_{\nu_\tau} \gtrsim 1 \text{ eV}$ for $|\delta m_{\text{atmos}}^2| \approx 10^{-2.5} \text{ eV}^2$ (see Fig. 2). Neutrino masses in the eV range have long been considered cosmologically interesting, because they would make a significant contribution to the energy density of the universe. In the standard big bang model, the contribution of massive standard neutrinos to the energy density is given by the well known formula

$$\Omega_\nu = \frac{\sum_\alpha m_{\nu_\alpha}}{h^2 92 \text{ eV}}, \quad (139)$$

²⁶We have numerically checked this by looking at the case $\sin^2 2\theta_{\mu e'} = 10^{-7}$ and found almost identical results. We have also checked smaller $\sin^2 2\theta_{\mu e'}$. For $\sin^2 2\theta_{\mu e'} \lesssim 10^{-9}$ the oscillations begin to become so non-adiabatic that the oscillations start to become less effective.

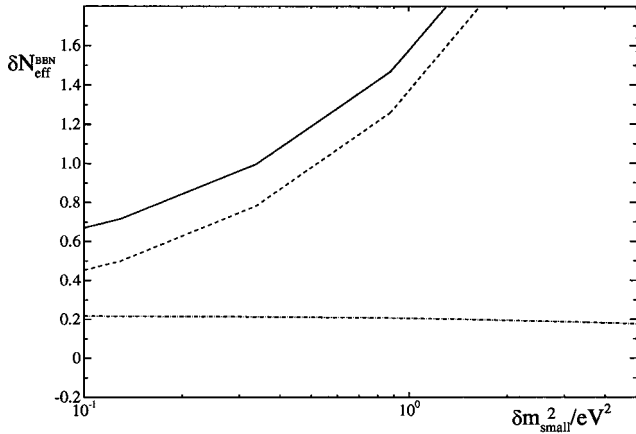


FIG. 16. Same as Fig. 13 except $L_{\nu_\tau} > 0$ (and hence $L_{\nu_e} < 0$) is considered.

where h is the usual cosmological parameter parametrizing the uncertainty in the Hubble constant. Thus, neutrinos in the eV mass range are a well known and well motivated candidate for hot dark matter.

Before the advent of information at high redshift values [50], large scale structure formation studies strongly favored a hot plus cold dark matter mixture with $\Omega_\nu \approx 0.20$ – 0.25 [51]. While recent work incorporating the new high redshift large scale structure data has reduced the need for a hot dark matter component, it remains an interesting possibility. Given that ν_τ masses greater than a few eV or so are well motivated from the combined requirements of the atmospheric neutrino anomaly and BBN, we see that the existence of neutrino hot dark matter is a generic prediction of the EPM.

There is an interesting complication in the hot dark matter story for the EPM (and models with sterile neutrinos) which we now discuss. We will take by way of concrete example that only the ν_τ (and ν'_τ) has an eV scale mass. Again for the sake of the example, we will consider the neutrino mass range required by what was the favored hot plus cold dark matter scenario [51],

$$3 \text{ eV} \leq m_{\nu_\tau} \leq 7 \text{ eV}, \quad (140)$$

even though the present situation is less clear. The point we want to make is that whatever a “favored neutrino hot dark matter mass range” might be at any given time, the situation is modified somewhat in the case of the EPM. The reason is that the $\nu_\tau \leftrightarrow \nu'_\mu$ and $\nu_\tau \leftrightarrow \nu'_e$ oscillations generate such a large L_{ν_τ} that the total number of tau neutrinos is actually significantly reduced. For the parameter region

$$10 \leq \delta m_{\text{large}}^2 / \text{eV}^2 \leq 300, \quad (141)$$

the final value of L_{ν_τ} is about 0.27. The large final lepton number occurs because about 70% of the anti-neutrinos have been depleted (for the $L_{\nu_\tau} > 0$ case) which means that the total number of tau neutrinos plus tau antineutrinos is roughly 0.65 of the standard expectation. (Note that the total number of neutrinos has not changed much: the missing

heavy tau antineutrinos have just been converted into light mirror states.) Also note that a small number of ν'_τ are also generated by the oscillations, and it turns out that the total number of ν_τ and ν'_τ (plus antiparticle) states is about 0.70 of the standard expectation. The effect of this is to change the “favored hot dark matter mass range” from what the expectation would be in the absence of mirror (or sterile) neutrinos. We can guess that in the context of the EPM the “favored” tau neutrino mass is actually about 50% larger than the naive expectation. (A full large scale structure computation would need to be performed to fully explore the consequences of a depleted ν_τ distribution.) Thus, in the EPM model, the hypothetical favored mass range of Eq. (140) becomes instead

$$5 \text{ eV} \leq m_{\nu_{\tau\pm}} \leq 10 \text{ eV}. \quad (142)$$

This means that $\delta m_{\text{large}}^2$ is expected to be in the range

$$25 \text{ eV}^2 \leq \delta m_{\text{large}}^2 \leq 100 \text{ eV}^2, \quad (143)$$

provided of course that the scenario of Eq. (140) is correct. The hypothetical hot dark matter region of Eq. (143) is the shaded band on Fig. 2. From this figure, we see that there is considerable overlap between the BBN allowed region and the hot dark matter region.

Finally, note that structure formation outcomes in hot plus cold dark matter models are generically sensitive to the number of eV neutrino flavors, not just to Ω_ν . These studies typically assume that the number of eV neutrino flavors (usually taken to be degenerate in mass) at the epoch of matter-radiation equality is an integer. It is important to understand that this is only true provided that mirror or sterile neutrinos do not exist. Indeed, as we have just explained above, we expect $N_\nu^{\text{heavy}} \approx 0.70$ in the EPM in the parameter space region of Eqs. (91), (92), and (141).

VII. IMPLICATIONS FOR THE COSMIC MICROWAVE BACKGROUND

During the next decade or so, high precision measurements of the anisotropy of the cosmic microwave background (CMB) will be performed by several experiments (such as the PLANCK and MAP missions). These satellites should be able to measure detailed spectral properties of the electromagnetic radiation in the universe at the epoch of photon-matter decoupling [52]. In this context it is important to note that mirror and sterile neutrinos can leave their “imprint” on the cosmic microwave background [53]. This information will complement knowledge obtained from BBN because (i) BBN and photon decoupling take place at different epochs and (ii) BBN is sensitive to both the expansion rate and the direct effect of L_{ν_e} on nuclear reaction rates whereas the CMB is insensitive to the direct effects of the asymmetry. Because of point (ii) we have to distinguish between *expansion rate* and *effective* neutrino flavor counting. So it is useful to introduce the quantities N_ν^{light} and N_ν^{heavy} which effectively count the number of light neutrino and heavy neutrino flavors, respectively, at the epoch of photon

decoupling. These quantities, which quantify expansion rates, are to be used in conjunction with $N_{\nu,\text{eff}}$ which contains both expansion rate and L_{ν_e} information. It is important to appreciate that the number of *relativistic* neutrino flavors may be different at the time of photon decoupling compared to BBN. So, in this context, “light” means much less than about 1 eV, making these neutrinos relativistic at the epoch of photon decoupling, and “heavy” means more than about 1 eV, making those neutrinos approximately non-relativistic. Of course in the minimal standard model of particle physics with its three massless neutrinos, $N_{\nu,\text{eff}}=N_{\nu}^{\text{light}}=3$ and $N_{\nu}^{\text{heavy}}=0$. However, in models with sterile or mirror neutrinos, $N_{\nu,\text{eff}}\neq N_{\nu}^{\text{light}}$ and $N_{\nu}^{\text{heavy}}\neq 0$ in general. It is also important to appreciate that in the EPM (or in models with sterile neutrinos), none of these quantities is in general an integer.

The CMB implications of the EPM depend on the neutrino parameter region. If we take by way of example the mass hierarchy of Eqs. (91) and (92), with $m_{\nu_{\tau\pm}}\gtrsim 1$ eV (as suggested by Fig. 2), then

$$N_{\nu}^{\text{heavy}}\simeq\frac{n_{\nu_{\tau}}+n_{\nu'_{\tau}}+\text{antiparticles}}{2n_0},$$

$$N_{\nu}^{\text{light}}=\frac{\rho_{\nu_e}+\rho_{\nu_{\mu}}+\rho_{\nu'_e}+\rho_{\nu'_{\mu}}+\text{antiparticles}}{2\rho_0}, \quad (144)$$

where n_i (ρ_i) is the mass (energy) density of species i with n_0 (ρ_0) being the mass (energy) density of a Weyl fermion distribution with zero chemical potential. Taking $\delta m_{\text{large}}^2$ in the range, Eq. (141), we find that

$$N_{\nu}^{\text{heavy}}\approx 0.70, \quad N_{\nu}^{\text{light}}\approx 2.3. \quad (145)$$

This should be distinguishable from the minimal standard model expectation.

We conclude by emphasizing that in general the precise measurements of the CMB may well prove to be quite useful in distinguishing between various competing explanations of the neutrino anomalies, since each model should leave quite a distinctive imprint on the CMB.

VIII. CONCLUSION

The exact parity model is theoretically well motivated by the neurotic desire of some to have the full Lorentz group as an exact symmetry of nature. It is very interesting that this model can, essentially as a by-product, provide an elegant explanation of the atmospheric and solar neutrino problems in a way that is fully compatible with the LSND results. In this paper, we explored the novel cosmological phenomena implied by the existence of mirror neutrinos.

We focussed on the parameter space region

$$m_{\nu_{e+}}\approx m_{\nu_{e-}}\lesssim m_{\nu_{\mu+}}\approx m_{\nu_{\mu-}}\lesssim m_{\nu_{\tau+}}\approx m_{\nu_{\tau-}} \quad (146)$$

with all intergenerational vacuum mixing angles obeying

$$10^{-10}\lesssim\sin^2 2\theta\ll 1. \quad (147)$$

The mass splittings among the e -like and μ -like states were chosen to solve the solar and atmospheric neutrino problems, respectively. The evolution of the neutrino and mirror neutrino ensembles was then calculated for the cosmological epoch between $T=m_{\mu}$ and big bang nucleosynthesis. Generic outcomes were obtained for significant regions of parameter space because (i) *some* of the final neutrino asymmetries turned out to be independent of the oscillation parameters for a range of those parameters and (ii) *many* of the modes were adiabatic and hence independent of vacuum mixing angles.

The most important specific conclusions were the following:

(1) The $\nu_{\mu}\rightarrow\nu'_{\mu}$ solution to the atmospheric neutrino problem is consistent with big bang nucleosynthesis for the parameter space region illustrated in Fig. 2. The ν_{τ} mass implied by this region makes the ν_{τ} a hot dark matter particle. This calculation improves on that discussed in Ref. [32] through the use of quantum kinetic equations.

(2) The effect of EPM neutrino oscillations on the primordial helium abundance has been computed. We find that a large change to the effective number of neutrino flavors during big bang nucleosynthesis is produced for a range of parameters. In particular, a change equivalent to adding or removing about one neutrino flavor is obtained when the $\nu_e-\nu_{\mu}$ mass splitting is in the LSND range.

ACKNOWLEDGMENTS

R.F. would like to thank S. Blinnikov for interesting correspondence and for sending him a copy of one of his papers. R.F. and R.R.V. are supported by the Australian Research Council.

APPENDIX A: DETAILS OF THE HELIUM ABUNDANCE COMPUTATION

The modification of the ν_e and $\bar{\nu}_e$ distributions due to the creation of L_{ν_e} affects big bang nucleosynthesis. This is primarily due to the modification of the $n\leftrightarrow p$ reaction rates. The result of this is a modification of the neutron/proton ratio. The most important observable effect of a small change to the neutron/proton ratio is a modification to the prediction for the helium mass fraction Y_p . This effect can be expressed as a change in the predicted $N_{\nu,\text{eff}}$ through the well-known relation $\delta Y_p\approx 0.012\delta N_{\nu,\text{eff}}$.²⁷ In computing the modification of Y_p due to the modified neutrino distributions, N_{ν_e} and $N_{\bar{\nu}_e}$, we do not need to use a full nucleosynthesis

²⁷Of course we are not saying that this equivalence is exact. It is not. The change in Y_p due to the modification of the ν_e and $\bar{\nu}_e$ distributions cannot be exactly represented as a change in $N_{\nu,\text{eff}}$. This is because these two effects will have different impacts on the other primordial element abundances. However, because a small modification in the ν_e and $\bar{\nu}_e$ distributions, or a small change in $N_{\nu,\text{eff}}$, primarily affects Y_p , our use of the relation $\delta Y_p\approx 0.012\delta N_{\nu,\text{eff}}$ is reasonable. We prefer to express our results in terms of $\delta N_{\nu,\text{eff}}$ rather than δY_p just because $\delta N_{\nu,\text{eff}}$ is a more familiar unit.

code. The reason is that the effects of the modified neutrino distributions are only important for temperatures $T \gtrsim 0.4$ MeV, well before nucleosynthesis actually occurs. A review of standard helium synthesis which we found useful was Ref. [46]. Our approach and notation follows this treatment quite closely.

Recall that the primordial helium mass fraction, Y_P , is related to the ratio of neutrons to nucleons, X_n , by $Y_P = 2X_n$, just before nucleosynthesis. X_n is governed by the differential equation

$$-\frac{dX_n}{dt} = \lambda(n \rightarrow p)X_n - \lambda(p \rightarrow n)(1 - X_n), \quad (\text{A1})$$

where

$$\begin{aligned} \lambda(n \rightarrow p) &\equiv \lambda(n + \nu_e \rightarrow p + e^-) + \lambda(n + e^+ \rightarrow p + \bar{\nu}_e) \\ &\quad + \lambda(n \rightarrow p + e^- + \bar{\nu}_e), \\ \lambda(p \rightarrow n) &\equiv \lambda(p + e^- \rightarrow n + \nu_e) + \lambda(p + \bar{\nu}_e \rightarrow n + e^+) \\ &\quad + \lambda(p \rightarrow n + e^+ + \nu_e). \end{aligned} \quad (\text{A2})$$

The rates for these processes are given by

$$\begin{aligned} \lambda(n + \nu_e \rightarrow p + e^-) &= A \int \frac{\nu_e E_e^2 \tilde{N}_{\nu_e}}{1 + \exp(-E_e/T)} dp_\nu, \\ \lambda(n + e^+ \rightarrow p + \bar{\nu}_e) &= A \int \frac{p_e^2 (p_\nu^2 - \tilde{N}_{\bar{\nu}_e})}{1 + \exp(E_e/T)} dp_e, \\ \lambda(n \rightarrow p + e^- + \bar{\nu}_e) &= A \int \frac{\nu_e E_e^2 (p_\nu^2 - \tilde{N}_{\bar{\nu}_e})}{1 + \exp(-E_e/T)} dp_\nu, \\ \lambda(p + e^- \rightarrow n + \nu_e) &= A \int \frac{p_e^2 (p_\nu^2 - \tilde{N}_{\nu_e})}{1 + \exp(E_e/T)} dp_e, \\ \lambda(p + \bar{\nu}_e \rightarrow n + e^+) &= A \int \frac{\nu_e E_e^2 \tilde{N}_{\bar{\nu}_e}}{1 + \exp(-E_e/T)} dp_\nu, \\ \lambda(p + e^- + \bar{\nu}_e \rightarrow n) &= A \int \frac{\nu_e E_e^2 \tilde{N}_{\bar{\nu}_e}}{1 + \exp(E_e/T)} dp_\nu, \end{aligned} \quad (\text{A3})$$

where $\nu_e = p_e/E_e$ is the velocity of the electron (we use $\hbar = c = 1$ throughout) and \tilde{N}_ν is related to the neutrino distribution functions by $\tilde{N}_\nu \equiv 2\pi^2 N_\nu$. The constant A can be expressed in terms of the vector and axial vector coupling constants of the nucleon [46],

$$A = \frac{g_V^2 + 3g_A^2}{2\pi^3}. \quad (\text{A4})$$

Also, E_e and E_ν are related by

$$E_e - E_\nu = Q \quad \text{for } n + \nu_e \leftrightarrow p + e^-,$$

$$E_\nu - E_e = Q \quad \text{for } n + e^+ \leftrightarrow p + \bar{\nu}_e,$$

$$E_\nu + E_e = Q \quad \text{for } n \leftrightarrow p + e^- + \bar{\nu}_e, \quad (\text{A5})$$

where $Q \equiv m_n - m_p \approx 1.293$ MeV. The integrals of Eq. (A5) are taken over all positive values of p_ν and p_e allowed by these relations.

In order to compute Y_P we need to know the time when nucleosynthesis occurs and neutron decay ceases. This is handled approximately by simply stopping the evolution of X_n at a point where agreement with the expected value of $Y_P \sim 0.24$ occurs, which we find to be roughly when $t \approx 300$ s. This approximation does not affect the accuracy of our results at all since we are only interested in the difference between Y_P using the modified ν_e and $\bar{\nu}_e$ distributions and Y_P using the standard distributions (i.e. Fermi-Dirac distributions with zero chemical potentials). Thus, to a excellent approximation, the modification of Y_P due to the non-standard neutrino distributions has the form

$$\delta Y_P \approx 2 \delta X_n(t=300 \text{ s}), \quad (\text{A6})$$

where $\delta X_n(t=300 \text{ s})$ is the difference between $X_n(t=300 \text{ s})$ computed using the neutrino momentum distributions N_{ν_e} and $N_{\bar{\nu}_e}$ and $X_n(t=300 \text{ s})$ using the standard momentum distributions. Of course the distributions N_{ν_e} and $N_{\bar{\nu}_e}$ typically depend on the time, so that the evolution of $X_n^{(0)}(t)$ must be computed concurrently with the evolution of N_{ν_e} and $N_{\bar{\nu}_e}$. In solving the differential equation (A1), we employ the usual the initial condition $X_n = 0.5$.

We have checked our code against some previous calculations. For example, in Ref. [47] they consider the case of a time independent neutrino chemical potential (taken to arise from some unknown physics at high temperature). From Fig. 2 of Ref. [47], they find that $\delta Y_P \approx -0.020$ for $\mu_\nu/T = -\mu_{\bar{\nu}}/T \approx 0.09$ (for constant η). Our code also gives exactly the same results under the same conditions.

Finally note that at low temperatures $T \lesssim m_e$, the e^+e^- annihilation process increases the temperature of the photons relative to the neutrinos. It also affects the time-temperature relation. In our numerical work, we take these effects into account using the equations given in Ref. [46] (suitably modified to incorporate three light neutrino flavors instead of two). Of course this detail actually does not affect our results much, since most of the effects of neutrino asymmetries are only important for temperatures $T \gtrsim m_e$. Nevertheless, following Mallory [54] we include it because it is there.

APPENDIX B: THE QUANTUM KINETIC EQUATIONS FOR THE MODES WITH $\delta M^2 = \delta M_{\text{small}}^2$ IN CASE 2 OF SEC. V

This appendix deals with the case defined by Eq. (133), where there are a class of modes having $\delta m_{\text{large}}^2$ [see Eq. (93)] and another class of modes having $\delta m_{\text{small}}^2$ [see Eq. (134)]. As discussed in Sec.V, the $\delta m_{\text{large}}^2$ and $\delta m_{\text{small}}^2$ modes approximately decouple from each other provided that $\delta m_{\text{large}}^2 \gtrsim 50 \delta m_{\text{small}}^2$. The evolution of the $\delta m_{\text{large}}^2$ oscillations

can be evaluated using the adiabatic formalism of Sec. VB. The $\delta m_{\text{small}}^2$ modes can be neglected initially because their resonance momenta satisfy $p_{1,2}/T \ll 1$. By the time $T = T_x$ [see Eq. (138)], the $\delta m_{\text{small}}^2$ modes begin to be important, and provided that $\delta m_{\text{large}}^2 \geq 50 \delta m_{\text{small}}^2$ is satisfied, the $\delta m_{\text{large}}^2$ modes can be neglected because $P_i/T \geq 10$. To compute the effects of the $\delta m_{\text{small}}^2$ modes we must numerically integrate the quantum kinetic equations. Thus, we start the quantum kinetic equations at $T = T_x$ with the initial values of N_{ν_α} , $N_{\nu'_\alpha}$, L_{ν_α} and $L_{\nu'_\alpha}$ obtained from the previous evolution involving the $\delta m_{\text{large}}^2$ modes.

In this Appendix we do not follow exactly the notation of Sec. IV. We adopt an equivalent but simplifying change of variables which is very useful for complicated coupled-mode systems such as the one we are currently dealing with.

For each of the four oscillation modes, we assign a density matrix $P_{x,y,z,0}^i$ ($i = 1, \dots, 4$). In solving this system, it is convenient to use the variables $P_x^i, P_y^i, N_{\nu_\alpha}, N_{\nu'_\alpha}, N_{\bar{\nu}_\alpha}$ and $N_{\bar{\nu}'_\alpha}$ rather than the variables P_0^i, P_x^i, P_y^i and P_z^i . The $P_{0,z}^i$ are related to the N 's as follows:

$$\begin{aligned} P_0^1(p) &= \frac{N_{\bar{\nu}_\mu}^-(p) + N_{\bar{\nu}'_e}(p)}{N^{\text{eq}}(p, T, 0)}, & P_z^1(p) &= \frac{N_{\bar{\nu}_\mu}^-(p) - N_{\bar{\nu}'_e}(p)}{N^{\text{eq}}(p, T, 0)}, \\ P_0^2(p) &= \frac{N_{\nu_e}(p) + N_{\nu'_\mu}(p)}{N^{\text{eq}}(p, T, 0)}, & P_z^2(p) &= \frac{N_{\nu_e}(p) - N_{\nu'_\mu}(p)}{N^{\text{eq}}(p, T, 0)}, \\ P_0^3(p) &= \frac{N_{\bar{\nu}_\mu}^-(p) + N_{\bar{\nu}'_e}(p)}{N^{\text{eq}}(p, T, 0)}, & P_z^3(p) &= \frac{N_{\bar{\nu}_\mu}^-(p) - N_{\bar{\nu}'_e}(p)}{N^{\text{eq}}(p, T, 0)}, \\ P_0^4(p) &= \frac{N_{\bar{\nu}'_\mu}(p) + N_{\bar{\nu}'_e}(p)}{N^{\text{eq}}(p, T, 0)}, & P_z^4(p) &= \frac{N_{\bar{\nu}'_\mu}(p) - N_{\bar{\nu}'_e}(p)}{N^{\text{eq}}(p, T, 0)}. \end{aligned} \quad (\text{B1})$$

The evolution of the number densities has a contribution from coherent effects and a contribution from the subsequent repopulation. Thus,

$$\begin{aligned} \frac{dN_{\nu_\alpha}}{dt} &= \frac{dN_{\nu_\alpha}}{dt} \Big|_{\text{osc}} + \frac{dN_{\nu_\alpha}}{dt} \Big|_{\text{repop}}, \\ \frac{dN_{\bar{\nu}_\alpha}}{dt} &= \frac{dN_{\bar{\nu}_\alpha}}{dt} \Big|_{\text{osc}} + \frac{dN_{\bar{\nu}_\alpha}}{dt} \Big|_{\text{repop}}. \end{aligned} \quad (\text{B2})$$

The contribution from coherent effects can be broken up among the four modes as follows:

$$\begin{aligned} \frac{dN_{\nu_e}}{dt} \Big|_{\text{osc}} &= \frac{dN_{\nu_e}}{dt} \Big|_{\nu'_\mu \leftrightarrow \nu_e}, & \frac{dN_{\bar{\nu}_e}}{dt} \Big|_{\text{osc}} &= \frac{dN_{\bar{\nu}_e}}{dt} \Big|_{\bar{\nu}_\mu \leftrightarrow \bar{\nu}'_e}, \\ \frac{dN_{\nu_\mu}}{dt} \Big|_{\text{osc}} &= 0, & \frac{dN_{\bar{\nu}_\mu}}{dt} \Big|_{\text{osc}} &= \frac{dN_{\bar{\nu}_\mu}}{dt} \Big|_{\bar{\nu}_\mu \leftrightarrow \bar{\nu}'_e} + \frac{dN_{\bar{\nu}_\mu}}{dt} \Big|_{\bar{\nu}'_\mu \leftrightarrow \bar{\nu}'_e}, \end{aligned}$$

$$\begin{aligned} \frac{dN_{\nu'_e}}{dt} \Big|_{\text{osc}} &= 0, & \frac{dN_{\bar{\nu}'_e}}{dt} \Big|_{\text{osc}} &= \frac{dN_{\bar{\nu}'_e}}{dt} \Big|_{\bar{\nu}_\mu \leftrightarrow \bar{\nu}'_e} + \frac{dN_{\bar{\nu}'_e}}{dt} \Big|_{\bar{\nu}'_\mu \leftrightarrow \bar{\nu}'_e}, \\ \frac{dN_{\nu'_\mu}}{dt} \Big|_{\text{osc}} &= \frac{dN_{\nu'_\mu}}{dt} \Big|_{\nu'_\mu \leftrightarrow \nu_e}, & \frac{dN_{\bar{\nu}'_\mu}}{dt} \Big|_{\text{osc}} &= \frac{dN_{\bar{\nu}'_\mu}}{dt} \Big|_{\bar{\nu}'_\mu \leftrightarrow \bar{\nu}'_e}, \end{aligned} \quad (\text{B3})$$

with

$$\begin{aligned} \frac{dN_{\bar{\nu}_\mu}^-}{dt} \Big|_{\bar{\nu}_\mu \leftrightarrow \bar{\nu}'_e} &= - \frac{dN_{\bar{\nu}'_e}}{dt} \Big|_{\bar{\nu}_\mu \leftrightarrow \bar{\nu}'_e} = \frac{1}{2} \int \beta_1 \bar{P}_y^1 N^{\text{eq}}(p, T, 0) dp, \\ \frac{dN_{\nu'_\mu}}{dt} \Big|_{\nu'_\mu \leftrightarrow \nu_e} &= - \frac{dN_{\nu_e}}{dt} \Big|_{\nu'_\mu \leftrightarrow \nu_e} = - \frac{1}{2} \int \beta_2 P_y^2 N^{\text{eq}}(p, T, 0) dp, \\ \frac{dN_{\bar{\nu}_\mu}^-}{dt} \Big|_{\bar{\nu}_\mu \leftrightarrow \bar{\nu}'_e} &= - \frac{dN_{\bar{\nu}'_e}}{dt} \Big|_{\bar{\nu}_\mu \leftrightarrow \bar{\nu}'_e} = \frac{1}{2} \int \beta_3 \bar{P}_y^3 N^{\text{eq}}(p, T, 0) dp, \\ \frac{dN_{\bar{\nu}'_\mu}}{dt} \Big|_{\bar{\nu}'_\mu \leftrightarrow \bar{\nu}'_e} &= - \frac{dN_{\bar{\nu}'_e}}{dt} \Big|_{\bar{\nu}'_\mu \leftrightarrow \bar{\nu}'_e} = \frac{1}{2} \int \beta_4 \bar{P}_y^4 N^{\text{eq}}(p, T, 0) dp, \end{aligned} \quad (\text{B4})$$

where $\beta_i = -\delta m_{\text{small}}^2 \sin 2\theta_i/2p$ for $i = 1, 3, 4$ and $\beta_i = \delta m_{\text{small}}^2 \sin 2\theta_i/2p$ for $i = 2$. The rate of change of the number densities due to repopulation is handled approximately via the equation,

$$\frac{d}{dt} \frac{N_{\nu_\alpha}(p)}{N^{\text{eq}}(p, T, 0)} \Big|_{\text{repop}} \simeq \Gamma_\alpha(p) \left[\frac{N^{\text{eq}}(p, T, \mu)}{N^{\text{eq}}(p, T, 0)} - \frac{N_{\nu_\alpha}(p)}{N^{\text{eq}}(p, T, 0)} \right] \quad (\text{B5})$$

where $\Gamma_\alpha(p)$ is the total collision rate, and $N^{\text{eq}}(p, T, \mu)$ is the equilibrium distribution which is a function of the chemical potentials which can be computed from the lepton numbers (see Sec. III for further discussion).

The rates of change of the lepton numbers are given by

$$\begin{aligned} \frac{dL_{\nu_e}}{dt} &= \frac{dL_{\nu_e}}{dt} \Big|_{\bar{\nu}_\mu \leftrightarrow \bar{\nu}'_e} + \frac{dL_{\nu_e}}{dt} \Big|_{\nu'_\mu \leftrightarrow \nu_e}, \\ \frac{dL_{\nu_\mu}}{dt} &= \frac{dL_{\nu_\mu}}{dt} \Big|_{\bar{\nu}_\mu \leftrightarrow \bar{\nu}'_e} + \frac{dL_{\nu_\mu}}{dt} \Big|_{\bar{\nu}'_\mu \leftrightarrow \bar{\nu}'_e}, \\ \frac{dL_{\nu'_e}}{dt} &= \frac{dL_{\nu'_e}}{dt} \Big|_{\bar{\nu}_\mu \leftrightarrow \bar{\nu}'_e} + \frac{dL_{\nu'_e}}{dt} \Big|_{\bar{\nu}'_\mu \leftrightarrow \bar{\nu}'_e}, \\ \frac{dL_{\nu'_\mu}}{dt} &= \frac{dL_{\nu'_\mu}}{dt} \Big|_{\nu'_\mu \leftrightarrow \nu_e} + \frac{dL_{\nu'_\mu}}{dt} \Big|_{\bar{\nu}'_\mu \leftrightarrow \bar{\nu}'_e}, \end{aligned} \quad (\text{B6})$$

where

$$\begin{aligned}
 \left. \frac{dL_{\nu_\mu}}{dt} \right|_{\bar{\nu}_\mu \leftrightarrow \bar{\nu}'_e} &= - \left. \frac{dL_{\nu'_e}}{dt} \right|_{\bar{\nu}_\mu \leftrightarrow \bar{\nu}'_e} \\
 &= - \frac{1}{2n_\gamma} \int \beta_1 \bar{P}_y^1 N^{\text{eq}}(p, T, 0) dp, \\
 \left. \frac{dL_{\nu'_\mu}}{dt} \right|_{\nu'_\mu \leftrightarrow \nu_e} &= - \left. \frac{dL_{\nu_e}}{dt} \right|_{\nu'_\mu \leftrightarrow \nu_e} \\
 &= - \frac{1}{2n_\gamma} \int \beta_2 P_y^2 N^{\text{eq}}(p, T, 0) dp, \\
 \left. \frac{dL_{\nu_\mu}}{dt} \right|_{\bar{\nu}_\mu \leftrightarrow \bar{\nu}_e} &= - \left. \frac{dL_{\nu_e}}{dt} \right|_{\bar{\nu}_\mu \leftrightarrow \bar{\nu}_e} \\
 &= - \frac{1}{2n_\gamma} \int \beta_3 \bar{P}_y^3 N^{\text{eq}}(p, T, 0) dp,
 \end{aligned}
 \qquad
 \begin{aligned}
 \left. \frac{dL_{\nu'_\mu}}{dt} \right|_{\bar{\nu}'_\mu \leftrightarrow \bar{\nu}'_e} &= - \left. \frac{dL_{\nu'_e}}{dt} \right|_{\bar{\nu}'_\mu \leftrightarrow \bar{\nu}'_e} \\
 &= - \frac{1}{2n_\gamma} \int \beta_4 \bar{P}_y^4 N^{\text{eq}}(p, T, 0) dp. \quad (\text{B7})
 \end{aligned}$$

Actually it turns out that the effect of the $\bar{\nu}'_\mu \leftrightarrow \bar{\nu}'_e$ mode can be neglected because $N_{\bar{\nu}'_\mu}(p_4) \approx N_{\bar{\nu}'_e}(p_4)$. This is because the modes with $\delta m^2 = \delta m_{\text{large}}^2$ create approximately equal numbers of $\bar{\nu}'_\mu$ and $\bar{\nu}'_e$ states. Also, the $\bar{\nu}_\mu \leftrightarrow \bar{\nu}_e$ mode always has a lower resonance momentum than the $\bar{\nu}'_\mu \leftrightarrow \bar{\nu}'_e$ mode. This means that the change in $N_{\bar{\nu}'_e}(p)$ due to the $\bar{\nu}_\mu \leftrightarrow \bar{\nu}_e$ mode does not occur until the $\bar{\nu}'_\mu \leftrightarrow \bar{\nu}'_e$ resonance momentum has already passed by. By similar reasoning, the $\bar{\nu}_\mu \leftrightarrow \bar{\nu}_e$ mode can also be neglected to a good approximation.

-
- [1] T. D. Lee and C. N. Yang, Phys. Rev. **104**, 256 (1956); I. Kobzarev, L. Okun, and I. Pomeranchuk, Sov. J. Nucl. Phys. **3**, 837 (1966); M. Pavsic, Int. J. Theor. Phys. **9**, 229 (1974).
- [2] S. I. Blinnikov and M. Yu. Khlopov, Sov. J. Nucl. Phys. **36**, 472 (1982); Sov. Astron. **27**, 371 (1983); E. W. Kolb, M. Seckel, and M. S. Turner, Nature (London) **514**, 415 (1985); H. M. Hodges, Phys. Rev. D **47**, 456 (1993); G. Matsas *et al.*, hep-ph/9810456; N. F. Bell and R. R. Volkas, Phys. Rev. D **59**, 107301 (1999).
- [3] R. Foot, H. Lew, and R. R. Volkas, Phys. Lett. B **272**, 67 (1991).
- [4] R. Foot, H. Lew, and R. R. Volkas, Mod. Phys. Lett. A **7**, 2567 (1992); R. Foot, *ibid.* **9**, 169 (1994); R. Foot and R. R. Volkas, Phys. Rev. D **52**, 6595 (1995); see also Z. Silagadze, Phys. At. Nucl. **60**, 272 (1997).
- [5] B. Holdom, Phys. Lett. **166B**, 196 (1985); S. L. Glashow, *ibid.* **167B**, 35 (1986); M. Collie and R. Foot, Phys. Lett. B **432**, 134 (1998).
- [6] E. Carlson and S. L. Glashow, Phys. Lett. B **193**, 168 (1987).
- [7] H. Lew (unpublished).
- [8] S. Blinnikov, astro-ph/9801015; R. Foot, Phys. Lett. B **452**, 83 (1999). Also, a similar idea has been discussed recently in the context of a model where the masses of the mirror particles are scaled up by an arbitrary parameter. See R. Mohapatra and V. Teplitz, *ibid.* **462**, 302 (1999).
- [9] S. Blinnikov, astro-ph/9902305.
- [10] Z. Berezhiani and R. Mohapatra, Phys. Rev. D **52**, 6607 (1995); Z. G. Berezhiani, A. D. Dolgov, and R. N. Mohapatra, Phys. Lett. B **375**, 26 (1996); Z. G. Berezhiani, Acta Phys. Pol. B **27**, 1503 (1996); see also E. Kh. Akhmedov, Z. G. Berezhiani, and G. Senjanovic, Phys. Rev. Lett. **69**, 3013 (1992).
- [11] SuperKamiokande Collaboration, Y. Fukuda *et al.*, Phys. Lett. B **433**, 9 (1998); **436**, 33 (1998); Phys. Rev. Lett. **81**, 1562 (1998); **82**, 2644 (1999).
- [12] T. Haines *et al.*, Phys. Rev. Lett. **57**, 1986 (1986); Kamiokande Collaboration, K. S. Hirata *et al.*, Phys. Lett. B **205**, 416 (1988); **280**, 146 (1992); Y. Fukuda *et al.*, *ibid.* **335**, 237 (1994); IMB Collaboration, D. Casper *et al.*, Phys. Rev. Lett. **66**, 2561 (1989); R. Becker-Szendy *et al.*, Phys. Rev. D **46**, 3720 (1989); NUSEX Collaboration, M. Aglietta *et al.*, Europhys. Lett. **8**, 611 (1989); Frejus Collaboration, Ch. Berger *et al.*, Phys. Lett. B **227**, 489 (1989); **245**, 305 (1990); K. Daum *et al.*, Z. Phys. C **66**, 417 (1995); Soudan 2 Collaboration, W. W. M. Allison *et al.*, Phys. Lett. B **391**, 491 (1997); Kamiokande Collaboration, S. Hatakeyama *et al.*, Phys. Rev. Lett. **81**, 2016 (1998); MACRO Collaboration, M. Ambrosio *et al.*, *ibid.* **434**, 451 (1998); hep-ex/9808001.
- [13] See, for example, R. Foot, R. R. Volkas, and O. Yasuda, Phys. Lett. B **433**, 82 (1998).
- [14] R. Foot, R. R. Volkas, and O. Yasuda, Phys. Rev. D **58**, 013006 (1998).
- [15] P. Lipari and M. Lusignoli, Phys. Rev. D **58**, 073005 (1998); E. Akhmedov, P. Lipari, and M. Lusignoli, Phys. Lett. B **300**, 128 (1993).
- [16] T. Kajita, talk at the ‘‘Topical Workshop on Neutrino Physics,’’ National Institute of Theoretical Physics, University of Adelaide, 1996; F. Vissani and A. Yu. Smirnov, Phys. Lett. B **432**, 376 (1998); Q. Y. Liu and A. Yu. Smirnov, Nucl. Phys. **B524**, 505 (1998); Q. Y. Liu, S. P. Mikheyev, and A. Yu. Smirnov, Phys. Lett. B **440**, 319 (1998); J. G. Learned, S. Pakvasa, and J. L. Stone, *ibid.* **435**, 131 (1998); L. J. Hall and H. Murayama, *ibid.* **436**, 323 (1998); see also Refs. [14,15].
- [17] R. Foot and R. R. Volkas, hep-ph/9510312.
- [18] The general idea that the solar neutrino problem is due to vacuum neutrino oscillations was proposed by V. Gribov and B. Pontecorvo, Phys. Lett. **28B**, 463 (1969); this paper considered both energy independent averaged oscillations as well as mentioning the possibility that the oscillation length may be of

- the order of the astronomical unit. See also, for example, S. Nussinov, *ibid.* **63B**, 201 (1976); S. Bilenky and B. Pontecorvo, Phys. Rep. **41**, 225 (1978); V. Barger, R. J. N. Phillips and K. Whisnant, Phys. Rev. D **24**, 538 (1981); S. L. Glashow and L. Krauss, Phys. Lett. B **190**, 199 (1987); **445**, 412 (1999); J. Bahcall, P. Krastev, and A. Yu. Smirnov, Phys. Rev. D **58**, 096016 (1998). For a recent review, see for example V. Berezhinsky, hep-ph/9904259.
- [19] A. H. Guth, L. Randall, and M. Serna, J. High Energy Phys. **08**, 018 (1999).
- [20] V. Berezhinsky, G. Fiorentini, and M. Lissia, hep-ph/9811352; hep-ph/9904225; M. B. Smy, SuperKamiokande Collaboration, hep-ex/9903034.
- [21] SuperKamiokande Collaboration, Y. Fukuda *et al.* Phys. Rev. Lett. **82**, 2430 (1999).
- [22] J. N. Bahcall, S. Basu, and M. H. Pinsonneault, Phys. Lett. B **433**, 1 (1998).
- [23] LSND Collaboration, C. Athanassopoulos *et al.*, LSND Collaboration, Phys. Rev. C **54**, 2685 (1996); Phys. Rev. Lett. **77**, 3082 (1996); **81**, 1774 (1998).
- [24] R. Foot, M. J. Thomson, and R. R. Volkas, Phys. Rev. D **53**, 5349 (1996).
- [25] R. Foot and R. R. Volkas, Phys. Rev. D **55**, 5147 (1997).
- [26] R. Foot and R. R. Volkas, Phys. Rev. D **56**, 6653 (1997); **59**, 029901(E) (1999).
- [27] N. F. Bell, R. Foot, and R. R. Volkas, Phys. Rev. D **58**, 105010 (1998).
- [28] R. Foot, Astropart. Phys. **10**, 253 (1999).
- [29] N. F. Bell, R. R. Volkas, and Y. Y. Y. Wong, Phys. Rev. D **59**, 113001 (1999).
- [30] P. Langacker, University of Pennsylvania Report No. UPR 0401T, 1989; R. Barbieri and A. Dolgov, Phys. Lett. B **237**, 440 (1990); Nucl. Phys. **B349**, 743 (1991); K. Kainulainen, Phys. Lett. B **244**, 191 (1990); K. Enqvist, K. Kainulainen, and M. Thomson, Nucl. Phys. **B373**, 498 (1992); J. Cline, Phys. Rev. Lett. **68**, 3137 (1992); X. Shi, D. N. Schramm, and B. D. Fields, Phys. Rev. D **48**, 2563 (1993); G. Raffelt, G. Sigl, and L. Stodolsky, Phys. Rev. Lett. **70**, 2363 (1993); C. Y. Cardall and G. M. Fuller, Phys. Rev. D **54**, 1260 (1996).
- [31] R. Foot and R. R. Volkas, Phys. Rev. Lett. **75**, 4350 (1995).
- [32] R. Foot and R. R. Volkas, Astropart. Phys. **7**, 283 (1997).
- [33] J. Bowes and R. R. Volkas, J. Phys. G **24**, 1249 (1998); A. Geiser, Phys. Lett. B **444**, 358 (1999); P. Langacker, Phys. Rev. D **58**, 093017 (1998); Y. Koide and H. Fusaoka, *ibid.* **59**, 053004 (1999); W. Krolikowski, hep-ph/9808307; see also C. Giunti, C. W. Kim, and U. W. Kim, Phys. Rev. D **46**, 3034 (1992); M. Kobayashi, C. S. Lim, and M. M. Nojiri, Phys. Rev. Lett. **67**, 1685 (1991).
- [34] J. Bunn, R. Foot, and R. R. Volkas, Phys. Lett. B **413**, 109 (1997); R. Foot, R. R. Volkas, and O. Yasuda, Phys. Rev. D **57**, 1345 (1998).
- [35] K. Enqvist, K. Kainulainen, and J. Maalampi, Nucl. Phys. **B349**, 754 (1991).
- [36] D. P. Kirilova and M. V. Chizhov, Phys. Lett. B **393**, 375 (1997); Nucl. Phys. **B534**, 497 (1998).
- [37] X. Shi, Phys. Rev. D **54**, 2753 (1996).
- [38] R. A. Harris and L. Stodolsky, Phys. Lett. **116B**, 464 (1982); **78B**, 313 (1978); A. Dolgov, Sov. J. Nucl. Phys. **33**, 700 (1981).
- [39] L. Stodolsky, Phys. Rev. D **36**, 2273 (1987); M. Thomson, Phys. Rev. A **45**, 2243 (1991).
- [40] B. H. J. McKellar and M. J. Thomson, Phys. Rev. D **49**, 2710 (1994) and references therein.
- [41] L. Wolfenstein, Phys. Rev. D **17**, 2369 (1978); S. P. Mikheyev and A. Yu. Smirnov, Nuovo Cimento C **9**, 17 (1986); see also V. Barger *et al.*, Phys. Rev. D **22**, 2718 (1980).
- [42] D. Notzold and G. Raffelt, Nucl. Phys. **B307**, 924 (1988).
- [43] See the paper by Enqvist *et al.* [30].
- [44] For some recent studies, see e.g. N. Hata *et al.*, Phys. Rev. Lett. **75**, 3977 (1995); P. J. Kernan and S. Sarkar, Phys. Rev. D **54**, 3681 (1996); K. A. Olive and D. Thomas, Astropart. Phys. **11**, 403 (1999); S. Burles *et al.*, Phys. Rev. Lett. **82**, 4176 (1999).
- [45] See, for example, K. Kainulainen, H. Kurki-Suonio, and E. Sihvola, Phys. Rev. D **59**, 083505 (1999).
- [46] S. Weinberg, *Gravitation and Cosmology* (Wiley, New York, 1972), Chap. 15.
- [47] K. A. Olive, D. N. Schramm, D. Thomas, and T. P. Walker, Phys. Lett. B **265**, 239 (1991).
- [48] T. P. Walker *et al.*, Astrophys. J. **376**, 51 (1991).
- [49] Chorus Collaboration, hep-ex/9807024; Nomad Collaboration, CERN Report No. CERN-EP-99-032 (unpublished).
- [50] A. Riess *et al.*, Astron. J. **116**, 1009 (1998); S. Perlmutter *et al.*, Astrophys. J. (to be published), astro-ph/9812133.
- [51] R. K. Schaefer, Q. Shafi, and F. W. Stecker, Astrophys. J. **347**, 575 (1989); J. Holtzman, Astrophys. J., Suppl. Ser. **74**, 1 (1989); J. Primack, J. Holtzman, A. Klypin, and D. O. Caldwell, Phys. Rev. Lett. **74**, 2160 (1995). For a review, see e.g. J. Primack, astro-ph/9610078.
- [52] R. E. Lopez, S. Dodelson, A. Heckler, and M. S. Turner, Phys. Rev. Lett. **82**, 3952 (1999), and references therein.
- [53] S. Hannestad and G. Raffelt, Phys. Rev. D **59**, 043001 (1999).
- [54] G. Mallory (private communication).